

Evaluation and Synthesis of Sugar 1-Phosphate Substrates for
Nucleotidyltransferases

by

Stephen A. Beaton

Submitted in Partial Fulfilment of the
Requirements for the degree of Master of Science

at

Dalhousie University
Halifax, Nova Scotia
April 2010

© Copyright by Stephen A. Beaton, 2010

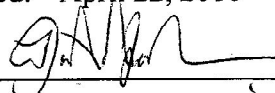
DALHOUSIE UNIVERSITY

DEPARTMENT OF CHEMISTRY

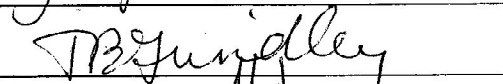
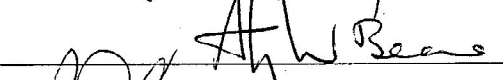

The undersigned hereby certify that they have read and recommend to the Faculty of Graduate Studies for acceptance a thesis entitled "Evaluation and Synthesis of Sugar 1-Phosphate Substrates for Nucleotidyltransferases" by Stephen A. Beaton in partial fulfilment of the requirements for the degree of Master of Science.

Dated: April 22, 2010

Supervisor:



Readers:

DALHOUSIE UNIVERSITY

DATE: April 22, 2010

AUTHOR: Stephen A. Beaton

TITLE: Evaluation and Synthesis of Sugar 1-Phosphate Substrates for
Nucleotidyltransferases

DEPARTMENT OR SCHOOL: Department of Chemistry

DEGREE: MSc CONVOCATION: October YEAR: 2010

Permission is herewith granted to Dalhousie University to circulate and to have copied for non-commercial purposes, at its discretion, the above title upon the request of individuals or institutions.


Signature of Author

The author reserves other publication rights, and neither the thesis nor extensive extracts from it may be printed or otherwise reproduced without the author's written permission.

The author attests that permission has been obtained for the use of any copyrighted material appearing in the thesis (other than the brief excerpts requiring only proper acknowledgement in scholarly writing), and that all such use is clearly acknowledged.

To my friends and family

TABLE OF CONTENTS

LIST OF FIGURES.....	viii
LIST OF TABLES	x
LIST OF SCHEMES	xi
ABSTRACT	xii
LIST OF ABBREVIATIONS AND SYMBOLS USED	xiii
ACKNOWLEDGEMENTS	xvii
CHAPTER 1 INTRODUCTION	1
1.1 Thymidyltransferases	1
1.2 Homology.....	1
1.3 Enzymatic Mechanism	3
1.3.1 Crystallographic Studies of Enzyme-Substrate Interactions.....	4
1.3.2 Role of the Divalent Metal Cation	7
1.3.3 Substrate Specificities	7
CHAPTER 2 PHOSPHONATES AS PROBES FOR ENZYMES.....	10
2.1 <i>O</i> -Glycosides vs. <i>C</i> -Glycosides: Comparisons of Physiochemical Properties	12
2.2 Synthesis of the Phosphono Analogue of Glucose 1-Phosphate.....	14
2.2.1 Synthesis of <i>C</i> -Glycosyl Halides	15
2.2.2 Conversion of <i>C</i> -Glycosyl Halides into Phosphonates	16
2.3 Alternative Methods for the Synthesis of Phosphono Mimics.....	18
2.4 Conclusion.....	21
2.5 Project Objectives	22
CHAPTER 3 RESULTS AND DISCUSSION: SUBSTRATE SPECIFICITY STUDIES WITH CPS2L.....	23
3.1 Phosphono Analogues of Sugar 1-Phosphates.....	23
3.1.1 Introduction.....	23
3.1.2 Progress Curves and Kinetic Characterization	23
3.1.3 Scale-up and Isolation of the Phosphono Analogue of dTDP-Glc	24
3.2 Glucopyranose-1-Boranophosphates	25
3.2.1 Attempted Progress Curves and Kinetic Characterization.....	26
3.3 2-Deoxy-2-Fluorosugar 1-Phosphates	28
3.3.1 Progress Curves and Kinetic Characterization	29

3.3.2 ¹ H NMR and MS Studies to Evaluate the Stereoselectivity of Cps2L for 32	29
3.3.3 Attempted Inhibition Studies	31
3.4 α-D-Glucose 1C-Difluorophosphonate.....	32
3.5 α-D-Glucose 1C-Thiophosphonate.....	34
3.6 Determination of Apparent Kinetic Parameters.....	36
3.7 Conclusions of Enzymatic Assays	39
CHAPTER 4 RESULTS AND DISCUSSION: SYNTHETIC STUDIES	43
4.1 Towards the Preparation of Fluoro Derivatives of α-D-Glucose 1C-Phosphonate	43
4.1.1 Fluoromethylenediphosphonates	43
4.1.2 Fluoro Derivatives of α-D-Glucose 1C-Phosphonate	45
4.2 Preparation of α-D-Glucose 1C-Thiophosphonate.....	50
4.3 Toward the Synthesis of α-D-Glucose 1C-Bisphosphonate.....	52
4.3.1 Synthesis of Methanetrisphosphonate.....	52
4.3.2 Synthesis of α-D-Glucose 1C-Bisphosphonate	53
CHAPTER 5 CONCLUSIONS.....	55
5.1 Future Work	56
5.1.2 Revision of Synthetic Strategy to Prepare α-D-Glc 1C-Phosphonate.....	56
5.1.3 Proposed Synthesis of Glucose 1C-Phosphonate Analogues	56
CHAPTER 6 EXPERIMENTAL.....	59
6.1 General Procedures and Instrumentation for Cps2L Studies	59
6.1.1 Purification of Cps2L.....	59
6.1.2 Determination of Progress Curves.....	60
6.1.3 Determination of Apparent Kinetic Parameters.....	61
6.1.4 Attempted Cps2L Inhibition Assays.....	62
6.1.5 Characterization of Enzymatically Prepared Sugar Nucleotides.....	62
6.2 Synthetic Procedures.....	63
6.2.1 3,4,5,7-Tetra- <i>O</i> -benzyl-1,2-dideoxy-D-glucoheptenitol (6)	64
6.2.2 <i>C</i> -(1-Deoxy-2,3,4,6-tetra- <i>O</i> -benzyl-α-D-glucopyranosyl) iodomethane (7)	65
6.2.3 Diethyl <i>C</i> -(1-deoxy-2,3,5,6-tetra- <i>O</i> -benzyl-α-D-glucopyranosyl) methanephosphonate (8)	65
6.2.4 Ammonium <i>C</i> -(1-deoxy-α-D-glucopyranosyl)methane phosphonate (1)....	66

6.2.5 Phosphono Analogue of dTDP- α -D-Glucopyranose (dTDP-1CP-Glc) (25)	67
6.2.6 Tetraisopropyl Mono- and Difluoromethylenediphosphonate (39,40)	69
6.2.7 Mono- and Difluoromethylenediphosphonic acid (39a, 40a)	70
6.2.8 Diethyl C-(1-deoxy 2,3,4,6-tetra- <i>O</i> -benzyl- α -D-glucopyranosyl) difluoromethanephosphonate (41)	71
6.2.9 Ammonium C-(1-deoxy- α -D-glucopyranosyl)methane difluorophosphonate (36)	72
6.2.10 Diethyl C-(1-deoxy 2,3,4,6-tetra- <i>O</i> -benzyl- α -D-glucopyranosyl)methane thiophosphonate (49)	73
6.2.11 Ammonium C-(1-Deoxy- α -D-glucopyranosyl)methane thiophosphonate (37)	74
6.2.12 Diethyl tetraisopropyl methylenetrisphosphonate (52)	75
6.2.13 Diethyl C-(1-deoxy 2,3,4,6-tetra- <i>O</i> -benzyl- α -D-glucopyranosyl)methane bisphosphonate (53)	76
REFERENCES	78
APPENDIX 1. SELECTED NMR SPECTRA OF REPRESENTATIVE COMPOUNDS	83
(a) ^1H NMR spectrum of 25	83
(b) COSY NMR spectrum of 25	84
(c) ^{31}P NMR spectrum of 25	84
(d) $^{13}\text{C}\{^1\text{H}\}$ NMR spectrum of 25	85
(a) ^{13}C - ^1H HSQC spectrum of 25	85
(a) ^1H NMR spectrum of 41	86
(b) ^{31}P NMR spectrum of 41	87
(a) ^1H NMR spectrum of 49	88
(b) ^{31}P NMR spectrum of 49	89
(a) ^1H NMR spectrum of 53	90
(b) ^{31}P NMR spectrum of 53	91

LIST OF FIGURES

Figure 1: Sequence alignment of representative thymidyltransferases (A-D).....	2
Figure 2: Interactions between E _p and the nucleoside of the dTTP substrate.....	4
Figure 3: The position of the catalytic metal in the active site of E _p	5
Figure 4: Interactions between E _p and the glucose moiety in the sugar binding pocket ...	6
Figure 5: Structure of 3- <i>O</i> -alkyl- α -D-glucopyranosyl phosphates.....	9
Figure 6: Isosteric and non-isosteric analogues of natural phosphates.....	10
Figure 7: Comparison of sugar 1-phosphate vs. an isosteric sugar 1C-phosphonate	11
Figure 8: Bond angles and lengths of a phosphate versus a phosphonate	13
Figure 9: Structures of phosphono analogues of various sugar 1-phosphates	14
Figure 10: Structures of phosphono analogues of sugar 1-phosphates prepared for evaluation as substrates for Cps2L	23
Figure 11: Typical analytical RP-HPLC chromatograms for Cps2L assays	24
Figure 12: HPLC trace of preparative reaction of 25	25
Figure 13: Structures of four glucopyranose 1-boranophosphates evaluated as substrates for Cps2L	25
Figure 14: HPLC trace for the enzyme coupled reaction of disodium α -D-glucopyranosyl boranophosphate (31) and dTTP.....	26
Figure 15: ¹ H NMR of the attempted enzymatic reaction of 31 and dTTP.. ..	27
Figure 16: Structures of the five 2-deoxy-2-fluorosugars evaluated as substrates for Cps2L.....	29
Figure 17: ¹ H NMR spectrum displaying the enzyme-catalyzed reaction containing 32 and dTTP as substrates.....	30
Figure 18: ESI-MS/MS EPI scan data of enzyme-catalyzed production dTDP-2-deoxy- 2-fluoro- α -D-glucose (34).....	31
Figure 19: Structure of 36	32
Figure 20: Fluorinated phosphonates as phosphate isosteres and associated pK _{a2} values	33
Figure 21: Structure of 37	35
Figure 22: ESI-MS/MS EPI scan of the enzymatic coupling of 37 with dTTP.....	35
Figure 23: Michaelis-Menten and Lineweaver-Burk plots for the determination of apparent kinetic parameters	36
Figure 24: Summary of percent conversions to sugar nucleotide for tested substrates ...	39

Figure 25: Graphical summary of substrate conversions observed for the formation of sugar nucleotides by Cps2L	42
Figure 26: ³¹ P NMR spectrum of the reaction mixture for the fluorination of tetraisopropyl methylenediphosphonate	44
Figure 27: ³¹ P NMR spectrum displaying signals associated with the crude reaction mixture of 41	48
Figure 28: Structure of by-product 41a	48
Figure 29: ³¹ P NMR of 37 in D ₂ O following purification using cellulose chromatography	51
Figure 30: Structure of target compound 50	52
Figure 31: Structures of the proposed analogues of 1	55
Figure 32: Structures of the sugar nucleotides characterized by ESI-MS/MS	62
Figure 33: NMR spectra of purified phosphono analogue of dTDP- α -D-glucopyranose (25).....	83
Figure 34: NMR spectra of diethyl C-(1-deoxy 2,3,4,6-tetra- <i>O</i> -benzyl- α -D-glucopyranosyl) difluoromethanephosphonate (41)	86
Figure 35: NMR spectra of diethyl C-(1-deoxy 2,3,4,6-tetra- <i>O</i> -benzyl- α -D-glucopyranosyl) methane thiophosphonate (49).....	88
Figure 36: NMR spectra of diethyl C-(1-deoxy 2,3,4,6-tetra- <i>O</i> -benzyl- α -D-glucopyranosyl) methane bisphosphonate (50)	90

LIST OF TABLES

Table 1: Physical Properties of <i>O</i> - and <i>C</i> -glycosyl linkages.....	12
Table 2: Apparent kinetic parameters for Cps2L substrates with dTTP	37
Table 3: Comparison of retention times and percentage conversions to sugar nucleotides after 30 min and 24 h.....	41
Table 4: Retention times of NDP, NTP and thymidine standards	41
Table 5: Summary of reaction conditions for optimization of the fluorination methodology	46

LIST OF SCHEMES

Scheme 1: Mechanism of nucleotidyltransferases.	4
Scheme 2: Metabolite glycosylation.	11
Scheme 3: Synthesis of the phosphono analogue of α -D-glucose 1-phosphate	15
Scheme 4: Mercuriocyclusation favours C-pyranosyl formation.....	15
Scheme 5: Iodocyclization favours C-furanosyl formation.....	16
Scheme 6: Formation of phosphonate via the Michaelis-Arbuzov reaction	17
Scheme 7: Deprotection of benzyl ethers by iodotrimethylsilane.....	18
Scheme 8: Deprotection of diethyl phosphonate by iodotrimethylsilane.....	18
Scheme 9: Formation of enitols by stereoselective vinylation of pentoses.....	19
Scheme 10: Oxazolidine formation of the reaction of methylenetriphenylphosphorane with 2-acetamido-2-deoxy-3,4,6-tri-O-benzyl-D-glucopyranose	19
Scheme 11: Mercuriocyclusation of aminosugar derivatives	20
Scheme 12: Introduction of amino function after the phosphono function.....	20
Scheme 13: Formation of the phosphonate analogues of <i>N</i> -acetyl- α -D-mannosamine and <i>N</i> -acetyl- α -D-glucosamine 1-phosphate	21
Scheme 14: Synthetic strategy employed for the preparation of monofluoro (39) and difluoro (40) derivatives of tetraisopropyl methylenediphosphonate.	43
Scheme 15: General scheme for the synthesis of fluoro derivatives of 1	45
Scheme 16: Proposed Wittig reaction of difluoroolefin.....	49
Scheme 17: Dissociation mechanism of Lawesson's Reagent	50
Scheme 18: Thionation mechanism of Lawesson's Reagent.....	50
Scheme 19: Synthesis of α -D-glucose-1 C-thiophosphonate (37).....	51
Scheme 20: Synthesis of the trisphosphonate (52).....	53
Scheme 21: Oxidation of P(III) to P(V) species using hydrogen peroxide.....	53
Scheme 22: Synthesis of 'supercharged' analogue of 1 (53)	54
Scheme 23: Modified synthetic strategy for the preparation of 8	56
Scheme 24: Proposed synthesis of 'supercharged' analogues of 1	58

ABSTRACT

The study of many of glycosyltransferases is limited due to an inadequate access to sugar nucleotides. Preparation of sugar nucleotides through the use of nucleotidyltransferases with broad substrate specificities is gaining significant interest and offers high yields and stereospecificity. Physiologically, the glucose 1-phosphate thymidyltransferase catalyzes the condensation of α -D-glucose 1-phosphate and deoxythymidine triphosphate to yield deoxythymidine diphospho glucose. Exploiting and targeting these enzymes also has the potential of yielding new therapeutics.

Cps2L is a thymidyltransferase isolated from *Streptococcus pneumoniae*, with broad substrate flexibility. The substrate specificity of Cps2L was evaluated with new sugar 1-phosphate analogues to gain further insight into substrate and inhibitor requirements. Several sugar 1-phosphate analogues including sugar 1C-phosphonates (and analogues thereof), 2-deoxy-2-fluorosugar 1-phosphates, and glucopyranose 1-boranophosphates have been used to probe the sugar 1-phosphate modification tolerance of Cps2L. In addition, NMR spectroscopy was used to determine the anomeric stereochemistry of 2-deoxy-2-fluorosugars nucleotide products. For those substrates that were accepted by Cps2L, steady-state kinetic parameters were determined. The enzyme is able to almost equally form Michaelis complexes with different sugar substrates, whereas the turnover values for obtaining the corresponding sugar nucleotide were different. The evaluation of the substrate tolerance of Cps2L, as well as the synthesis of α -D-glucose-1C-thiophosphonate, a difluoro and a bisphosphono analogue of α -D-glucose 1C-phosphonate will be described.

LIST OF ABBREVIATIONS AND SYMBOLS USED

ADP	adenosine 5'-diphosphate
Araf	arabinofuranose
ATP	adenine 5'-triphosphate
Bn	benzyl
br.	broad
BuLi	butyllithium
calcd.	calculated
CDP	cytidine 5'-diphosphate
COSY	correlation spectroscopy
mCPBA	<i>meta</i> -chloroperoxybenzoic acid
CTP	cytidine 5'-triphosphate
CV	column volume(s)
d	doublet
DCM	dichloromethane
dd	doublet of doublet
DMF	<i>N,N</i> -dimethylformamide
dTDP	deoxythymidine 5'-diphosphate
dTTP	deoxythymidine 5'-triphosphate
eq	equivalent
EPI	enhanced product ion
ESI	electrospray ionization

Et	ethyl
EtOAc	ethyl acetate
EU	enzyme unit
Fuc	fucose
Gal	galactose
GDP	guanosine 5'-diphosphate
Glc	glucose
GT	glycosyltransferase
GTP	guanosine 5'-triphosphate
HPLC	high performance liquid chromatography
HRMS	high-resolution mass spectrometry
Hz	hertz
IC ₅₀	half maximal inhibitory concentration
<i>J</i>	coupling constant
<i>k</i> _{cat}	turnover number of an enzyme
<i>k</i> _{cat} / <i>K</i> _m	efficiency of an enzyme
KDA	potassium diisopropylamide
<i>K</i> _m	Michaelis constant
LC	liquid chromatography
LR	Lawesson's reagent
LRMS	low-resolution mass spectrometry
m	multiplet
Me	methyl

MeCN	acetonitrile
MeOH	methanol
MS	mass spectrometry
NaHMDS	sodium hexamethyldisilazide
NBS	<i>N</i> -bromosuccinimide
NIS	<i>N</i> -iodosuccinimide
NDP	nucleoside 5'-diphosphate
NFSI	<i>N</i> -fluorobenzenesulfonimide
NMR	nuclear magnetic resonance
NT	nucleotidyltransferase
NTP	nucleoside 5'-triphosphate
P	phosphate
PP _i	inorganic pyrophosphate
ppm	parts per million
q	quartet
R	organic substituent
R _f	retention factor
Rha	rhamnose
rt	room temperature
s	singlet
Selectfluor®	1-chloromethyl-4-fluoro-1,4-diazobicyclo[2.2.2]octane bis(tetrafluoroborate)
S _N 2	substitution nucleophilic bimolecular
THF	tetrahydrofuran

TLC	thin layer chromatography
TMSI	trimethylsilyl iodide
t_R	retention time
UDP	uridine 5'-diphosphate
UTP	uridine triphosphate
UV	ultraviolet
v/v	volume per unit volume
δ	chemical shift
ϵ	molar extinction coefficient
λ	wavelength

ACKNOWLEDGEMENTS

I would first like to thank my supervisor, Dr. David Jakeman, who has provided me with guidance and knowledge throughout the course of this work. Having had the opportunity to work in Dr. Jakeman's lab allowed me to develop my skills as a chemist and as a researcher. I would like to thank my enthusiastic lab mates, past and present, for many valuable discussions. Past colleagues include Ali Sadeghi-Khomami, Jessica Pearson, Cathy Graham, Patricia Jiang, Ishrat Jalal, and Zakia Biwas. Current members include, Steph Dupuis, Matt Loranger, Andrew Robertson, Thomas Veinot, Gaia Aish, Debabrata Bhattasali, and Erin Feldman. Thanks are due to these colleagues for providing a fun and stimulating lab environment.

I also wish to acknowledge my supervisory committee, Dr. Stephen Bearne, Dr. T. Bruce Grindley, who both taught me stimulating graduate courses in their respective fields. I also thank Dr. Norm Schepp for agreeing to be a third reader for my defense. I would also like to extend my thanks to Dr. Mike Lumsden and Dr. Kathy Robertson at the Nuclear Magnetic Resonance Research Resource (NMR-3) for training and advice, as well as Dr. Ray Syvitski for his assistance at the National Research Council Canada Institute for Marine Biosciences.

Special thanks are also due to my personal friends in chemistry at Dalhousie: Dan Beach, Aaron Rowe, Vincent Martin, Ben Tardiff, and Jon Moulins. I am also very much obliged to Eamonn Conrad for being an outstanding friend.

Lastly, I would like express my gratitude to my parents, Rod and Josepha Beaton, for their patience, support, and encouragement over the years. Finally, I would like to thank Claire Kanasewich, my best friend, who has supported me through this academic journey. Without these people, I would not have been able to reach the goals that I set out for myself.

CHAPTER 1 INTRODUCTION

1.1 Thymidyltransferases

A large number of nucleotidyltransferases (also known as sugar nucleotide (NDP-sugar) pyrophosphorylases) are found in nature, with an estimated 14,000 nucleotidyltransferase sequences in GenBankTM.¹ One class of nucleotidyltransferases known as a glucose 1-phosphate thymidyltransferases are found in many bacterial species. Protein sequences from 46 different bacterial sources show homology to the glucose 1-phosphate thymidyltransferase from *Salmonella enterica* (RmlA) and are involved in catalysing the first step of the rhamnose biosynthetic pathway.² The enzyme has a molecular weight of 32 kDa and catalyzes both the biosynthesis of dTDP-Glc, as well as its pyrophosphorylysis³ according to the following chemical reaction:



The superfamily of nucleoside triphosphate enzymes includes a number of bacterial thymidyltransferases, including RmlA (*Streptococcus mutans*), Cps2L (*Streptococcus pneumoniae* R6); uridylyltransferases, such as yeast UDP-glucose pyrophosphorylase⁴ and adenylyltransferases like GlgC.⁵ All of these nucleotidyltransferases possess the same essential catalytic residues, assume the same general fold,⁶ and require the presence of a divalent metal cation cofactor (Mg^{2+}). The necessity of the Mg^{2+} , the homology, and similar fold provides good evidence that all of these aforementioned nucleotidyltransferases act by a common mechanism.⁷

1.2 Homology

A sequence alignment (ClustalW) comparing four representative thymidyltransferases

is shown in Figure 1. With respect to Figure 1, **A-C** have been previously cloned and studied in the Jakeman laboratory, whereas **D** is the thymidyltransferase most characterized in the literature. The sequence alignment compares the amino acid sequences in such a way as to uncover structural, functional, and evolutionary relationships. All of the sequences shown in the figure have overall amino acid identity of greater than 60%. The sequence homology between enzymes from one biochemical pathway to enzymes in other species is particularly striking (88% identity between Cps2L in *Streptococcus pneumoniae* and RmlA in *Streptococcus mutans* RmlA). Thus deductions made involving one enzyme will likely have similar implications for enzymes from other organisms.⁸ This strongly implies that substrate acceptance (or inhibition) of one specific enzyme may result in similar substrate acceptance (or inhibition) of many other homologs and is of critical significance in developing broad-spectrum antibiotics.

```

CLUSTAL 2.0.12 multiple sequence alignment

A_F.aeruginosa_RmlA      MK-RKGIILAGGSGTRLHPATLAISKQLLPVYDKPMIYYPLSTLMLAGIREILIIISTPQD 59
D_S.enterica_Ep         MKTRKGIILAGGSGTRLYPVTMAVSKQLLFIYDKPMIYYPLSTLMLAGIRDILIIISTPQD 60
B_S.pneumoniae_Cps2L    ---MKGIILAGGSGTRLYPPLTRATSKQLMPVYDKPMIYYPLSTLMLAGIKDILIIISTPQD 57
C_S.mutans_RmlA        ---MKGIILAGGSGTRLYPPLTRAASKQLMPVYDKPMIYYPLSTLMLAGIKDILIIISTPQD 57
                        *****:* * * * * :*****:*****:*****:*****:*****:*****:

A_F.aeruginosa_RmlA      TFRFQQLLGDGGSNWGLDQYAVQPSFDGLAQAFIIGESFIGNDLSALVLDGDNLYYGHDFH 119
D_S.enterica_Ep         TFRFQQLLGDGGSQWGLNLQYKVPQSPFDGLAQAFIIGEEFIGHDDCALVLDGDNIFYGHDLF 120
B_S.pneumoniae_Cps2L    LFRFKDLLLDGSEFGIRLSYAEQPSFDGLAQAFIIGEDFIGDSDVALILGDNIIYHGPGLS 117
C_S.mutans_RmlA        LFRFKELLQDGSEFGIKLSYAEQPSFDGLAQAFIIGEEFIGDDHVALILGDNIIYHGPGLS 117
                        *****:*****:* * * * * :*****:*****:*****:*****:*****:

A_F.aeruginosa_RmlA      ELLGSASQRQTGASVPFAYHVLDPERYGVVVEFDQGGKAISLEEKPLEPKSNYAVTGLYFYD 179
D_S.enterica_Ep         KLMEAAVNKESGATVPFAYHVNDPERYGVVVEFDQKGTAVSLEEKPLQPKSNYAVTGLYFYD 180
B_S.pneumoniae_Cps2L    KMLQKTVSKKSGATVPFGYQVNDPERFQVVEFDENMNAISIEEKPECPKSNYAVTGLYFYD 177
C_S.mutans_RmlA        RMLQKAASKESGATVPFGYQVNDPERFQVVEFDNDRNAISIEEKPEHPKSHYAVTGLYFYD 177
                        :.. : ..:*****:* * * * * :*****:*****:*****:*****:*****:

A_F.aeruginosa_RmlA      QQVVDIARDLKPSFRGELEITDVNRAYLERGQLSVEIMGRGYAWLDTGTHDSLLEAGQFI 239
D_S.enterica_Ep         NSVVEMAKNLKPSARGELEITDINRIYMEQGRLSVAMMGRGYAWLDTGTHQSLIEASNFI 240
B_S.pneumoniae_Cps2L    NDVVEIAKSIKPSARGELEITDVNKAYLDRGNLSVEVMGRGFPAWLDTGTHESLLEASQYI 237
C_S.mutans_RmlA        NSVVDIAKNIKPSFRGELEITDVNKAYLDRGDLSEVVMERGFPAWLDTGTHESLLEAAQYI 237
                        :.*****:*****:*****:*****:*****:*****:*****:*****:*****:

A_F.aeruginosa_RmlA      ATLENRQGLKLVACFEEIAYRQKWIDAAQLEKLAAPLAKNGYGYQLKRLLTETVY 293
D_S.enterica_Ep         ATIEERQGLKLVSCFEEIAYRKNFINAQVIELAGPLSKNDYKGYLLKMKVGL-- 292
B_S.pneumoniae_Cps2L    ETVQRMQNQVANLEEIAYRMGYISREDVLELAQPLKKNYEGQYLLRLIGEV-- 289
C_S.mutans_RmlA        ETVQRMQNQLQVANLEEIAYRMGYITADQVRELAQPLKKNYEGQYLLRLRIGEA-- 289
                        *..* .:..* : *****: * * * * * : : : * * * * * * * * * * * : : :

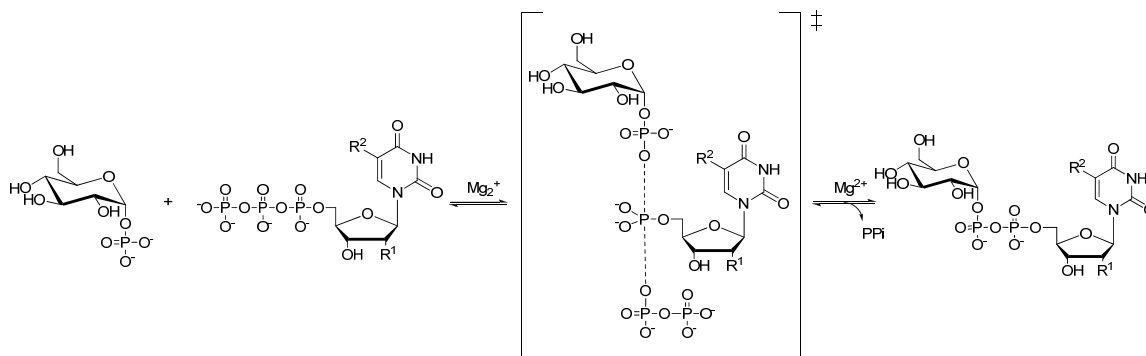
```

Figure 1: Sequence alignment of representative thymidyltransferases (**A-D**), where “*” indicates that the residues in that column are identical, “:” indicates that conserved substitutions have been observed, and “.” indicates that semi-conserved substitutions are observed.

1.3 Enzymatic Mechanism

Analysis of the crystal structures of a thymidyltransferase isolated from *Pseudomonas aeruginosa* complexed with its substrate and product⁸ have given insight into the proposal of an ordered Bi Bi reaction mechanism. This mechanism involves dTTP binding non-covalently to the enzyme active site first, followed by binding of glucose 1-phosphate and then nucleophilic attack of glucose 1-phosphate on the dTTP α -phosphate group, resulting in the release of inorganic pyrophosphate (PP_i), followed by dTDP-glucose. The active site of the enzyme accommodates the mutual positioning of the first substrate relative to the second one.⁸ This hypothesis is in agreement for kinetic studies involving the same enzyme.³ Additionally, Frey and co-workers⁹ proposed a single-displacement mechanism for the whole nucleotidyltransferase family. The evidence for this came from a study involving a UDP-glucose pyrophosphorylase which revealed that the α -phosphate of the UTP possessed an inverted geometry upon attack by Glc-1-P.

This was explicitly stated more recently by Thorson and co-workers¹⁰ who suggested that the phosphoryl oxygen nucleophile of Glc-1-P directly attacks, in an S_N2 fashion, the α -phosphate of dTTP. In turn, this would result in the simultaneous formation and cleavage of the phosphodiester bonds on opposite sides of the α -phosphate atom. Thus, catalysis occurs via the formation of a trigonal bipyramidal phosphoryl transition state in which the nucleophile and the leaving group (pyrophosphate) occupy apical positions around the trigonal bipyramidal α -phosphorus atom with concurrent accumulation of negative charge on the oxygen atoms bound to phosphorus (Scheme 1).



Scheme 1: Mechanism of nucleotidyltransferases. R¹=H and R²=CH₃ (dTTP) for thymidyltransferases; and R¹=OH and R²=H (UTP) for uridylyltransferases¹²

1.3.1 Crystallographic Studies of Enzyme-Substrate Interactions

Of late, the three-dimensional structures of four mesophilic glucose 1-phosphate thymidyltransferases have been reported. These include RmlA, named E_P, from *Salmonella enterica* LT2,¹⁰ RmlA3 from *Pseudomonas aeruginosa*,⁸ RffH and RmlA from *Escherichia coli*.^{2,7}

Thorson and co-workers¹⁰ probed the substrate specificity of *Salmonella enterica* LT2 *rmlA* encoded thymidyltransferase, E_P, in which dTTP and UTP are readily accepted as substrates while CTP is not. Hydrogen bonds are formed between an active site residue (Gln 83) and the exocyclic N-3 and O-4 ring atoms of deoxythymidine and uridine (Figure 2). Moreover, hydrogen bonds between the O-4

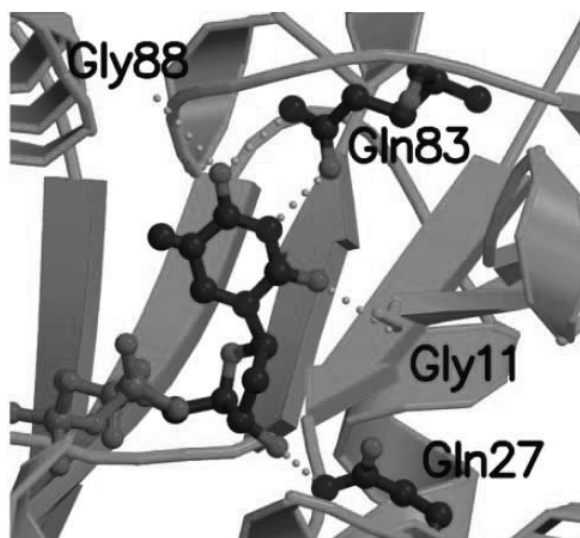


Figure 2: Interactions between E_P and the nucleoside of the dTTP substrate.¹⁰

and the main chain nitrogen residue (Gly 88) are observed as well as between O-2 and the main nitrogen chain of another active site residue (Gly 11). Hydrogen bond formation between the 3'-hydroxyl group of the ribose and Gln 27 was reported. These interactions are of great consequence to the binding of the nucleoside triphosphate. CTP is a poor substrate because it lacks these favourable interactions, but also possesses unfavourable interactions between the amino group at position four and two active site residues (Gln 83 and Gly 88). In addition to hydrogen bonds, a large number of van der Waals interactions are observed when dTTP is the substrate, with all cumulating in a hydrophobic “bed” for the nucleoside. The pocket of the active site allows for pyrimidine bases to fit without difficulty, but purine bases do not fit this pocket as well because they are too big. With regards to the acceptance of UTP as an alternative substrate, UTP is bound with interactions that are similar to dTTP as a result of structural similarities. Additionally, since there is no specific interaction with the methyl group of the thymidine ring, and a pocket for the 2-OH of ribose exists, UTP has been observed to be an excellent alternative substrate for the enzyme.¹⁰ The phosphate groups of the dTTP substrate are held in place by a number of interactions including interactions with a divalent metal cofactor, Mg²⁺ (Figure 3).

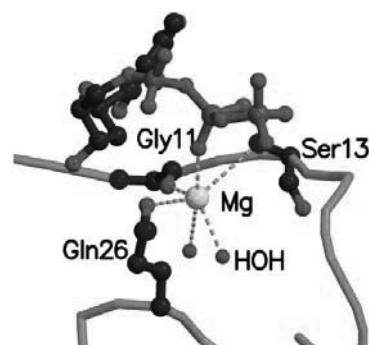


Figure 3: The position of the catalytic metal in the active site of E_p.¹⁰

As for the glucose moiety, the hydroxyl groups at positions 2, 3, and 4 interact directly with the enzyme active site through hydrogen bonds, while the hydroxyl group at position 6 is bound to the enzyme by a water molecule (Figure 4). A total of four water molecules form a bridge between the glucose moiety and the enzyme, E_p.¹⁰ A number of

active site residues also contribute to van der Waals interactions with the base of the hexose ring. Another set of residues creates a closure for the glucose binding pocket, which prevents disaccharides and other bulky sugars from binding. E_p (as well as a number of other thymidyltransferases) possess broad sugar substrate specificity.¹⁰⁻¹⁵ One major factor that contributes to this is that the O-6 of the glucose does not

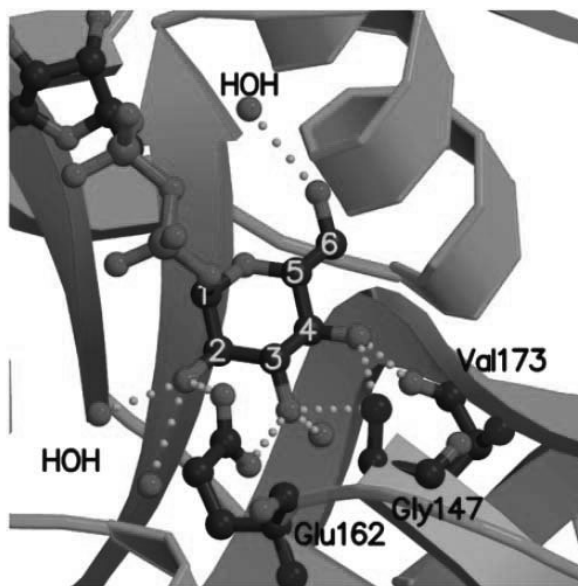


Figure 4: Interactions between E_p and the glucose moiety in the sugar binding pocket¹⁰

come into direct contact with the enzyme, thus allowing for various substituents at position 6.

Additional insight into the substrate specificity of thymidyltransferases can be obtained from the crystal structure of a homologous nucleotidyltransferase, RmlA from *Pseudomonas aeruginosa*, bound to the product dTDP-glucose.⁸ Adjacent to the active site of the enzyme, a pocket is present which permits the binding of substrates containing unnatural (and extended) functional groups from the C3-OH of the glucose moiety. This pocket has also been observed in the crystal structure of the RmlA with dTDP- β -L-rhamnose. Based on these observations, the enzymatic preparation of lipophilic sugar nucleotides using a series of 3-O-alkyl sugar 1-phosphates has been described.¹² Furthermore, crystal structures of RmlA in complex with its substrates, as well as with dTDP- β -L-rhamnose (an inhibitor), reveals that substrates and the inhibitor bind at the

catalytic site. The location of the phosphate groups differ between the substrate and inhibitor complexes, especially the interaction between the β -phosphate of dTDP- β -L-rhamnose and the R194 residue in the inhibitor complex.^{3,8} This observation suggests a strategy for development of inhibitors by targeting increased hydrogen bonding interactions with residue R194.

1.3.2 Role of the Divalent Metal Cation

All nucleotidyltransferases require the divalent metal cation, Mg^{2+} .⁷ The activity of the enzyme strongly depends on the presence of Mg^{2+} ; the role of the cation is to stabilize the departure of PP_i , which results as a by-product.¹⁶ Not only does Mg^{2+} act through electrostatic stabilization of the PP_i , but also works by coordinating the region of the enzyme responsible for substrate binding. This provides the most favourable position for the NTP during catalysis.

1.3.3 Substrate Specificities

Several reports have demonstrated that both prokaryotic and eukaryotic nucleotidyltransferases possess broad *in vitro* substrate specificity for sugar 1-phosphates.^{1,4,11,13,17} This has been expanded upon in several of these studies to utilize RmlA's broad sugar 1-phosphate tolerance to enzymatically synthesize a large collection of dTDP- and UDP-based sugar nucleotide libraries; in some instances, structure-based engineering was beneficial.^{10,15,18} Impressively, more than 30 different sugar 1-phosphates have been described as being substrates for RmlA as well as mutants of RmlA.¹ Provided that the sugar substrate resembles glucose 1-phosphate, a wide number

of wild-type thymidyltransferases are capable of accepting dTTP and UTP as nucleotide substrates, without a significant discrepancy in yields.

In comparison to a number of characterized nucleotidyltransferases with promising substrate flexibility, for example thermostable UDPG-PPase (*Pyrococcus furiosus* DSM 3638),¹⁹ and E_p (*Salmonella enterica* LT2),^{14,20} Cps2L (as well as RmlA and RmlA3) exhibits higher flexibility towards tolerating variant sugar 1-phosphates and nucleoside triphosphate substrates *in vitro*.¹¹ In addition, the high conversions to product catalyzed by Cps2L demonstrates the potential synthetic utility of the enzyme. The physiological sugar substrate, glucose 1-phosphate, upon incubation with either dTTP or UTP, results in excellent conversions to their respective NDP-sugars. This indicates that Cps2L readily accepts UTP as an alternative nucleoside triphosphate substrate with glucose 1-phosphate. In addition, glucosamine 1-phosphate displays similarly high yielding conversions with dTTP and UTP. Cps2L also produces ADP-Glc, CDP-Glc, and GDP-Glc in reasonable conversions using the appropriate nucleoside triphosphate.

With dTTP as a substrate, Cps2L readily accepts the largest number of alternative α -sugar substrates including galactose 1-phosphate, mannose 1-phosphate, and *N*-acetyl glucosamine 1-phosphate. Other sugar substrates that have been accepted by Cps2L include furanosyl sugars¹³ and 3-*O*-alkyl glucose 1-phosphate substrates.¹² In the case of furanosyl 1-phosphates with dTTP, conversion was observed but to a lesser extent than those observed for the physiological reaction with glucopyranose 1-phosphate, as well as other hexopyranosyl 1-phosphates. A plausible reason for the lower conversions may be the lack of optimal interactions within the binding site of Cps2L for furanosyl 1-phosphates. Determination of kinetic parameters for Cps2L with respect to α -D-Glc 1-P

and β -L-Araf 1-P revealed the fact that both sugar substrates have similar affinity in terms of binding to Cps2L ($K_m = 139 \mu\text{M}$ and $90 \mu\text{M}$, respectively) but the furanosyl substrates experience significantly more sluggish reactivity ($k_{\text{cat}} = 27.6 \text{ min}^{-1}$ and 0.00218 min^{-1} , respectively). With respect to the alkyl sugar phosphates (Figure 5) being coupled to dTTP, quantitative conversions were observed. However, the lengthier alkyl chain derivatives took longer to convert to product in comparison to the shorter chain derivatives. Likewise, bulkier substrate analogues also appear to be accommodated for by Cps2L in which branched chain sugar derivatives were readily converted to product.

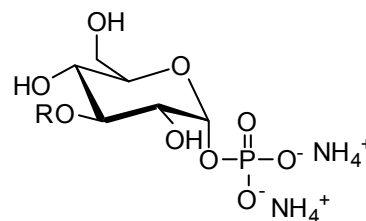


Figure 5: Structure of 3-*O*-alkyl- α -D-glucopyranosyl phosphates
 $R = (\text{CH}_2)_n\text{CH}_3$, $n = 0, 3, 5, 7, 11, 15$

These substrates were reported to have increased $\text{p}K_{\text{a}2}$ values (increase of 0.6 units) due to the inductive donating effect of the alkyl group onto the sugar 1-phosphate.¹² This decrease in the acidity of the phosphate does not show any indication of impeding the catalytic action of the enzyme. However no catalytic parameters were determined for the 3-*O*-alkyl-glucose 1-phosphates and so it is difficult to obtain further insight.

CHAPTER 2 PHOSPHONATES AS PROBES FOR ENZYMES

For many years, carbohydrates have been a source of great scientific interest because of their abundance in nature, and due to the synthetic challenges brought upon by their polyhydroxylated structures.²¹ It is well known that glycosyl phosphates play a key part in the metabolism of carbohydrates. Glycosyl phosphates are the primary metabolic precursors, and are precursors of glycosyl donors involved in the biosynthesis of glycoconjugates.²² Glycosyl phosphates have been demonstrated to be regulators of metabolic processes in some cases.²² Glycosyl phosphates are important in glycosylation, either as substrates in non-Leloir pathways, or indirectly as precursors to nucleoside diphosphates in the Leloir pathway.

A prominent drawback to the use of *O*-glycosyl phosphates to study carbohydrate mediated interactions is that they are potential substrates as a result of the labile phosphate linkage or their inability to withstand acidic and basic conditions. To overcome these issues of stability, phosphonates, structural mimics of phosphates, can be synthesized and studied. A number of drugs have been developed that contain phosphonates including clinical antiretroviral²³ and osteoporosis drugs.²⁴

There are two distinct classes of phosphonates that can be prepared. The first class, known as isosteric analogues, involves the phosphoester oxygen being replaced by

one carbon atom. On the other hand, non-isosteric phosphonates entail either the complete removal of the bridging oxygen or its replacement by two or more carbon atoms. Figure 6 shows an isosteric

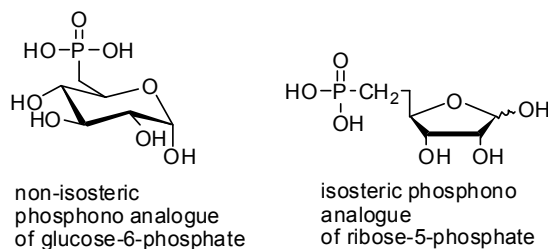
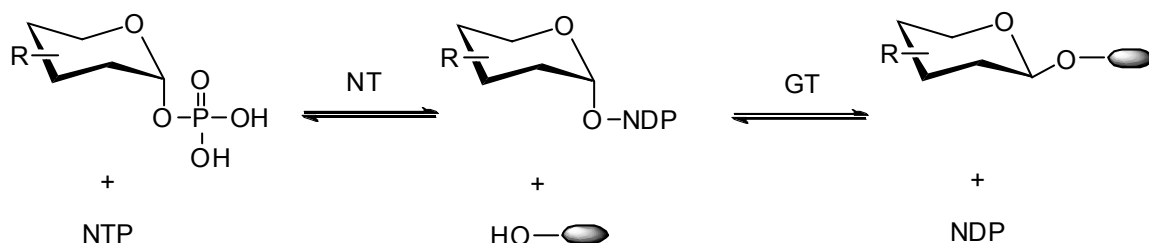


Figure 6: Isosteric and non-isosteric analogues of natural phosphates

analogue of ribose-5-phosphate and an non-isosteric analogue of glucose 6-phosphate.²⁵

The importance of isosteric phosphono analogues of pyranosyl 1-phosphates stems from their chemical and biological relevance. The substitution of the glycosidic oxygen by a methylene unit gives rise to compounds containing a non-hydrolyzable ‘pseudoglycosidic’ linkage. As a consequence, these compounds may act as inhibitors of carbohydrate processing enzymes. It is known that glycosyltransferases reversibly^{26,27} catalyze the transfer of a donor sugar to an acceptor substrate with simultaneous release of a pyrophosphoryl unit, typically in the form of a nucleoside diphosphate (Scheme 2).²⁸



Scheme 2: Metabolite glycosylation. NT = nucleotidyltransferase, GT = glycosyltransferase, NTP = ATP, CTP, GTP, dTTP, UTP; NDP = ADP, CDP, GDP, dTDP, UDP

The facility of controlling glycosylation by developing glycosyltransferase inhibitors, such as phosphonate sugars, could provide a variety of new classes of enzyme inhibitors (Figure 7).²⁹ This would result in a non-hydrolyzable C-glycosidic phosphonate

nucleotide that may act as a competitive inhibitor. The phosphono analogue of UDP-GlcNAc has recently been shown to

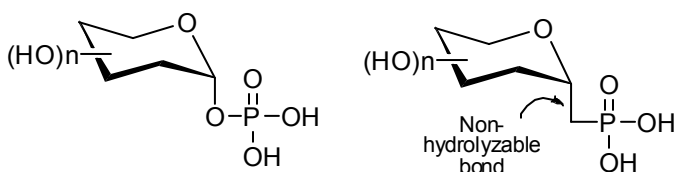


Figure 7: Comparison of sugar-1-phosphate vs. an isosteric sugar-1C-phosphonate

be a competitive inhibitor of *N*-acetylglucosaminyltransferase I (GnT I).³⁰

2.1 O-Glycosides vs. C-Glycosides: Comparisons of Physiochemical Properties

The substitution of a methylene unit for an oxygen atom results in a modification in both the electronic properties, as well as the size of the glycosyl linkage, when comparing a native *O*-glycosyl phosphate with its phosphonate analogue (Figure 7, Table 1).

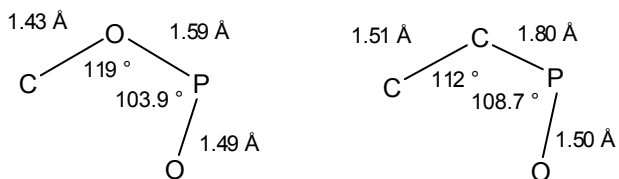
Table 1: Physical Properties of *O*- and *C*-glycosyl linkages²¹

Property	Oxygen	Carbon
van der Waals radius	1.52 Å (ether)	2.0 Å (methylene)
hydrogen bonding	acceptor	none
electronegativity (Pauling values)	3.51	2.35
dipole moment	0.8 D (C-O)	0 D (C-C)

The size and electronic properties of a glycosyl linkage are altered when a methylene group is substituted for an oxygen atom.²¹ In turn, *C*- and *O*-glycosides largely differ from one another with regards to their chemical reactivities. Table 1 shows that *C*-glycosides have moderately more steric hindrance, significantly less hydrogen bonding ability and fewer dipole interaction capabilities. This may result in the loss of binding functions of the esterified phosphate oxygen, and could create a variation in biological or physiological activity. Despite these differences, *C*-glycosides have an important role in protein-ligand studies.³¹ Overall the conformational similarity of *C*-glycosides to their parent compounds in solution is more important than the above differences. Additionally, the *O*-linkage is better solvated in an aqueous environment than the *C*-linkage because of its dipole moment and hydrogen bonding ability. Thus, the more hydrophobic *C*-glycoside will have a larger entropic advantage for interaction with protein acceptors.³²

Phosphonate analogues are capable of fitting into the active sites, as well as the receptors, of the parent phosphates. This is attributed to the fact that the geometry of the

phosphate is not significantly varied by the replacement of the phosphoester oxygen with a carbon atom (Figure 8).³³ The phosphonate analogue has slightly longer bond lengths (10%) between the



C-C-P in contrast to the bond lengths of C-O-P. In addition, the bond angles associated with the C-C and the C-P of phosphonates are marginally smaller (6%) than those of the C-O and the O-P of the corresponding phosphate.³³ Another advantage of phosphonates is that the cleavage of the carbon-phosphorus bond (the main enzymatic transformation) cannot occur which often results in an enzymatic process being inhibited.³⁴

In regards to the acidity of the compounds, the substitution of the methylene unit, an electron-donating alkyl group, for the exocyclic oxygen results in a significant decrease in the acidity of the resultant phosphorus acid functional group.³⁵ With this change, the analogue will likely possess a different state of dissociation with respect to the naturally occurring phosphate at physiological pH. The second pK_a is of interest for both the phosphonate and the physiological phosphate as they are near physiological pH, whereas the first pK_a is around 2. A study examining the effect of primary alkyl groups attached to phosphorus on their pK_{a2} 's revealed them to be within the range of 7.7-8.2.³³ Additional branching of the alkyl group resulted in a decrease of acidity. This decrease in acidity for the addition of a methylene unit is also apparent for the phosphono analogue of α -D-glucose 1-phosphate in which its pK_{a2} was half a unit higher than the physiological substrate (7.0 vs. 6.4).^{36,37}

2.2 Synthesis of the Phosphono Analogue of Glucose 1-Phosphate

The first synthesis of a phosphono analogue of a glycosyl phosphate occurred in 1981.³⁸ The key step involved in the synthesis is the carbon chain extension. The formation of the new C-C bond involves the reaction of either a Wittig reagent or an organometallic reagent which will be discussed in 2.2.1 and 2.3, respectively.

As a consequence of the difficulties associated with the direct introduction of the methylenephosphonic acid group at the anomeric centre of the sugar, indirect methods have been made available. These indirect synthetic procedures typically involve introducing the phosphonic acid group to an electrophilic carbon atom that was previously obtained by carbon chain extension. Thus, the preparation normally follows the creation of a *C*-glycoside, followed by the conversion of the *C*-glycosidic carbon atom into a halide, and finally its conversion into a phosphonate by the Arbuzov reaction and removal of the protecting groups.

Many phosphono analogues of sugar 1-phosphates have been prepared by forming a *C*-glycosyl halide and reacting it with a trialkylphosphite. Those phosphono analogues that have been prepared in this manner include the phosphono analogue of α -D-glucose 1-phosphate (**1**),^{17,39} α -D-galactose 1-phosphate (**2**),^{17,40} α -D-mannose 1-phosphate (**3**),⁴¹ and α -L-rhamnose 1-phosphate (**4**)^{42, 43} (Figure 9).

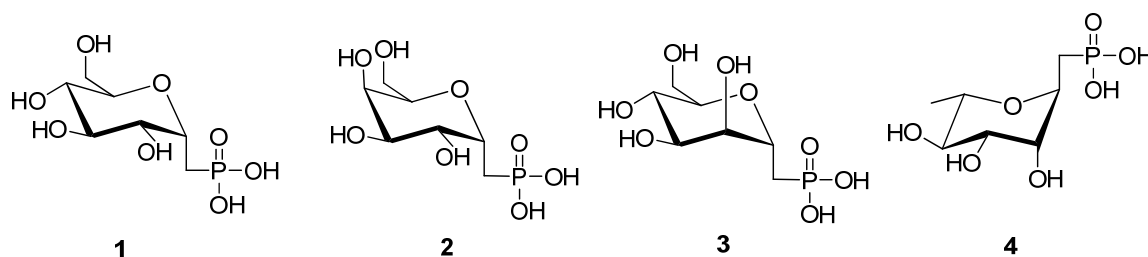
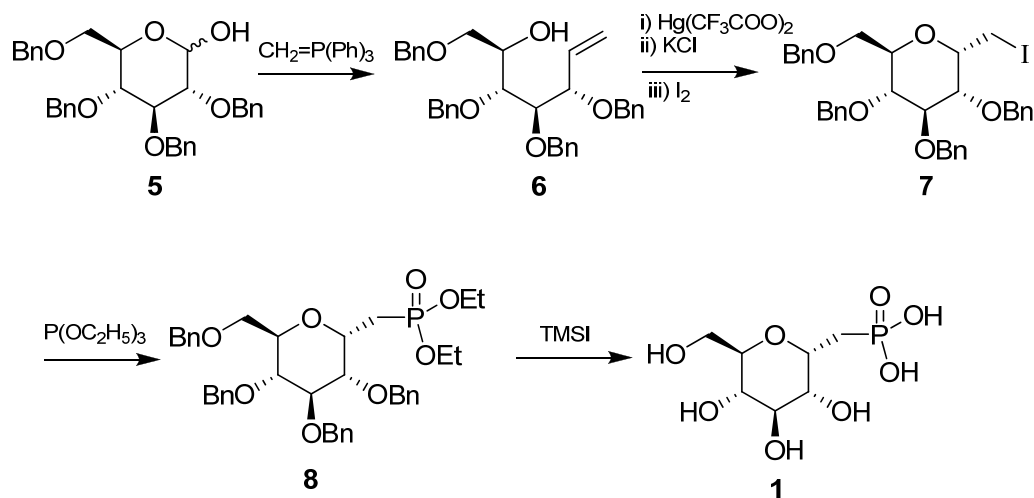


Figure 9: Structures of phosphono analogues of various sugar 1-phosphates

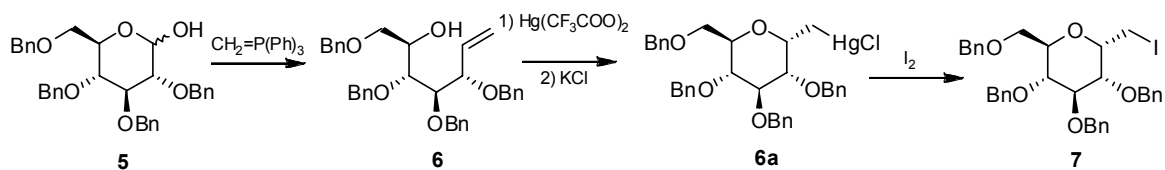
Most of the reported syntheses require the use of *C*-glycosyl halides (via a Wittig chain extension, mercuriocyclization, and iodination) which undergo the Arbuzov reaction with trialkyl phosphite to afford the related phosphonate. The steps associated with this method for the preparation of the phosphono analogues of α -D-glucose 1-phosphate^{17, 39} (Scheme 3) will be discussed in 2.2.1 and 2.2.2.



Scheme 3: Synthesis of the phosphono analogue of α -D-glucose 1-phosphate^{39, 44}

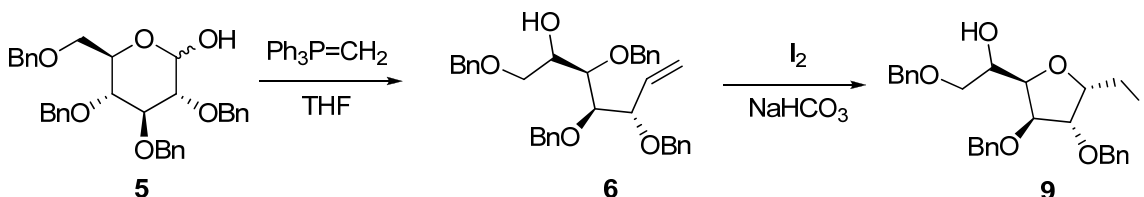
2.2.1 Synthesis of *C*-Glycosyl Halides

C-glycosyl halides have been stereoselectively synthesized by different *C*-glycosylation methods. One of the more expedient methods involves the mercuriocyclization of the unsaturated glycoenitol derivative (**6**), obtained by conducting a Wittig reaction with methylenetriphenylphosphorane ($\text{Ph}_3\text{PMeBr}^-$, BuLi) and commercially available 2,3,4,6-tetra-*O*-benzyl-D-glucopyranose (**5**) (Scheme 4).⁴⁵ The stereospecific



Scheme 4: Mercuriocyclisation favours *C*-pyranosyl formation

mercuriocylation of the glycoenitol yields mercurio derivative **6a**. The activation of the double bond by electrophiles such as iodine⁴⁶ and mercury salts^{45, 47} promotes the cyclization. The *C*-glycosyl-mercurioderivatives are acquired stereoselectively with a 1,2-*cis* arrangement. In the case of electrophilic activation by iodine, the benzyloxy functionality is a nucleophilic competitor for the free hydroxyl group. This favours the formation of five-membered rings over six-membered rings. Generally, mercuriocylation favours *C*-pyranosyl generation while iodocyclisation favours *C*-furanosyl formation (e.g. **9**) (Scheme 5).⁴⁶ The subsequent halide can be then easily obtained through by treating the derivative with I₂, Br₂, NBS, or NIS. In the case of glucose, the mercurioderivative (**6a**) is converted into the corresponding iodide (**7**), which is then subjected to an Arbuzov reaction.

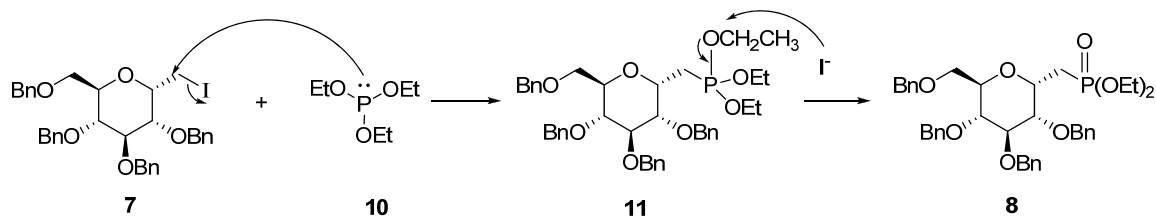


Scheme 5: Iodocyclization favours *C*-furanosyl formation

2.2.2 Conversion of *C*-Glycosyl Halides into Phosphonates

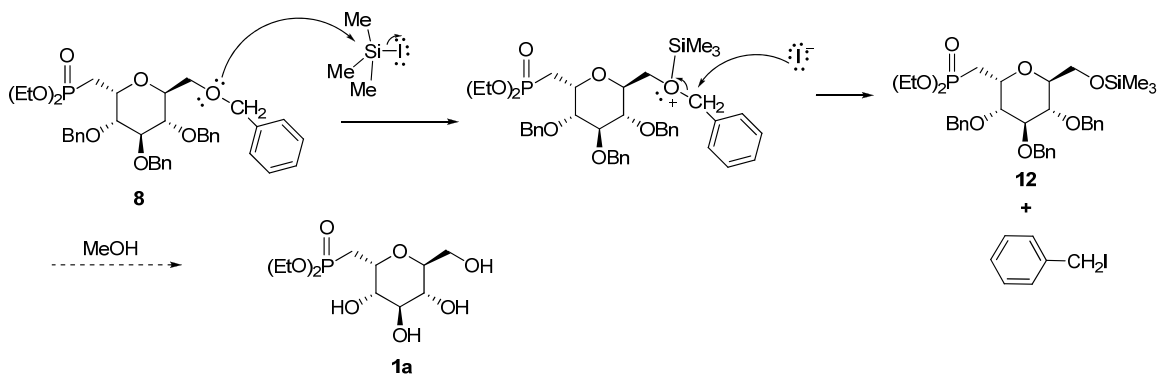
In order to obtain the related phosphonate, the *C*-glycosyl halide is treated with a phosphate via the Arbuzov reaction. Steric hindrance of both the halide and the phosphite influence the yield of phosphonate. The impending conversion to the free phosphonic acid from the phosphonic ester is conventionally simplified with phosphites such as tris(trimethylsilyl)phosphite as well as ethyl diphenyl phosphite. However, lower yields are associated with these phosphites due to their steric hindrance.

The Michaelis–Arbuzov reaction (Scheme 6) is initiated with the S_N2 reaction of the nucleophilic phosphite (**10**) with the electrophilic *C*-glycosyl halide (**7**) to give a phosphonium intermediate (**11**). The displaced halide anion reacts via another S_N2 reaction with the phosphonium intermediate to give the desired phosphonate (**8**) and another alkyl halide ($\text{CH}_3\text{CH}_2\text{I}$).



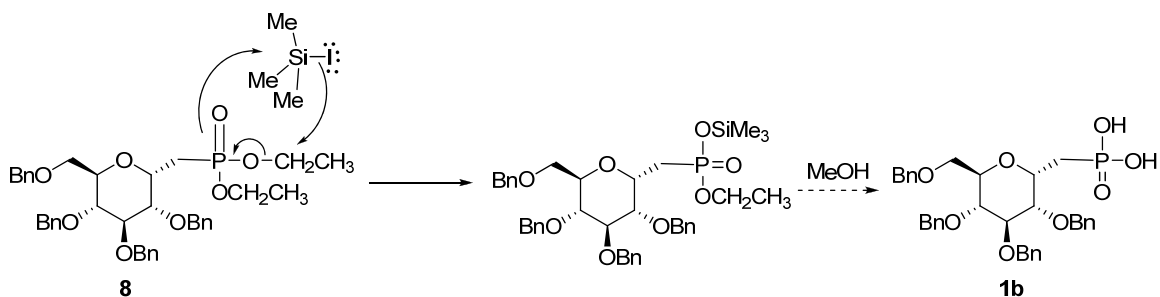
Scheme 6: Formation of phosphonate via the Michaelis-Arbuzov reaction

The completion of the synthesis of the phosphono analogue of α -D-glucose 1-phosphate is accomplished by the treatment of **8** with iodotrimethylsilane. This treatment converts the phosphonate ester into a bis(trimethylsilyl) ester which upon hydrolysis yields the free acid form and concomitantly cleaves the benzyl protecting groups. The mode of action for the deprotection varies depending on functional group that is involved (i.e. ether vs. ester). With respect to the cleavage of the benzyl protecting groups (Scheme 7), the silicon atom coordinates with the oxygen atom, while the iodide attacks the methylene carbon associated with the benzyl group. In turn, the ether oxygen is converted into a good leaving group. The leaving group is then displaced by the iodide ion to form an iodoalkane and an alkyl silyl ether (**12**). This silyl ether then undergoes solvolysis with methanol yielding the unprotected sugar (**1a**).



Scheme 7: Deprotection of benzyl ethers by iodotrimethylsilane

With regards to the deprotection of the ethyl esters of the phosphonate, the deprotection occurs via the formation of phosphonium ion intermediates (Scheme 8). The final alkyl silyl phosphoester is also cleaved via solvolysis with methanol leading to the formation of the free acid form of the phosphonate (**1b**).

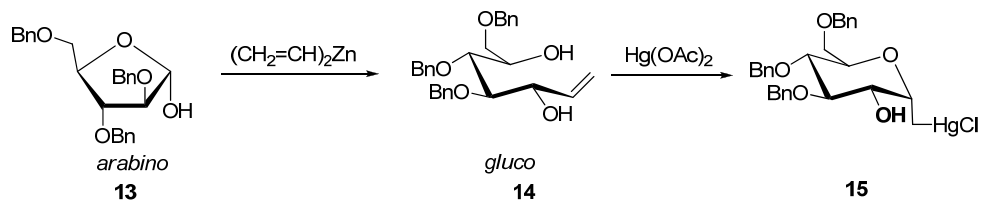


Scheme 8: Deprotection of diethyl phosphonate by iodotrimethylsilane

2.3 Alternative Methods for the Synthesis of Phosphono Mimics

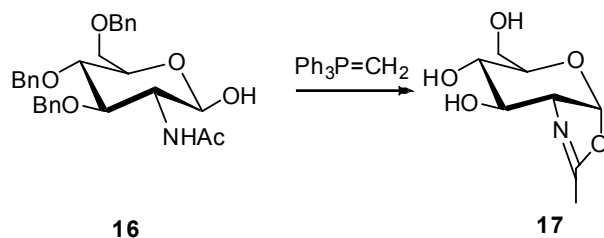
Though it is an expeditious route to the formation of glycoenitols, the exploitation of the Wittig reaction of the aldose with methylenetriphenylphosphorane is not universal. The Wittig reaction may give low yields,^{47, 48} and in some cases it causes an epimerization at C-2 of the starting sugar.⁴⁸ In addition, this route has had no success for aminosugars such as D-glucosamine and its derivatives.²⁵ One option that has been explored to

overcome this drawback is through the vinylation of an aldose (Scheme 9).⁴⁹ When divinylzinc is used as a vinyllating agent with an aldose one carbon shorter than that desired (**13**), the stereochemistry of the reaction can be controlled resulting in the desired glycoenitol (**14**). Mercuriocyclization of the obtained glycoenitols stereoselectively affords the *C*-glycosyl mercurio-derivatives (**15**) with the corresponding 1,2-*cis* relationship. An attractive aspect of the *C*-glycosides obtained via this method is that the hydroxyl group at C-2, derived from the starting sugar's carbonyl group, is the only one deprotected. As a result, the deprotected hydroxyl group may be altered to obtain 2-amino, 2-fluoro, or 2-deoxy-*C*-glycosides. Thus a variety of tri-*O*-benzyl-D-pentoses can be used to stereoselectively obtain the desired products.



Scheme 9: Formation of enitols by stereoselective vinylation of pentoses

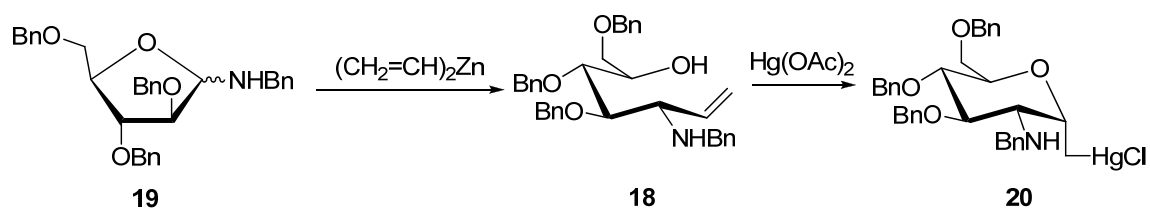
Preparation of phosphono analogues of *N*-acetyl- α -D-glucosamine 1-phosphate are of interest due to their potential biological activities including interfering in the formation of bacterial cell walls.⁵⁰ As previously stated, the synthesis of *C*-glycosides and *C*-glycosyl halides of D-glucosamino derivatives have been



Scheme 10: Oxazolidine formation of the reaction of methylenetriphenylphosphorane with 2-acetamido-2-deoxy-3,4,6-tri-*O*-benzyl-D-glucopyranose

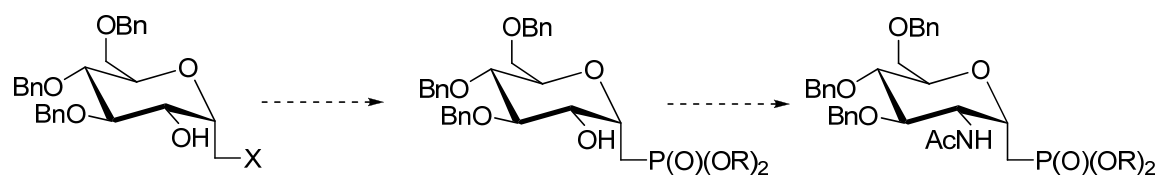
glucosamine derivative with methylenetriphenylphosphorane did not result in the desired

enitol product. In some cases, there was no reaction while in the case of 2-acetamido-2-deoxy-3,4,6-tri-*O*-benzyl-D-glucopyranose (**16**), the reaction ultimately yielded oxazolidine **17** (Scheme 10). Nicotra and co-workers investigated a separate path in which vinylmagnesium bromide was used to obtain 2-amino-2-deoxy-gluconitol (**18**) from *N*-benzyl(2,3,5-tri-*O*-benzyl-D-arabinofuranosyl)amine (**19**).⁵⁰ Mercuriocyclisation (Scheme 11) of the obtained aminogluconitol results in the α -D-glucopyranoside (**20**), but its subsequent conversion to the related halide was ineffective. The reasoning for the lack of reactivity was hypothesized to be associated with the nucleophilic character of the amino function and its proximity to the electrophilic carbon of the targeted halide.



Scheme 11: Mercuriocyclisation of aminosugar derivatives

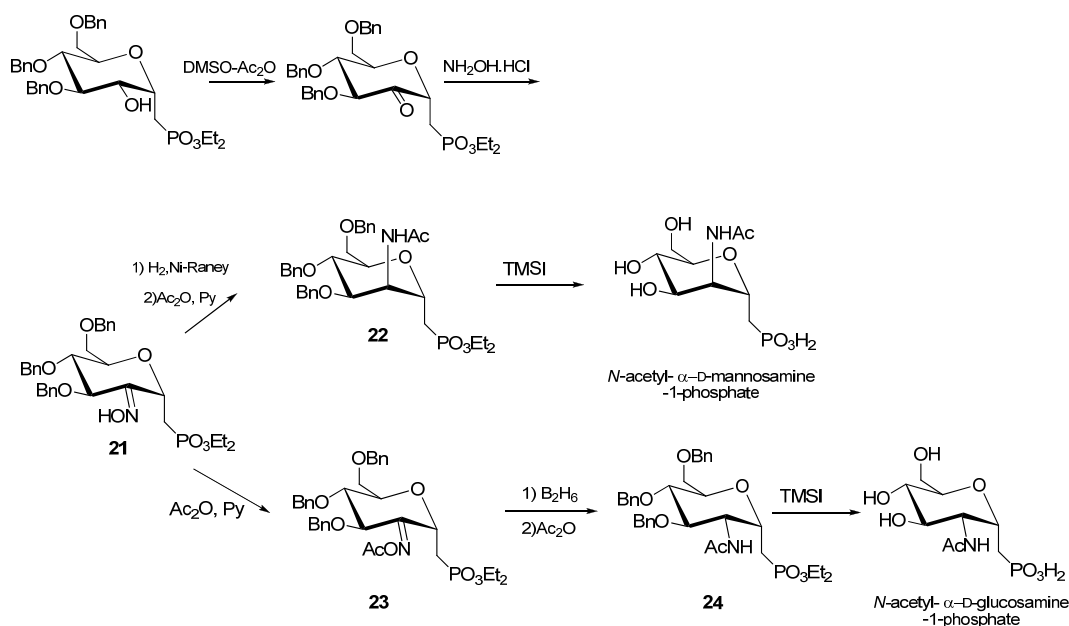
Overcoming these complications involved introducing the amino function after the introduction of the phosphono function. An α -*C*-glucopyranoside with a deprotected hydroxyl group at C-2 is required for this synthesis whereby the amino function will be added at the end of the synthesis of the phosphonate (Scheme 12).



Scheme 12: Introduction of amino function after the phosphono function

The strategy involves similar mercuriocyclisation, halogenation, Arbuzov, and deprotection steps as described in Section 2.2. The conversion to an amino group at C-2

from the free hydroxyl group can be obtained from oxidation, oximation, and reduction of the oxime through catalytic hydrogenation or treatment with diborane (Scheme 13). The preferentially formed product, starting from the α -anomer, is the 2-aminosugar obtained with the *gluco* configuration.^{25,51} The catalytic hydrogenation of α -oxime **21** with Raney nickel affords, following acetylation, the *manno*-isomer **22**. The metal catalyst appears to coordinate with the α -oriented phosphonate. This results in a favoured attack of the hydrogen from the α -face. With that observation, the *gluco*-isomer **24** can be obtained by utilizing diborane, a non-coordinating reducing agent, to reduce acetyloxime **23**.



Scheme 13: Formation of the phosphonate analogues of *N*-acetyl- α -D-mannosamine and *N*-acetyl- α -D-glucosamine 1-phosphate

2.4 Conclusion

The promise of affecting carbohydrate processing enzymes by employing glycosyl phosphate mimics has created a research area of growing interest. A variety of procedures

have been reported including the direct introduction of a methylenephosphonate group at the anomeric centre of the sugar. However, a more encompassing strategy for the preparation of these compounds consists of the preparation of a *C*-glycosyl halide followed by its conversion into a phosphonate. Though this synthesis appears to be quite universal, its application in the preparation of phosphono analogues of D-aminosugars has been unfruitful. The limitation of this procedure can be overcome by introducing the amino functionality in the final step of phosphonate synthesis.

The accessibility of these analogues of glycosyl phosphates allows for the preparation and evaluation of their NDP-derivatives and analogues.

2.5 Project Objectives

The aims of the project are as follows:

- To evaluate the substrate specificity of Cps2L with new sugar 1-phosphate analogues to gain further insight into the substrate and inhibitor requirements.
- To synthesize analogues of sugar 1-phosphates with interesting properties to be used either as inhibitors of Cps2L or, following enzymatic coupling to the corresponding sugar nucleotide, as inhibitors of other biosynthetic enzymes.

CHAPTER 3 RESULTS AND DISCUSSION: SUBSTRATE SPECIFICITY STUDIES WITH CPS2L

3.1 Phosphono Analogues of Sugar 1-Phosphates

3.1.1 Introduction

The synthesis of the phosphono analogue of α -D-glucose 1-phosphate (**1**) was accomplished as described by Nicotra³⁹ with adjustments to the purification step by Malcolm Huestis, a technician in the Jakeman group.

Similarly, the synthesis of the

phosphono analogue of α -D-

galactose 1-phosphate (**2**) was

carried out by Ali Sadeghi-

Khomami, a PDF in the Jakeman group, as a part of his Ph.D. thesis.⁴⁰ The structures of these analogues are shown in Figure 10.

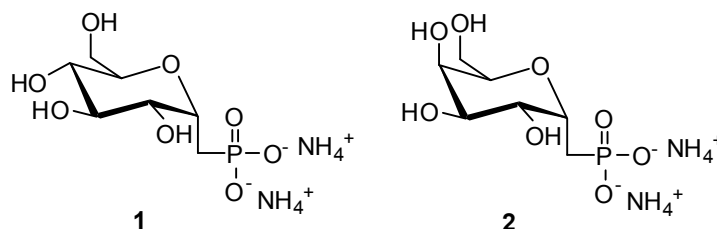


Figure 10 : Structures of phosphono analogues of sugar 1-phosphates prepared for evaluation as substrates for Cps2L: C-(1-deoxy- α -D-glucopyranosyl)methane phosphonate (**1**) and C-(1-deoxy- α -D-galactopyranosyl)methane phosphonate (**2**)

3.1.2 Progress Curves and Kinetic Characterization

Compounds **1** and **2** were assayed with five nucleoside triphosphates (ATP, CTP, GTP, dTTP, and UTP) using Cps2L as the enzyme. The enzyme (2 EU) was incubated with phosphonate **1** or **2** (2 mM), MgCl₂ (2.2 mM), and dTTP (1 mM), Tris-HCl buffer (20 mM final buffer concentration, pH 7.4), and inorganic pyrophosphatase (0.5 EU) at 37 °C for 30 min and 24 h. HPLC analysis of quenched aliquots was used to confirm the formation of product based on conversion of NTP. A thirty minute incubation of **1** with either dTTP (Figure 11) or UTP resulted in the formation of sugar nucleotide products in conversions of 95% (**25**) and 70% (**26**) respectively. This portion of the study indicates

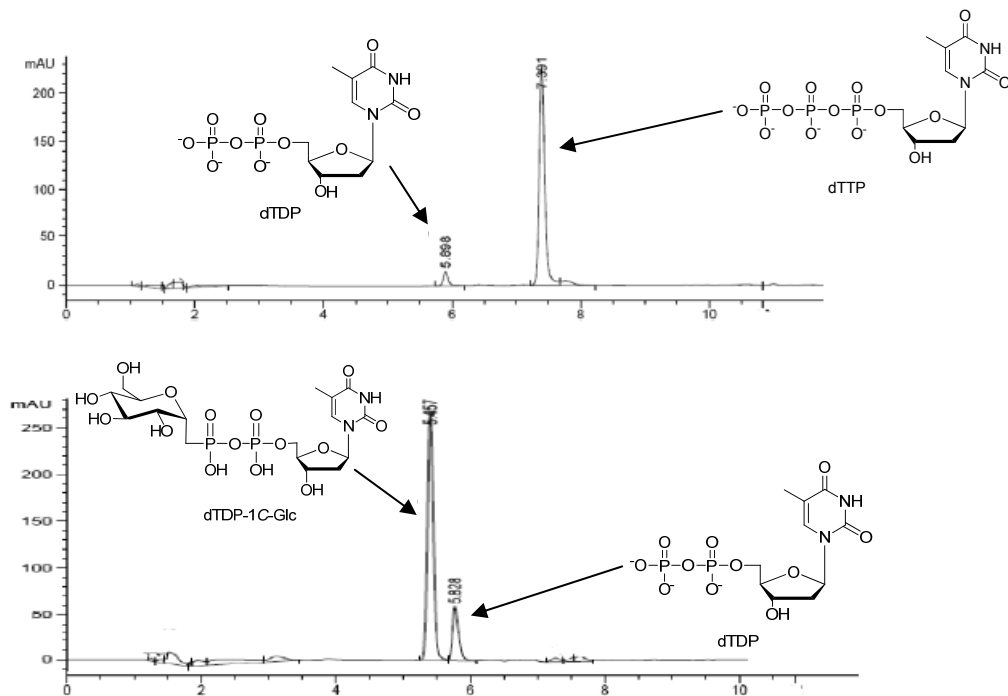


Figure 11: Typical analytical RP-HPLC chromatograms for Cps2L assays. HPLC trace of the dTTP control void of Cps2L (top); the Cps2L coupled reaction of **1** and dTTP (bottom)

that **1** is promptly accepted as an alternative substrate for Cps2L. On the other hand, incubating **2** with either dTTP or UTP under identical assay conditions only resulted in the production of the phosphono analogue of dTDP-Gal (**27**) with a conversion of 40%. With regard to assays containing ATP, CTP, or GTP, significant product was observed, but only when **1** was the sugar substrate (**28**, **29**, or **30** respectively). The yields observed for these conversions were within the range of 15-20% with lengthier incubation times (~24 h).

3.1.3 Scale-up and Isolation of the Phosphono Analogue of dTDP-Glc

A successful attempt was made to scale-up the enzymatic reaction containing **1** and dTTP. Purification of **25** was performed using a weakly acidic ion-pair buffer (10 mM tributyl ammonium bicarbonate, pH 6) following purification methods previously described in the lab for chromatographic separations of sugar nucleotides.⁵² Following

steps of subsequent cation exchange using Dowex® 50W-X8 cation exchange resin (100-200 mesh, Na⁺ form, 18 mm x 14 cm) to bind tributyl ammonium cations and generate the sodium salt of the desired sugar nucleotide, and gel filtration (Sephadex G10 column (1.5 cm x 100 cm)), the phosphono sugar nucleotide product was successfully purified with minimal loss or degradation of product (Figure 12). This method of purification proved better than

other purification methods attempted previously where either salt or basic pH initiated product breakdown. We were

not the first to report instabilities of sugar

nucleotides, as Lowary and co-workers have observed product decomposition under such conditions.⁵³

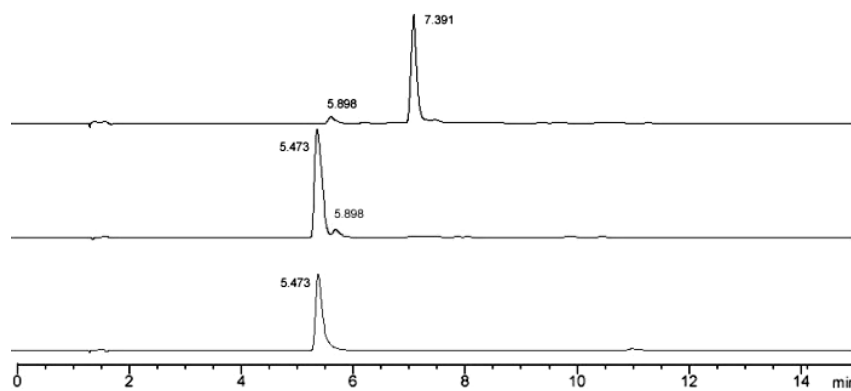


Figure 12: HPLC trace of preparative reaction of **25**. Reversed-phase ion-pair HPLC traces. HPLC trace for the dTTP control void of enzyme (top); the enzyme coupled reaction of **1** and dTTP (middle), and the final purified product

3.2 Glucopyranose-1-Boranophosphates

In collaboration with Dr. Takeshi Wada's group at the University of Tokyo, a series of

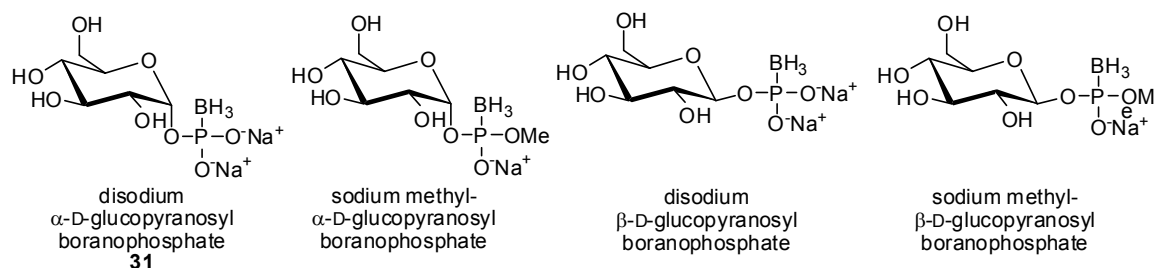


Figure 13: Structures of four glucopyranose-1-boranophosphates evaluated as substrates for Cps2L

four boranophosphates were evaluated as substrates for Cps2L (Figure 13). The four sugars were synthesized by Wada and co-workers as precursors to the formation of glycosyl boranophosphate triesters.⁵⁴ A boranophosphate is isosteric to the neutral methyl phosphonate group, and is similar to the phosphate and phosphorothioate groups in the fact that it maintains a similar negative charge.⁵⁵ In addition, the borane group is isoelectronic with the oxygen occurring in the phosphate. Boranophosphates are also more lipophilic than phosphates, despite possessing high water solubility.⁵⁵ It was anticipated that these boranophosphates could be accepted as substrates by Cps2L in such a way as to enzymatically obtain new types of modified sugar nucleotides. If there is no success as substrates, the possibility of the boranophosphates being inhibitors for Cps2L will be explored.

3.2.1 Attempted Progress Curves and Kinetic Characterization

Enzymatic assays were conducted in a similar fashion to those described for the formation of

phosphono

analogues of

sugar nucleotides.

After having

performed a

number of assays

using HPLC, ESI-

MS/MS, and ¹H NMR analysis by varying the concentration of Cps2L from 2 EU to 10

EU, as well as the concentration of the boranophosphate from 2 mM to 40 mM, there was

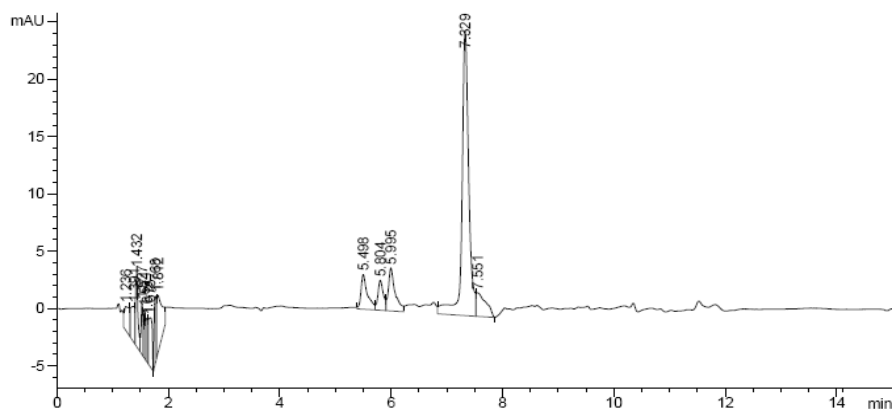


Figure 14: HPLC trace for the enzyme coupled reaction of disodium α -D-glucopyranosyl boranophosphate (**31**) and dTTP (T_R 7.4 min). The formation of sugar nucleotide was not observed, despite the emergence of other absorbance peaks (T_R 5.5-5.8 min)

no indication for the formation of sugar nucleotide indicating that reaction did not occur. Analysis by HPLC is typically the best indicator for the formation of sugar nucleotides, indicated by the appearance of a new absorbance peak. Of interest is the HPLC trace for α -D-glucopyranosyl boranophosphate (**31**) (Figure 14). In comparison to the dTTP control trace ($T_R=7.329$ min dTTP, 5.985 min decomposition to dTDP) there was the appearance of two small absorbance peaks. These two small absorbance peaks ($T_R=5.498$ min and 5.804 min) were of interest due to the anticipation of **31** being accepted by the enzyme as a substrate. However, attempts to confirm the formation of the borano sugar nucleotide analogue were unsuccessful. No product signals were observed following analysis with ESI-MS/MS, nor was there any observation of changes in the intensity and shift of the anomeric proton following an ^1H NMR experiment (Figure 15). Repetition of the experiment consistently showed the production of the two small absorbance peaks on the HPLC trace. The occurrence of these two additional peaks appears to be something other than the desired product.

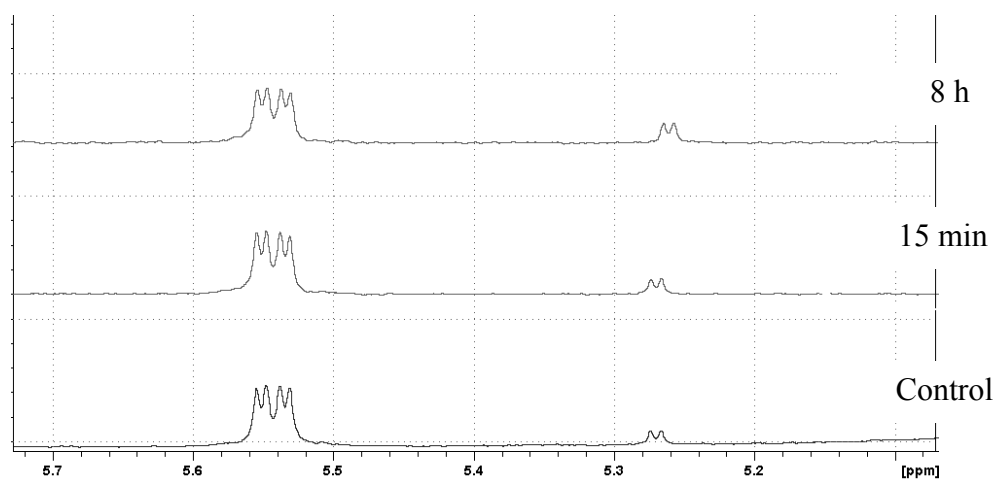


Figure 15: ^1H NMR of the attempted enzymatic reaction of **31** and dTTP. No change in intensity or shift was observed over time. The reaction mixture without the enzyme (control) is shown on the bottom. The next two spectra were obtained following the addition of enzyme (Cps2L) showing no change in the anomeric proton following 15 min and 8 h.

Similar assays were conducted using the other nucleotidyltransferases RmlA, RmlA3, AtUSP (*Arabidopsis thaliana* galactose 1-phosphate uridylyltransferase, purified by Ali Sadeghi-Khomami), and UDPGlc PP (UDP-glucose pyrophosphorylase from baker's yeast, commercially available), but as with Cps2L, the desired sugar nucleotide was not formed. These assays were once again conducted by varying the concentration of enzyme (2-10 EU), as well as varying the concentration of **31** (2 mM to 40 mM) along with incubation times (1-24 h).

The compounds were then investigated as inhibitors of the physiological reaction catalyzed by Cps2L. Increasing the concentrations (2 mM, 10 mM, 20 mM, and 50 mM) of all four of the boranophosphate sugars (conducted at set time intervals from 30 min to 24 h) did not impede the reaction of dTTP and Glc 1-P, and cannot be classified as inhibitors.

Despite not detecting any substrate or inhibitor actions from these boranophosphate sugars, these sugars have allowed for further insight into the substrate as well as the inhibitor requirements of Cps2L. A better understanding of these compounds could be obtained through determination of their pK_a values, although reasoning for the inability of these sugars to act as substrates presently remains unclear.

3.3 2-Deoxy-2-Fluorosugar 1-Phosphates

A set of fluoro analogues of sugar 1-phosphates (Figure 16) were synthesized by Stephanie Lucas and Shannon Timmons, former members of the Jakeman group. They were then evaluated as possible substrates/inhibitors of Cps2L.

3.3.1 Progress Curves and Kinetic Characterization

A series of enzymatic assays, similarly performed by incubating Cps2L (2 EU) with five fluoro analogues of sugar 1-phosphates (2 mM), MgCl₂ (2.2 mM), and NTP (1 mM) at 37 °C for up to 24 h to gain insight into the substrate specificity of Cps2L thymidyltransferase.

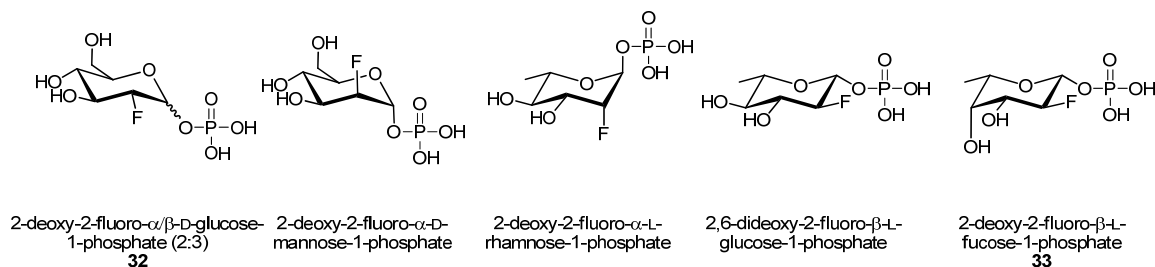


Figure 16: Structures of the five 2-deoxy-2-fluorosugars evaluated as substrates for Cps2L

The incubation of 2-deoxy-2-fluoro- α/β -D-glucose 1-phosphate (**32**) with either dTTP or UTP after 1 h gave conversions of 100% and 95%, generating the respective dTDP- and UDP-fluorosugar products (**34** and **35**). The ease of conversion associated with **32** indicates that Cps2L willingly accepts this fluoro analogue as a substitute substrate. Further assays involving **32** were observed to have product formation (< 15%) after prolonged incubation (24 h) when the nucleoside triphosphate was ATP, CTP, or GTP. Enzymatic assays of the other four fluorosugars, did not produce the corresponding sugar nucleotide product, when attempts were made to couple them with NTPs.

3.3.2 ¹H NMR and MS Studies to Evaluate the Stereoselectivity of Cps2L for **32**

A series of ¹H NMR experiments were conducted on the enzymatic coupling of **32** with dTTP. (Figure 17) The ¹H NMR spectra visibly established that Cps2L accepted and converted only the α -anomer (1,2-*cis*-phosphate) to the sugar nucleotide **34**. In addition,

after 12 h of incubation at ambient temperature, there was no decomposition of the non-productive β anomer.

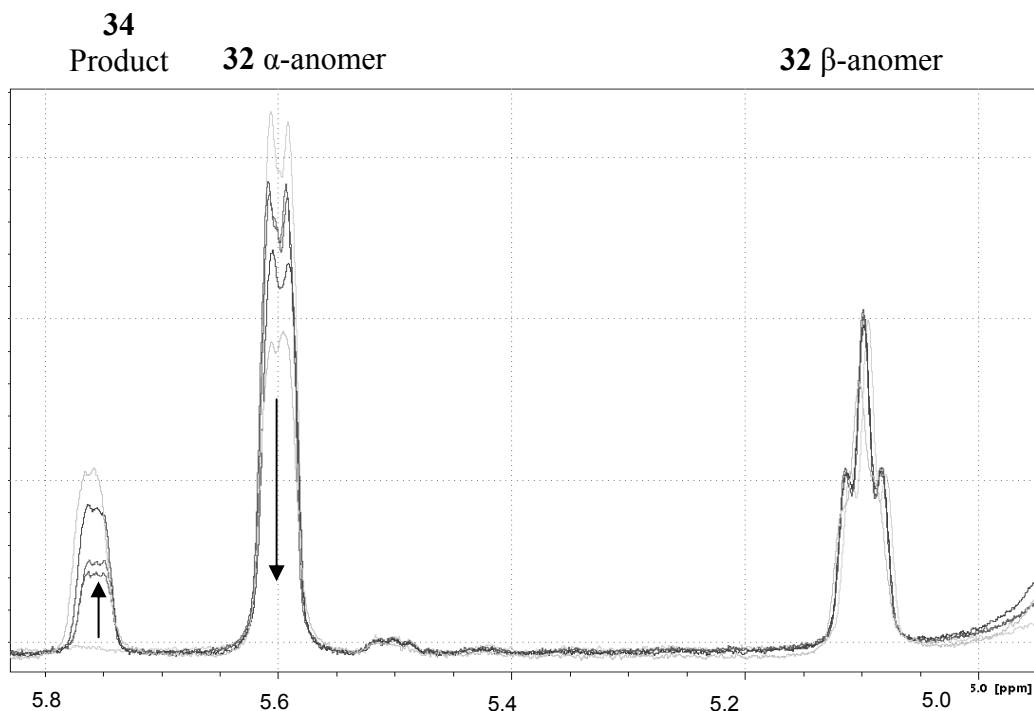


Figure 17: ^1H NMR spectrum displaying the enzyme-catalyzed reaction containing **32** and dTTP as substrates prior to the addition of enzyme. The remaining overlaid spectra show the reaction mixture at 1, 2, 6 and 12 h, respectively, showing the emergence of the anomeric signal for dTDP-2-deoxy-2-fluoro - α -D-glucose (**34**) (5.76 ppm) in conjunction with the diminishing of the anomeric signal for the α -anomer of **32** (5.60 ppm) as the signal for the β -anomer of **32** (5.09 ppm) remains constant.

The preferential binding of the α -anomer of the **32** was verified by investigation using ESI-MS/MS. This method, as described by Wolucka and co-workers⁵⁶ involves monitoring the mass spectrum of a hexopyranosyl nucleotide. The method has been applied for the mass spectral analysis of sugar nucleotides in the Jakeman lab.¹³ A primary fragmentation into a nucleoside 5'-monophosphate would indicate that a hexopyranosyl nucleotide has a 1,2-*cis* configuration, while an abundant fragment of a nucleoside 5'-diphosphate indicates that the hexopyranosyl nucleotide has a 1,2-*trans*

configuration. Submitting quenched reaction aliquots of the mixture containing **32** with dTTP resulted in a large signal at m/z 321.3 resulting from the fragmentation of the sugar nucleotide **34** (m/z 564.8) into a nucleoside 5'-monophosphate fragment (Figure 18). This indicates that the fluorosugar nucleotide product in question is 1,2-*cis*-linked, and substantiates the result obtained from the NMR experiments.

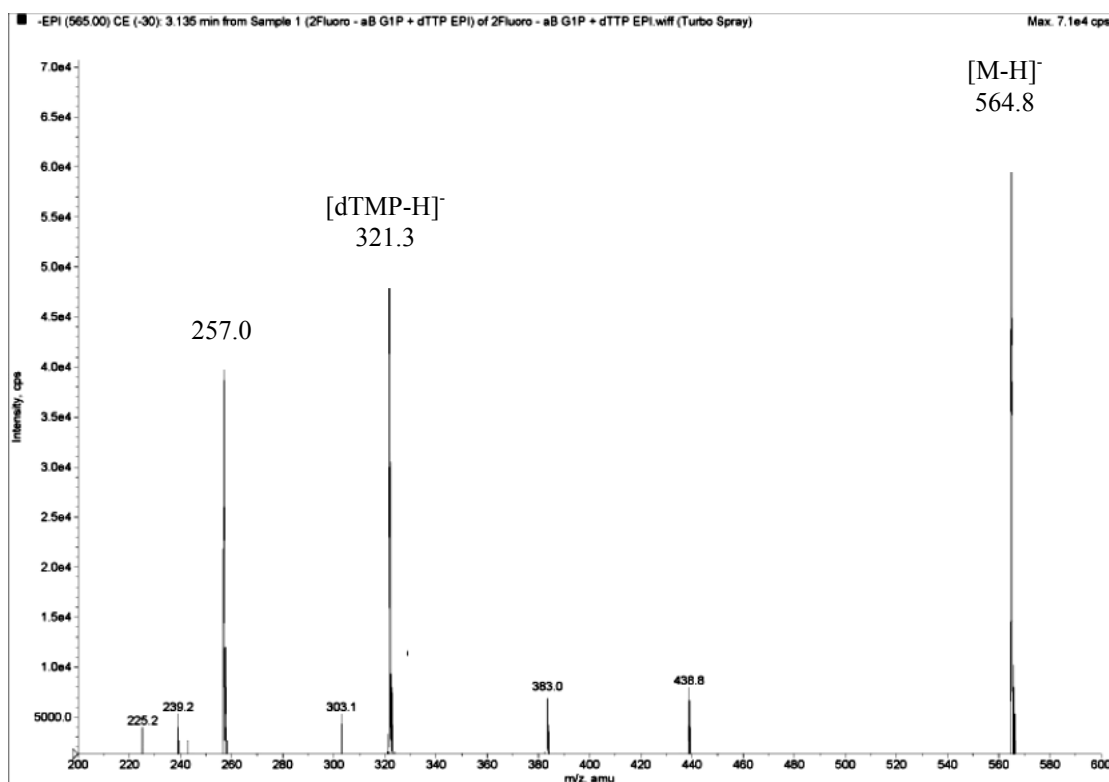


Figure 18: ESI-MS/MS EPI Scan data of enzyme-catalyzed production of dTDP -2-deoxy-2-fluoro- α -D-glucose (**34**). Key Fragments: 564.8 [M-H]⁻, 321.3 [dTMP-H]⁻. Presence of NMP (and absence of NDP) fragment indicates a 1,2-*cis* linkage.

3.3.3 Attempted Inhibition Studies

Only one of the unaccepted substrates, 2-deoxy-2-fluoro- β -L-fucose 1-phosphate (**33**) mildly inhibited the physiological reaction in the forward direction. However, high concentrations of inhibitor (~80 mM) were required. Reactions performed in triplicate showed a reduction in the conversion (~4%) to dTDP-Glc when a 10 mM of **33** was added in addition to the standard requirements for the physiological reaction mixture after

1 min. A dilution of Cps2L (0.2 EU) was used in order to obtain 50% conversion, and thus allowing the monitoring of potential decrease in conversion from a parallel reaction. The percent of conversion to product was compared between the physiological reaction and the reaction containing the inhibitor. The possibility of **33** acting as an inhibitor was further pursued by conducting assays with increased concentrations of **33** (20 mM, 40 mM, 80 mM), but the maximum reduction in conversion did not exceed 10%.

3.4 α -D-Glucose-1C-difluorophosphonate

The synthetically prepared difluoro analogue of **1** (**36**, Figure 19, see Section 4.1.2) was evaluated as a substrate for Cps2L. Fluorination of the methylene unit adjacent to the phosphorus is considered to have distinct advantages, such as reduced pK_a , and frequently results in improved binding in comparison to the parent compound due to the high electronegativity of fluorine.⁵⁷ The more effective

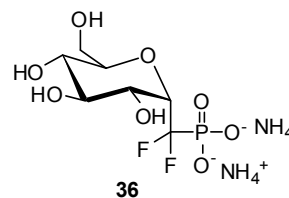


Figure 19: Structure of **36**

analogues of phosphonates are found to be the monofluoro- and difluoro derivatives in comparison to the non-fluorinated species. Fluorination of the methylene results in the alteration of the geometry (bond lengths and angles) of the phosphonate with respect to those of the parent phosphate.^{58, 59} Both the CHF and the CF₂ groups can mimic the bridging oxygen of the phosphate in respect to sterics and electronics. Thus, this alteration would result in the pK_{a2} to more closely parallel that of the phosphate as a result of the electron-withdrawing effect of fluorine.⁵⁸ In addition, fluorinated phosphonates, as compared to the non-fluorinated counterparts, result in a reduction of the pK_{a2} (Figure 20). For instance, the pK_{a2} of a phosphate group is approximately 6.5, while the simple phosphonate (CH₂) possesses a resultant pK_{a2} of 7.5-8^{58,59} (specifically

for **1** a pK_{a2} of 7 was determined¹⁷), which is less acidic. The CF_2 phosphonate has a significantly lower pK_{a2} of approximately 5.5-6^{58,59} as a result of the electron-withdrawing effect of the two fluorine atoms, while the occurrence of only one fluorine

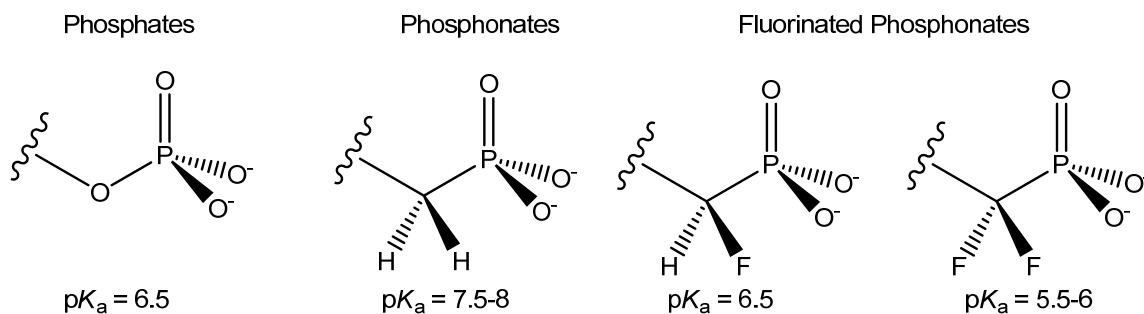


Figure 20: Fluorinated phosphonates as phosphate isosteres and associated pK_{a2} values

atom (i.e. CHF) moderately lowers the pK_{a2} to 6.5, nearly identical to that of the natural phosphate.^{58,59} Other additional parameters that are considered to favour fluorinated phosphonates include an increased dihedral angle for C- CF_2 -P. The crystal structures of some amino phosphinic acids have shown that P-C-C angle of the CF_2 -phosphonate (116°) falls within a similar range of the C-O-P angle (118°), as opposed to those of the CH_2 - and CHF-phosphonates (112° and 113° , respectively).⁶⁰ Moreover, the possibility of fluorine acting as a possible electron pair donor while preserving the role of being a hydrogen bond acceptor (C-F \cdots H-X) could result in imparting a possible additional binding site for enzymes.^{57, 60}

It was anticipated that the promising properties of the fluorinated phosphonate would result in interesting results with Cps2L. Attempts to couple **36** with dTTP were unproductive as no catalysis was observed despite varying the concentrations of enzyme (2-10 EU) as well as the concentration of **36** itself. Alternatively, investigating the potential of inhibiting catalysis by Cps2L with **36** was then explored. Using a set of concentrations (0, 1, 5, 10, 20, or 40 mM) of **36** and incubating with Cps2L (0.2 EU) for 1

min at 37 °C did not impede the reaction of dTTP and Glc 1-P, as compared to a parallel analysis of a physiological control (i.e. no inhibitor present). Pre-incubation of Cps2L with **36** for 1 h prior to the addition of the physiological substrates did not result in any noticeable decrease in sugar nucleotide production.

The lack of enzymatic activity toward **36** may be attributed to steric factors. Despite the favourable characteristics associated with fluorophosphonates mentioned above, the simple phosphonate is more inclined to be favoured by sterics.^{57,60} This is attributed to the fact that the fluorine atoms reside in the space previously occupied by the lone pairs of electrons on the oxygen. Accordingly, the simple phosphonate is considered to be the best isostere of the physiologically occurring phosphate because the C-F bond length of fluorinated phosphonates, falls within the range of 1.3-1.5 Å, which is on average 30-50% longer than the corresponding C-H bond.^{57,60} It remains to be seen whether the investigation of a monofluorophosphonate analogue will give rise to enzymatic interactions. A CHF unit α to the phosphoryl group gives rise to a phosphonate of similar acidity (iso-acidic) to the actual phosphate (Figure 20). The exploration of this type of monofluorophosphonate may yield particularly interesting results, and may provide insight for the lack of enzymatic activity of the difluoro analogue, considering the simple phosphonate was readily accepted by Cps2L.

3.5 α -D-Glucose 1C-thiophosphonate

The replacement of one of the non-bridging oxygen atoms present in a phosphonate with a sulfur atom, resulting in a thiophosphonate, will also reduce pK_a values in a similar fashion to phosphonates having one or two fluorine atoms at the α -methylene position.⁶¹ Similarly, these ensuing thiophosphonates mimic the naturally occurring phosphate esters

and, under physiological conditions, are hydrolytically stable. Investigations on the substrate properties of the synthetically prepared α -D-glucose-1C-thiophosphonate (**37**, Figure 21, see Section 4.1.3) as a substrate were performed. Enzymatic assays were

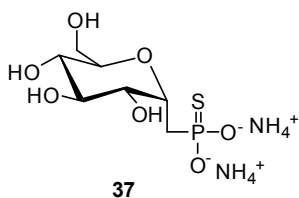


Figure 21: Structure of **37**

conducted to evaluate whether **37** was accepted as a substrate by Cps2L, as well as Cps2LQ24S, upon coupling to dTTP. At varying concentrations of enzyme (2 EU, 7 EU, and 12 EU), the maximum conversion to sugar nucleotide was 15%.

Analysis of ESI-MS/MS fragmentation of an aliquot of the enzyme assay revealed that the oxygen still operates as the nucleophile, rather than the sulfur atom, and in turn the oxygen is still the linkage between the sugar and the nucleotide (Figure 22).

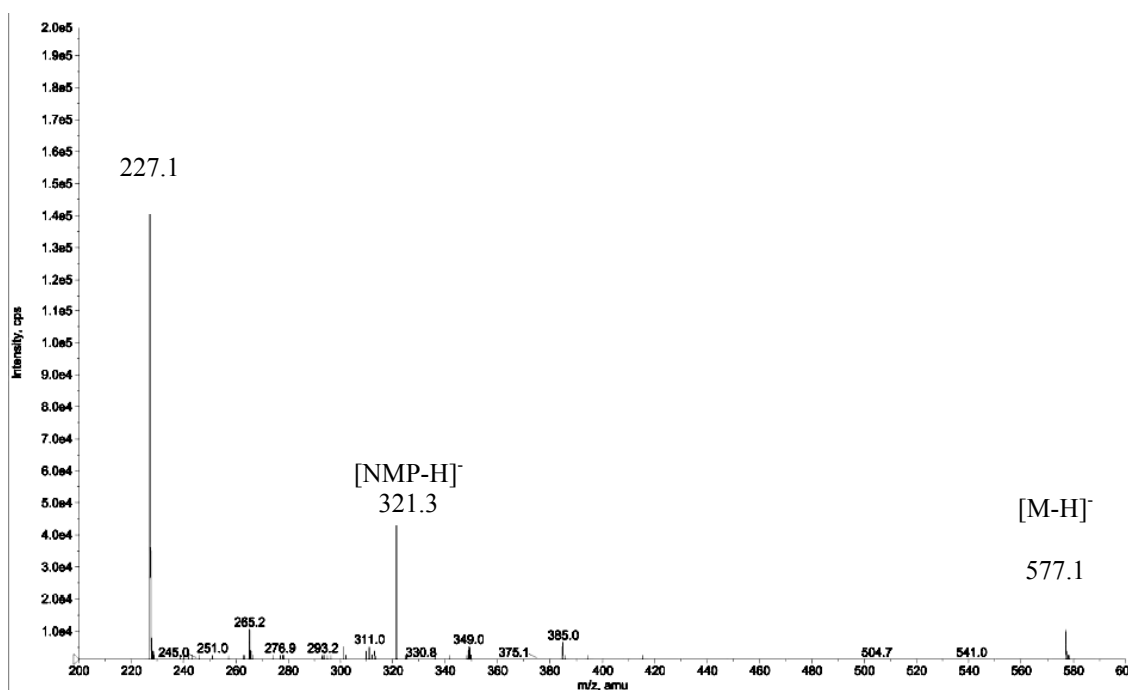


Figure 22: ESI-MS/MS EPI scan of the enzymatic coupling of **37** with dTTP. The resultant $[NMP-H]^-$ is indicative of the oxygen still operating as the nucleophile, as opposed to the sulfur atom, which would have resulted in a fragment of 377.

Subsequent experiments were then conducted to investigate whether **37** may display product inhibition when present in the physiological reaction. When the assays were monitored, comparable yields of the physiological sugar nucleotide were detected, and thus product inhibition was not arising.

3.6 Determination of Apparent Kinetic Parameters

The apparent kinetic parameters of Cps2L with respect to **1**, **2**, and **32** were determined in the forward reaction upon coupling to dTTP by varying the concentrations of sugar substrate from 50 μM to 300 μM to determine initial rates. Data were then plotted to create Michaelis-Menten and Lineweaver-Burk plots (Figure 23). In addition, these kinetic parameters were compared to those parameters associated with α -D-galactose 1-

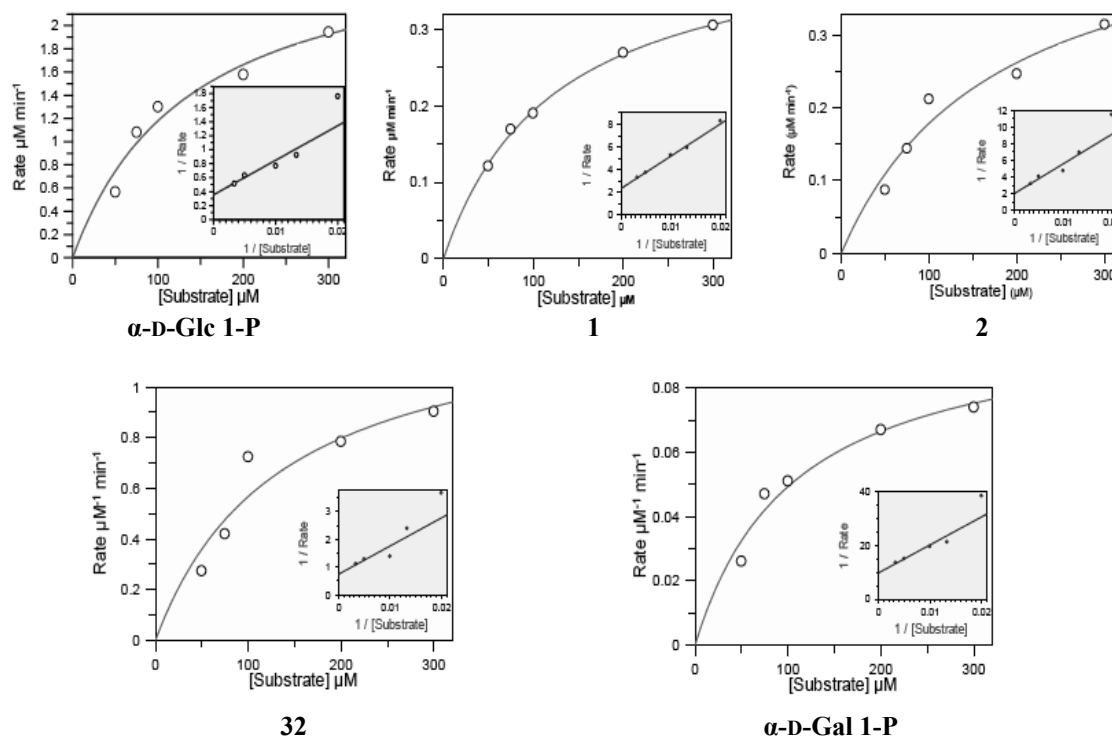


Figure 23: Michaelis-Menten and Lineweaver-Burk plots for the determination of apparent kinetic parameters. The values of V_{max} and K_m with respect to the sugar substrate were determined. (Table 2)

phosphate, as well as previously reported values for α -D-glucose 1-phosphate and β -L-arabinofuranose 1-phosphate.¹³ The kinetic values for all of these sugar substrates are given in Table 2.

Table 2: Apparent kinetic parameters for Cps2L substrates with dTTP

Parameter	α -D-Glc 1-P	1	32	2	α -D-Gal 1-P	β -L-Araf 1-P ¹³
V_{\max} ($\mu\text{M min}^{-1}$)	2.818	0.4321	1.33	0.493	0.1022	0.2801
K_m (μM)	139	124	136	176	107	90
k_{cat} (min^{-1})	27.6	0.198	0.491	0.00849	0.00335	0.00218
k_{cat}/K_m ($\mu\text{M}^{-1} \text{min}^{-1}$)	0.199	0.00166	0.00361	0.0000483	0.0000313	0.0000242

The K_m values for all of the sugar substrates are within the same magnitude indicating that the creation of an activated Michaelis complex is attained at relatively the same amount of substrate. This is in agreement with results from a similar study from Pohl and co-workers.⁴ Their study involved the use of a mechanistically similar nucleotidyltransferase (from yeast) and a number of deoxy glucose 1-phosphates in which the key observations involved limited differences in substrate binding, but overall large differences in yields for the deoxy glucose nucleotide products.

In regards to the kinetic parameters in our study, the substrates were all compared in relation to the physiological substrate. The substrate **1** displayed a 140-fold decrease in k_{cat} relative to the physiological substrate, α -D-Glc 1-P, while **32** exhibited a 56-fold decrease. On the other hand **2** displayed a 3200-fold decrease, while its parent sugar, α -D-Gal 1-P, displayed a decrease of 8200-fold.

By titration, Malcolm Huestis determined the $\text{p}K_a2$ of **1** to be half a unit higher than the physiological substrate, α -D-Glc 1-P (7 vs. 6.4), while Withers and Street determined the $\text{p}K_a2$ of **32** to be 5.9.⁴⁴ It is plausible that the decrease in turnover

efficiency of **2** versus α -D-Gal 1-P is attributed to these changes in ionization, and the geometry associated with the phosphonate. However, these geometric and ionization variations appear to have less of an effect on the amount of conversion being observed in comparison to the effects observed in changing the stereochemistry at C4. This can be seen by comparing the levels of conversion between α -D-Glc 1-P and α -D-Gal 1-P. This statement puts forward the premise that, in regards to the overall catalytic efficiency, the stereochemistry at C4 is of greater importance and lesser so is the ionization state of the phosphoryl centre. Thus, the configuration of the sugar has more of an effect on the lack reactivity than the electron density on the phosphoryl centre. Another study in the Jakeman group substantiates this detail by the fact that a furanosyl sugar 1-phosphate (β -L-arabinofuranose 1-phosphate) exhibited a much lower k_{cat} .¹³

There are two distinct observations when the sugar 1-phosphate analogues are compared to the naturally occurring sugar 1-phosphates. Of note here was that **1** and **32** possesses lower turnover to product relative to α -D-Glc 1-P. Secondly, **2** possesses a higher turnover to product versus its parent sugar 1-phosphate, α -D-Gal 1-P. Despite being remote from the reactive site, it is fascinating that a stereochemical change at C4 can, to some extent, be offset by alteration of the phosphate moiety, as seen in the case of **2**. It is possible that the trajectory of the phosphate may be misaligned by the stereochemistry at C4, while a methylene unit (substituting the anomeric oxygen) could potentially bring the nucleophile trajectory back into alignment owing to the geometric differences of the phosphonate. Alterations of the methylene unit (i.e. CF₂, **36**) may impose unfavourable steric effects, and decrease acceptance by the enzyme. The study of a similar nucleotidyltransferase from the Pohl group,⁶² showed that carbagluose 1-

phosphate, a carbocyclic analogue of the physiological substrate, resulted in a 725-fold decrease in k_{cat}/K_m with respect to the physiological substrate. In contrast, **1** as a substrate resulted in a decrease in k_{cat}/K_m of 120-fold. Thus, replacing the exocyclic anomeric oxygen substituent with a methylene unit more closely mimics the physiological substrate, than replacing the ring oxygen in the case of carbaglucose.

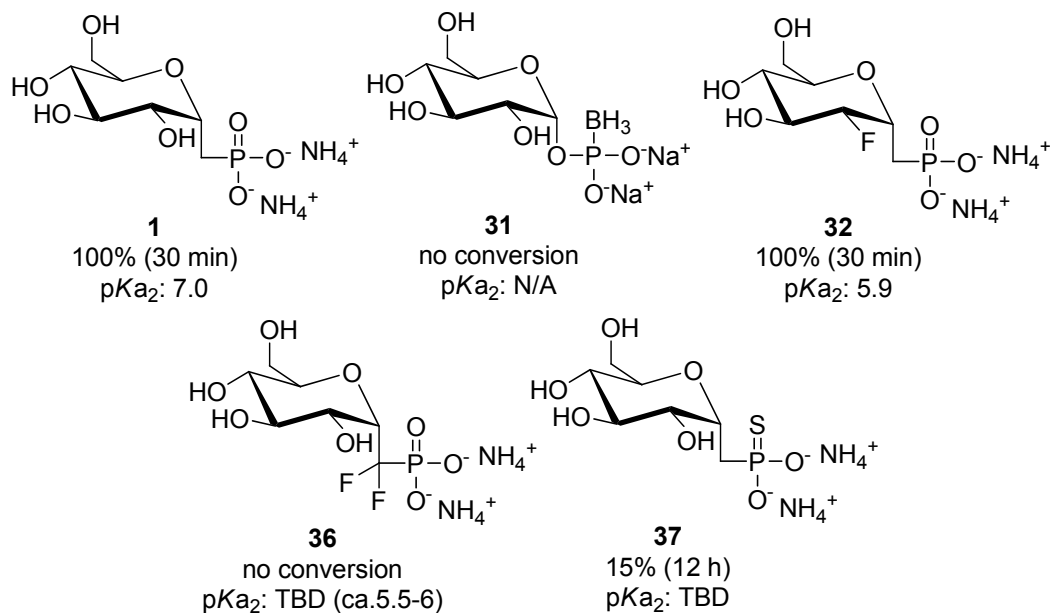


Figure 24: Summary of percent conversions to sugar nucleotide for tested substrates. The pK_{a2} values for the tested substrates are shown for comparison.

3.7 Conclusions of Enzymatic Assays

The issues related to low yields and prolonged reaction times for the formation of sugar nucleotides, in particular their phosphono analogues, has been overcome by utilizing nucleotidyltransferases. The retention times of sugar nucleotides and nucleoside triphosphate standards are shown in Table 3 and 4; a graphical summary of the percent conversions to NDP-sugar for different combinations of substrates is shown in Figure 25. Cps2L efficiently couples dTTP and UTP nucleotides with substrates that closely resemble the physiological substrate, such as **1** and **32**. Cps2L is more capable of

producing a phosphono analogue of dTDP-Gal, as opposed to dTDP-Gal. The differences in geometry of the phosphonate may result in a partial realignment of the nucleophile trajectory, and allow **2** to act as a better substrate than its parent sugar. Although these substrates all possess similar K_m values, the lower k_{cat} values associated with altering the stereochemistry at C4 suggest that the configuration of the OH at C4 plays a key role in the bond forming and breaking steps. This may be as a result of interactions with the active site residues of Cps2L, in which the equatorial OH may be better positioned to interact favourably with the residues. However, considering the conversions to product, the substituent at C3 plays less of a decisive role as established by probing Cp2SL with 3-*O*-alkyl substrates.¹²

Exploring the possibility of the sugar 1-boranophosphates, and studies on **37**, as substrates for Cps2L suggests that substitution of any of the oxygen atoms bound to the phosphate, other than the bridging oxygen involved in the glycosidic linkage, significantly decreases, or even impedes, the conversion to the desired sugar nucleotide. In combining this information, with that observed for the assays involving **36**, the pK_a of the sugar substrate appears to be a major factor in its potential acceptance as a substrate. Those substrates with pK_a values higher (+0.5) than that of α -D-Glc 1-P are readily accepted (also observed for the 3-*O*-alkyl-glucose 1-phosphates), whereas those with pK_a values lower (-1.5) than that of α -D-Glc 1-P are not accepted by Cps2L. Although further studies are required, this may be the result of a decrease in the nucleophilicity of **36**.

The conversion of **1**, **2** and **32** to their corresponding sugar nucleotide analogues highlights the promise of generating novel glycosyltransferase probes through the use of efficient enzymatic transformations.

Table 3: Comparison of retention times and percentage conversions to sugar nucleotides after 30 min and 24 h

Enzyme	Sugar 1-Phosphate	NTP	% Conversion ^a after 30 min	% Conversion ^a after 24 h	NDP-Sugar Retention Time (min)
Cps2L	1	ATP	6	19	5.36
Cps2L	1	CTP	10	16	5.79
Cps2L	1	GTP	1	16	5.13
Cps2L	1	dTTP	95	100	5.46
Cps2L	1	UTP	55	61	5.27
Cps2L	2	dTTP	42	--	5.52*
Cps2L	2	UTP	--	1	5.33
Cps2L	31	dTTP	0	0	--
Cps2L	31	UTP	0	0	--
Cps2L	32	dTTP	98	98	5.41
Cps2L	32	UTP	90	94	5.30
Cps2L	36	dTTP	0	0	--
Cps2L	36	UTP	0	0	--
Cps2L	37	dTTP	2	12	5.51

^a Percentage conversion = [NDP-sugar / (NDP-sugar + NTP)] x 100 where NDP-sugar is equal to the product peak integration and NTP is equal to the NTP peak integration.

* Product of **2** with dTTP broke down after 24 h incubation.

Table 4: Retention times of NDP, NTP and thymidine standards

Standard	Retention Time
ATP	7.29
CTP	7.11
GTP	7.16
dTTP	7.36
UTP	7.29
ADP	5.78
CDP	5.08
GDP	5.87
dTDP	5.84
UDP	5.69
thymidine	1.96

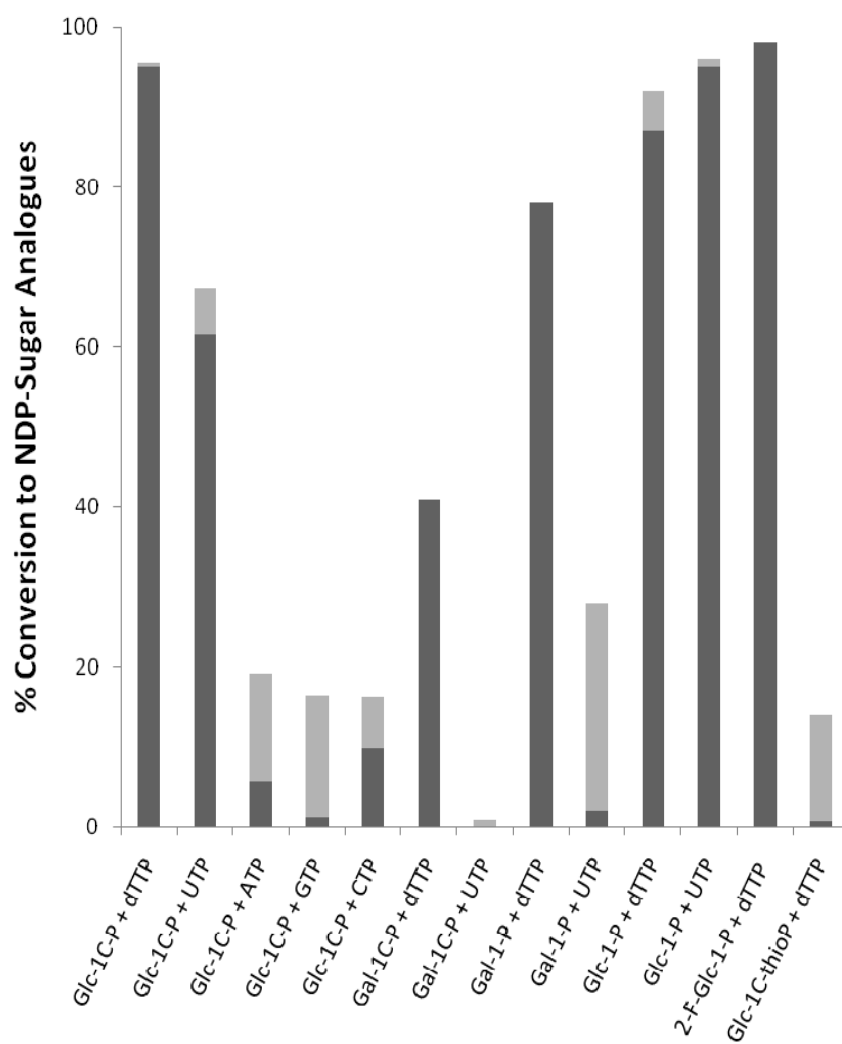


Figure 25: Graphical Summary of substrate conversions observed for the formation of sugar nucleotides by Cps2L after 30 min (dark shade) and 24 h (light shade) at 37 °C.

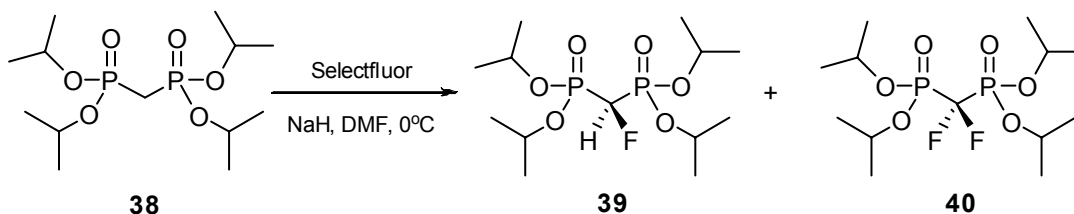
CHAPTER 4 RESULTS AND DISCUSSION: SYNTHETIC STUDIES

It is expected that the synthesis of new phosphono analogues may yield potential substrates for Cps2L. Modifying the phosphonate moiety, such as appending functional groups to the carbon of the methylene linker, could also result in the formation of potential inhibitors for the nucleotidylyltransferase. Furthermore, obtaining new derivatives of C-phosphonates can allow for the creation of additional hydrolytically stable sugar nucleotide analogues to potentially inhibit glycosyltransferases.

4.1 Towards the Preparation of Fluoro Derivatives of α -D-Glucose 1C-Phosphonate

4.1.1 Fluoromethylenediphosphonates

The initial synthetic strategy toward the preparation of a fluoro derivative of **1** was evaluated based on the synthesis of both a mono- and a difluoro analogue of tetraisopropyl methylenediphosphonate (**38**). The evaluation of the synthetic strategy to prepare fluorinated analogues of **38** was followed in order to optimize the reaction conditions, in addition to producing potentially interesting compounds for the investigation of the reverse reaction catalyzed by Cps2L. It was anticipated that the



Scheme 14: Synthetic strategy employed for the preparation of monofluoro (**39**) and difluoro (**40**) derivatives of tetraisopropyl methylenediphosphonate.

deprotection of **39** and **40** may be recognized as a substrate, or categorized as an inhibitor. The synthetic preparation of **39** and **40** (Scheme 14) is based on a procedure from the Jakeman lab, but with minor modifications to the purification method.⁶³ The synthesis involves employing an electrophilic fluorine donor, Selectfluor™ (F-TEDA-BF₄), to yield **39** and **40** from the enolate generated by sodium hydride. The reaction

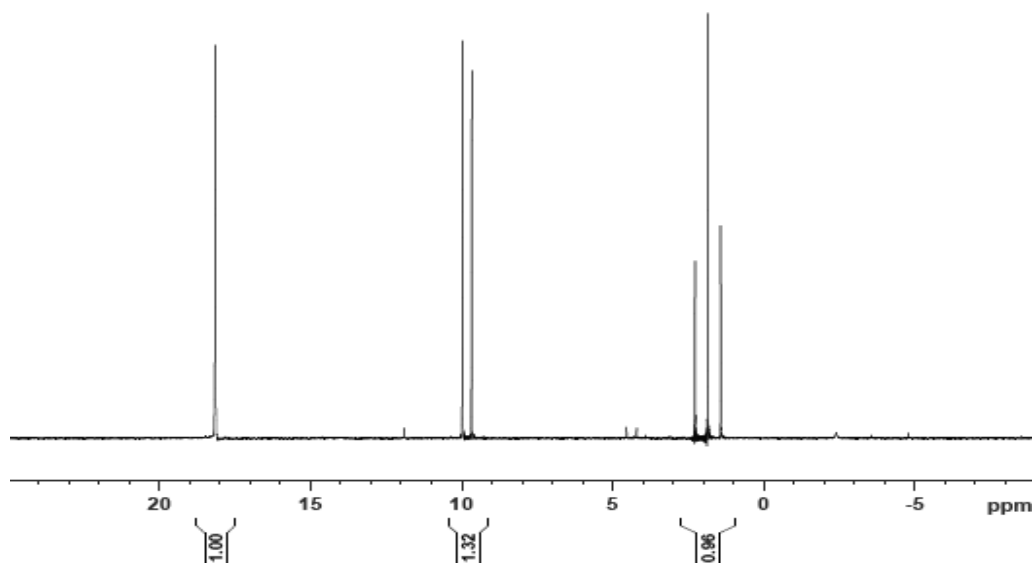
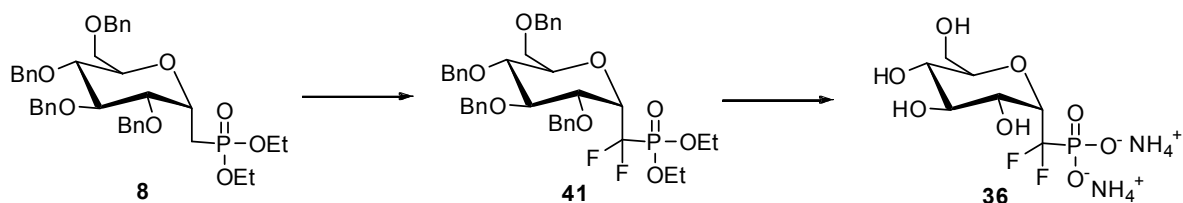


Figure 26: ³¹P NMR spectrum of the reaction mixture for the fluorination of tetraisopropyl methylene diphosphonate. Shown are signals for the presence of **38** (18.15), and the production of fluoro derivatives **39** (9.80), and **40** (1.85)

progress was monitored by removing small aliquots for ³¹P NMR spectroscopy [**38** 18.15(s); **39** 9.80, (d), ²J_{P,F} 61.76 Hz; **40** 1.85, (t), ²J_{P,F} 85.42 Hz], and the reaction was quenched when a ratio of approximately 1:1:1 was observed (Figure 26). The NMR data are consistent with published results.^{63,64} Both **39** and **40** were isolated using silica gel column chromatography (80/20 hexanes/EtOAc). Compound **39** was obtained in 40% yield, while **40** was obtained in 29% yield, for a combined yield of 69%. Assays using both **39** and **40** were then conducted by Ishrat Jalal (Biochemistry, 2009/2010 Honours Student) to examine potential inhibition of the reverse reaction catalyzed by Cps2L.

4.1.2 Fluoro Derivatives of α -D-Glucose 1C-Phosphonate

A similar synthetic strategy, namely the formation of an anion and treatment with the electrophilic fluoride source, was pursued with the purpose of preparing fluorinated derivatives of **1** (Scheme 14). All reactions were carried out on **8**.¹⁷ A number of reactions were attempted involving different bases, solvents, electrophilic fluorinating agents, and reaction conditions. These attempts are summarized in Table 5. The original attempt (Method A) for the synthesis of the desired compounds was built on the results from the optimized reactions for the production of **39** and **40**. However, upon carrying out a similar anhydrous procedure at 0 °C using sodium hydride and Selectfluor™, no



Scheme 15: General scheme for the synthesis of fluoro derivatives of **1**.

product was formed. A similar result was observed when the reaction was performed at -78 °C. The starting material could not be recovered from either reaction mixture, due to probable decomposition based on TLC and a complicated ³¹P NMR spectrum. It was then hypothesized that Selectfluor™, despite being a widely used electrophilic fluorinating agent applicable to organic substrates possessing carbanionic character,⁶⁵ may have not been reactive enough to overcome the potential instability of the carbanion. Manipulating the synthetic approach by utilizing an alternative electrophilic fluorinating agent, *N*-fluorobenzenesulfonimide (NFSI) was attempted (Method B).⁶⁶ Despite this alteration, the reaction did not proceed as expected, and similarly the starting material

could not be recovered. A plausible explanation for this may be attributed to the highly basic nature of the sodium hydride ($pK_a \sim 35$).^{67, 68}

To overcome the issue of decomposition, a similar method was employed involving the substitution of NaH for the less basic sodium hexamethyldisilazide (NaHMDS) ($pK_a \sim 26$).⁶⁹ It should be noted here that March states the contrary, where NaH is less basic than sodium amide, a strong base with similarities to NaHMDS.⁷⁰ The application of NaHMDS has gained significant use in a number of fluorination studies (typically when used in combination with the fluorinating agent NFSI) for its use as a sterically hindered base and as a nucleophile.^{71,72} Deprotonation of the methylene protons by NaHMDS, followed by the fluorination of the anion with NFSI (Method C) resulted in the production of the desired difluoro analogue **41** as judged by ³¹P NMR in a yield of 8.8% (6.5 ppm, Figure 27). In addition to the formation of **41**, a phosphorus containing by-product (~26%) was observed on the ³¹P NMR spectrum (16.4 ppm, Figure 27). With the intention of minimizing the by-product formation, efforts were then made to optimize the reaction conditions associated with Method C. In two independent attempts (Methods D and E) the number of molar equivalents of NFSI to be added to the reaction were

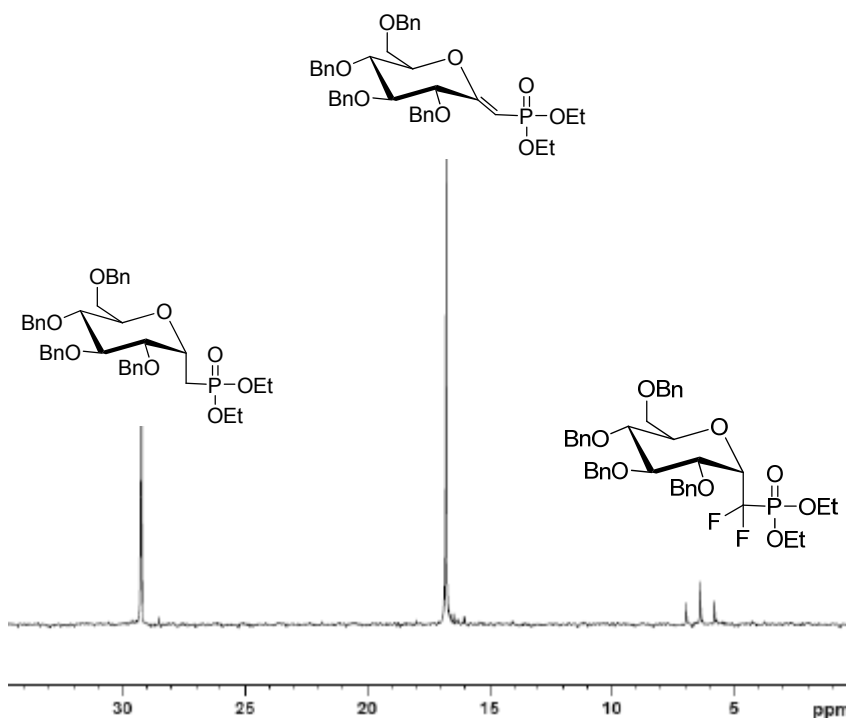
Table 5: Summary of reaction conditions for optimization of the fluorination methodology

Method A	Method B	Method C	Method D	Method E	Method F	Method G	Method H	Method I
DMF	DMF	THF	THF	THF	MeCN	Ether	Toluene	THF
NaH (2.5eq)	NaH (2.5eq)	NaHMDS (2.5eq)	NaHMDS (2.5eq)	NaHMDS (1.5eq)	NaHMDS (2.5eq)	NaHMDS (2.5eq)	NaHMDS (2.5eq)	KDA (2.5eq)
Selectfluor (2.5eq)	NFSI (2.5eq)	NFSI (2.5eq)	NFSI (5eq)	NFSI (1.5eq)	NFSI (2.5eq)	NFSI (2.5eq)	NFSI (2.5eq)	NFSI (2.5eq)
0°C & -78°C	0°C & -78°C	0°C & -78°C	-78°C	-78°C	0°C & -78°C	0°C & -78°C	0°C & -78°C	-78°C
--	--	Product - 8 (8.8%)	--	--	--	--	--	--

adjusted to push the reaction to completion. The addition of five equivalents of NFSI to promote reactivity impeded the formation of product. On the other hand, reducing the number of equivalents to a slight excess of one equivalent (so as to control the fluorination and yield solely the monofluoro derivative) exhibited a minute triplet at 6.32 ppm in the ^{31}P NMR, likely as a result of the formation of **41**. Subsequently, a set of reactions involving the effect of solvent on the reaction conditions of Method C (Methods F-H) were carried out. It was anticipated that performing the reactions in different solvents, such as acetonitrile, diethyl ether and toluene, would aid in directing the electrophilic fluorine.^{66, 71} Despite the reported success of these solvents,^{66, 71} there was no improvement on the outcome of the reaction; no product was observed and the starting materials were recovered.

The final effort to increase the yield of the reaction involved following a published procedure for the fluorination of alkyl phosphonate carbanions.⁷³ The reaction is carried out similarly to Method C with the exception of employing potassium diisopropylamide (KDA), generated *in situ* from LDA and potassium *t*-butoxide, for the deprotonation of the methylene protons. Differding and colleagues described that, particularly in the case of obtaining difluoro products, the yields of such a reaction were strongly dependent on the nature of the cation. Potassium diisopropylamide provided a better yield (66% vs. ~20%) of their respective difluorophosphonate product, as opposed to lithium diisopropylamide (LDA). However, this method (Method I) did not result in any improvements for the synthesis of **41**, and **8** was easily recovered.

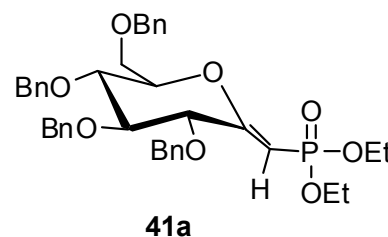
Despite efforts made to improve the yield of **41**, the reaction conditions associated with Method C were the most efficient route to furnish **41**. Analysis of the reaction mixture by TLC showed three spots including the starting material, and two unknown species. The ^{31}P NMR spectrum of the reaction mixture (Figure 27)



confirmed this observation. Isolation and purification of **41**

Figure 27: ^{31}P NMR spectrum displaying signals associated with the crude reaction mixture targeting the preparation of **41**. Chemical Shifts are as follows: **8**, 29 ppm, (s); exo-glycal, 16 ppm, (s); **41**, 6.95 ppm (t)

was completed via silica gel column chromatography (80:20 hexane/EtOAc) and was characterized by ^1H NMR, ^{13}C NMR, and ^{31}P NMR, as well as ESI-MS/MS. Typical P-F splitting patterns and coupling constants were observed in the ^{31}P NMR, and were indicative of the formation of a difluorophosphate. A by-product with a ^{31}P chemical shift of 17 ppm was also isolated via the same silica gel column. The by-product, exo-glycal **41a**, (Figure 28) was subsequently characterized



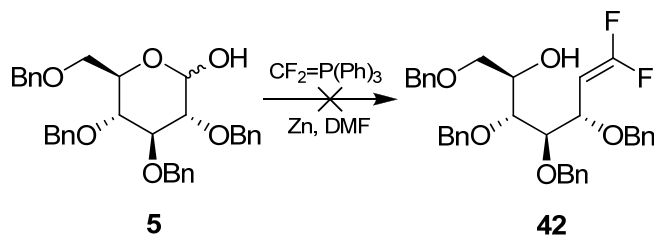
by ^1H NMR, ^{13}C NMR, ESI-MS/MS, in addition to ^{31}P

Figure 28: Structure of by-product **41a**

NMR. The mass spectrum of the by-product revealed a cluster of signals near m/z 695,

representing the sodiated product ($[M+Na]^+$). Despite performing the reaction at $-78\text{ }^\circ\text{C}$ to overcome the side reactions associated with less stabilized carbanions, it appears that a possible elimination reaction is favoured over the electrophilic attack by NFSI thus providing a low yield of desired product.

A final attempt was made to prepare a difluoro analogue via an alternate route through a Wittig reaction of fluorinated phosphonium ylides (Scheme 16). The strategy was to react difluoromethylene triphenylphosphonium ylide ($\text{Ph}_3\text{P}^+-\text{CF}_2^-$), obtained by zinc metal dehalogenation of (bromodifluoromethyl)triphenylphosphonium bromide, with **5** in a Wittig reaction to obtain the fluoro olefin (**42**). Despite the relatively common exploitation of zinc dehalogenation in the literature,⁷⁴⁻⁷⁶ the said reaction proved to be unsuccessful and starting materials were ultimately recovered.

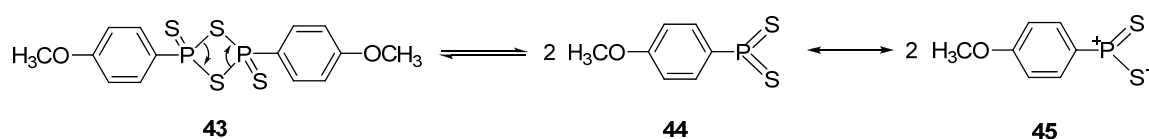


Scheme 16: Proposed Wittig reaction of difluoroolefin

At this stage, Method C was deemed as being the most appropriate method for the production of **41**. Treating **41** with iodotrimethylsilane resulted in the complete hydrolysis of the phosphonate ester into its free acid form as well as the cleavage of the benzyl protecting groups (**36**). The compound was characterized by ^1H NMR, ^{13}C NMR, ^{31}P NMR, as well as ESI-MS/MS.

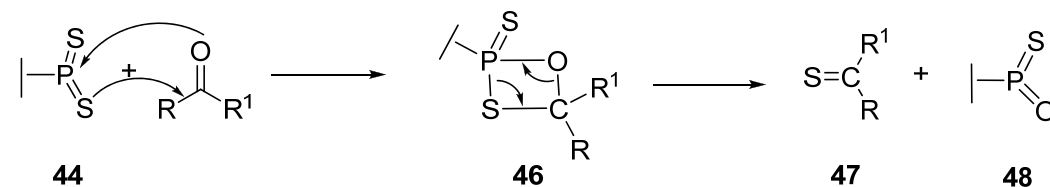
4.2 Preparation of α -D-Glucose 1C-Thiophosphonate

Lawesson's reagent (LR, **43**) (Scheme 17) was utilized for the transformation of **8** to its thiophosphonate derivative. The use of LR for the replacement of the oxo group of phosphorus (P=O) for the thio (P=S) is relatively common.⁷⁷



Scheme 17: Dissociation mechanism of Lawesson's Reagent

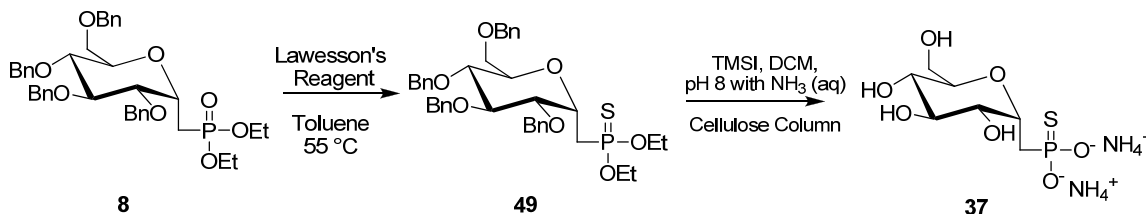
The usual method of thionation is performed in refluxing benzene, toluene, or xylene,⁷⁷ in which the possible mechanisms of both reagents were suggested to involve dissociation equilibria, which yield **44** and **45**. These decomposition products can then react with carbonyl functional groups to form four-membered rings **46**, which subsequently decompose to the corresponding thioketone **47** (Scheme 18). The P-O bond is much stronger than the P-S bond, which results in the formation of **48** which is the more thermodynamically stable product.⁷⁷ This is considered to be one of the key driving forces behind the mechanism of LR.



Scheme 18: Thionation mechanism of Lawesson's Reagent

This reaction was carried out in a slightly different manner than those described. After detailed experimentation, while many reports require refluxing toluene,^{77,78} the optimal reaction conditions were concluded to be heating at 55 °C for 12 h in dry toluene. Under these conditions, treatment of **8** with Lawesson's reagent yielded diethyl C-(1-

deoxy 2,3,4,6-tetra-*O*-benzyl- α -D-glucopyranosyl) methane thiophosphonate (**49**) which was obtained in 71.5% yield after purification (Scheme 19). It can be noted that the extreme downfield shift of the phosphorus atom in the ^{31}P NMR, 29.2 ppm for **8** compared to 96.8 ppm for **49**, is very diagnostic^{78, 79} and indicates that thionation took place on the phosphorus atom.



Scheme 19: Synthesis of α -D-glucose-1C-thiophosphonate (**37**)

The deprotected product, α -D-glucose-1C-thiophosphonate (**37**) was obtained in 42% yield by reacting **49** with iodotrimethylsilane and subsequent purification cellulose column chromatography (8:1:1 n-propanol- NH_3 - H_2O) (Figure 29).

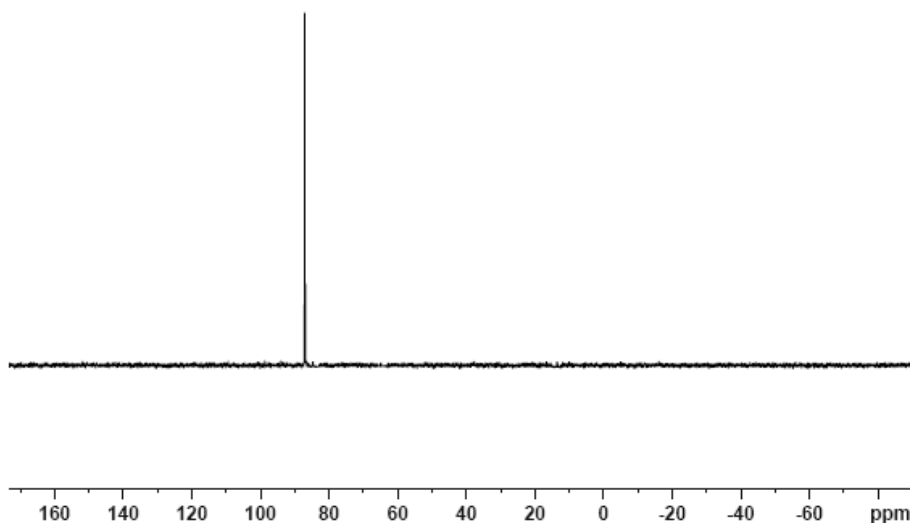


Figure 29: ^{31}P NMR spectrum of **37** (87.2 ppm (s)) in D_2O following purification using cellulose column chromatography

4.3 Toward the Synthesis of α -D-Glucose 1C-Bisphosphonate

The synthesis of a modified derivative of **1** (**50**, Figure 30) was pursued in order to allow for further exploration of the substrate specificity of Cps2L in an attempt to enzymatically prepare novel sugar nucleotides which may act inhibitors of glycosyltransferases. The preparation of a new C-glycosyl phosphonate mimic that

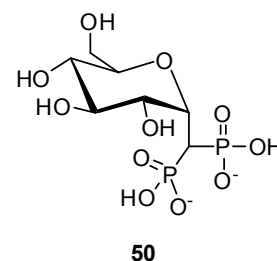


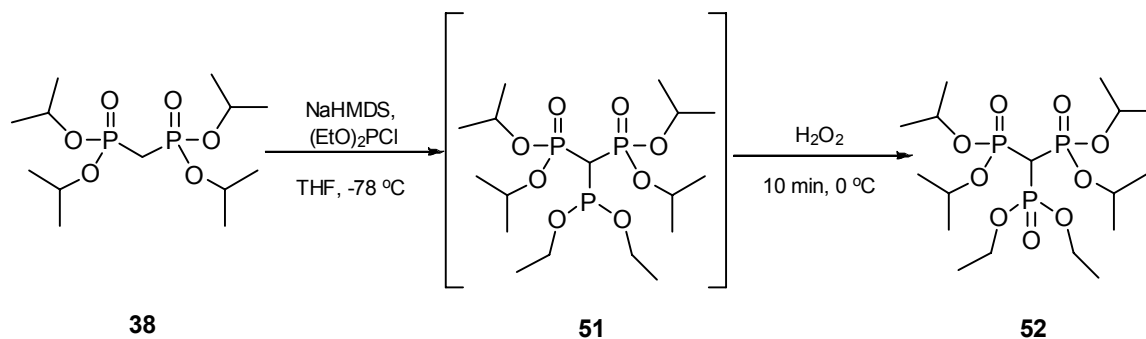
Figure 30: Structure of target compound **50**

possesses an anionic functional group on the exocyclic methylene carbon has been explored. Similar analogues of ATP have been synthesized and, due to their enhanced affinity for receptors, have been employed to resist enzymatic hydrolysis.^{80,81} This compound may inhibit Cps2L, thereby blocking the biosynthesis of L-Rha and also potentially inhibiting the specific glycosyltransferases that bind dTDP- β -L-Rha as a substrate. The bisphosphono compound is an isosteric phosphonate analogue relative to the parent **1**, and more closely resembles the transition state of the Cps2L reaction by incorporating additional negative charge.

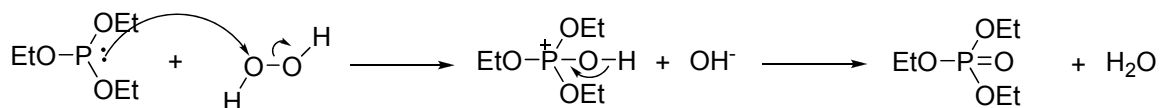
4.3.1 Synthesis of Methanetrисphosphonate

Initial explorations of the potential of this reaction were conducted with tetraisopropyl methylenebisphosphonate. Deprotonation of the methylene proton of the bisphosphonate with NaHMDS, followed by drop-wise addition of diethyl chlorophosphite resulted in the formation of a P(III) intermediate **51**. This intermediate was immediately oxidized *in situ* with hydrogen peroxide (30%)^{82,83} resulted in the formation of the corresponding trisphosphonate (**52**) in 72% yield (Scheme 20). Oxidation of the P(III) species by hydrogen peroxide (30%) was observed to be the most efficient reagent to attain the final P(V) species with respect to attempts using iodine in

pyridine–THF–water,⁸⁴ and mCPBA.⁸⁵ The mechanism for the oxidation of P(III) to P(V) is shown in Scheme 21. The rate determining step is governed by an S_N2 reaction, in which the phosphite species abstracts the hydroxyl oxygen of the phosphite. This results in an intermediate species which decomposes to yield the P=O, as a result of the oxidation to P(V).^{86, 87}



Scheme 20: Synthesis of the trisphosphonate (**52**)

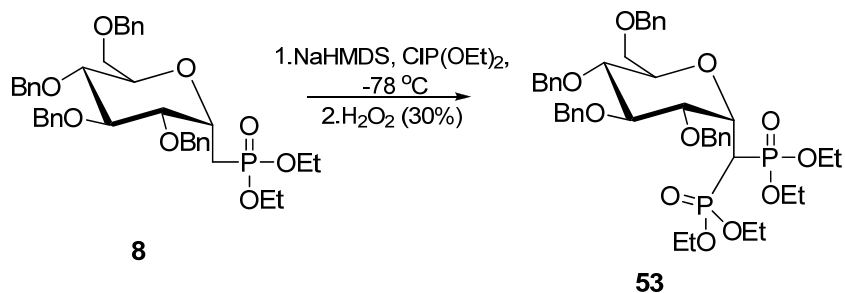


Scheme 21: Oxidation of P(III) to P(V) species using hydrogen peroxide⁸⁶

4.3.2 Synthesis of α -D-Glucose-1C-Bisphosphonate

The synthetic scheme outlined for the synthesis of trisphosphonate **52** was subsequently employed for the synthesis of the desired bisphosphono compound **53**. Similarly, **8** was reacted with diethyl chlorophosphite in the presence of NaHMDS at -78 °C (Scheme 22). The P(III) intermediate was subsequently oxidized *in situ* in a similar fashion by means of hydrogen peroxide (30%) addition in order to attain the final P(V) species. The optimal oxidation reaction time appears to be 10 min, whereas times longer than 30 minutes result in several phosphorus-containing by-products, as observed on ³¹P NMR.

The synthesis of the bisphosphono analogue of **8** was completed on a small scale (60 mg), and in low yield (13%). A fractional amount of **8** could be recovered, however a quantity of unidentified phosphorus species were observed on the ^{31}P NMR spectrum. A subsequent attempt to deprotect **53** using iodotrimethylsilane in anhydrous CH_2Cl_2 was unfruitful, likely as a result of low quantities of protected material. Due to difficulties in purifying the product, as well as the low yield of product, future work will entail re-synthesizing and optimizing the reaction conditions to obtain sufficient material to effectively remove all by-products and contaminants prior to deprotection and testing of the compound.



Scheme 22: Synthesis of ‘supercharged’ analogue of **1** (**53**)

CHAPTER 5 CONCLUSIONS

One of the major objectives in the Jakeman laboratory is to explore the substrate specificity of the thymidyltransferase, Cps2L. Advances have been made in the preparation of sugar nucleotides via enzymatic approaches for use as substrates for glycosyltransferases. Several analogues of α -D-glucose 1-phosphate were prepared synthetically, and were evaluated as substrates for Cps2L. Several of these substrates were accepted as substrates, producing structurally diverse sugar nucleotides. In addition, one of these enzymatic reactions was scaled up, and the corresponding sugar nucleotide product was purified.

5.1 Future Work

Continuation with the analysis of the substrate specificities and kinetic parameters of Cps2L with compounds discussed earlier is essential for better comprehension of its substrate requirements. The kinetic parameters of **1**, **32**, and their parent sugar (α -D-glucose 1-phosphate), will be investigated at pH intervals (pH 6-8) to observe potential ionization influences. I am then interested in synthesizing modified derivatives of **1** (**54-56**) (Figure 31), which will be used to further explore the substrate specificity of Cps2L in an attempt to enzymatically produce novel sugar nucleotides which may act as inhibitors of glycosyltransferases.

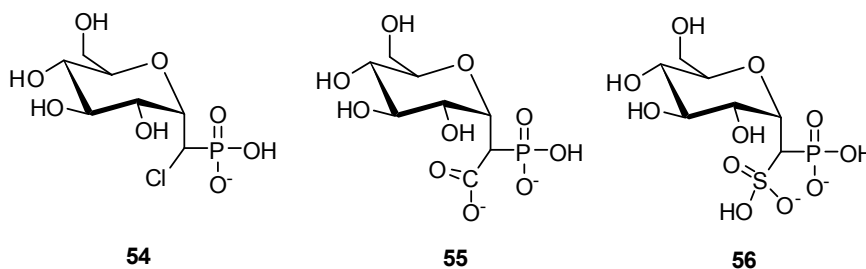


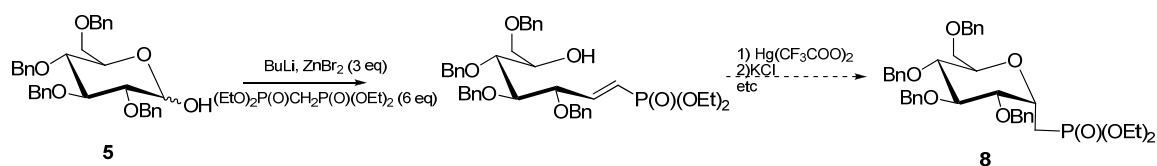
Figure 31: Structures of the proposed analogues of **1**

Enzymatic specificity constants of Cps2L will also be measured for those substrates that are accepted by the enzyme. Lastly, the substrate specificity of the enzymes RmlB-RmlD will be explored with products produced by Cps2L to generate novel sugar nucleotides.

5.1.2 Revision of Synthetic Strategy to Prepare α -D-Glc 1C-Phosphonate

Hultin and co-workers have recently described a short and efficient synthesis of the phosphono analogues of *N*-acetyl β -D-mannosamine- and *N*-acetyl β -D-glucosamine 1-phosphates.⁸⁸ The treatment of a protected glucosamine derivative with $(\text{EtO})_2\text{P}(\text{O})\text{CHLiP}(\text{O})(\text{OEt})_2$ in the presence of ZnBr_2 resulted in an α,β -unsaturated phosphonate in 85% yield. Subsequent Michael cyclization upon treatment with $\text{K}_2\text{CO}_3/\text{EtOH}$ gave the desired β -C-mannopyranosyl product.

A modification to this synthesis may provide a more expeditious route to the formation **8**. We would like to explore the possibility of using mercuric trifluoroacetate (Scheme 23), a reagent that yields predominantly α -products, rather than $\text{K}_2\text{CO}_3/\text{EtOH}$ to preferentially yield the desired α -product rather than the β -product as described by Hultin.



Scheme 23: Modified synthetic strategy for the preparation of **8**

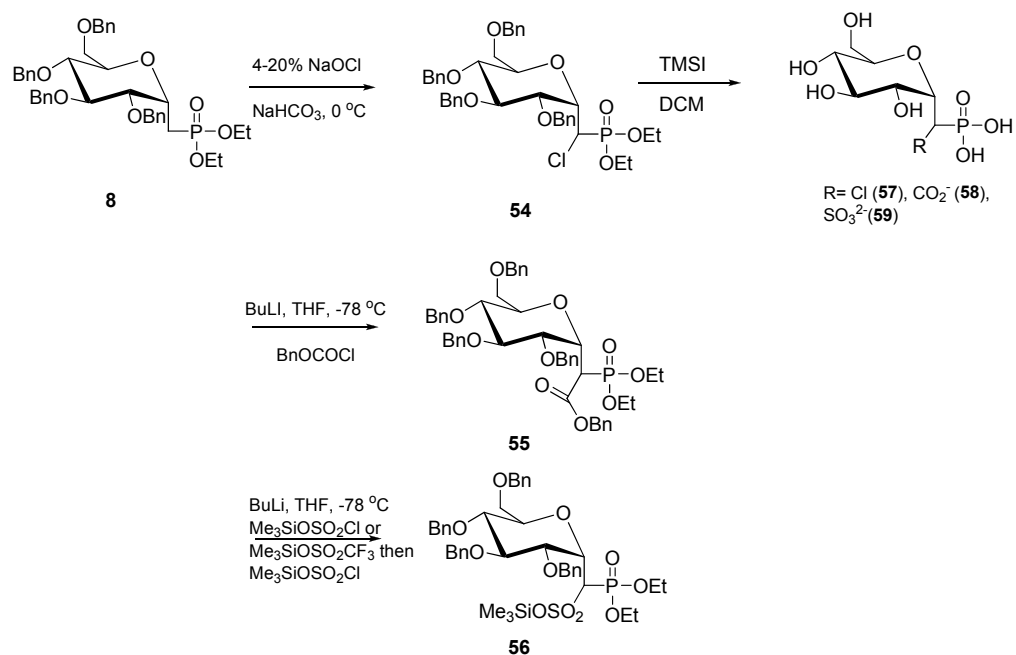
5.1.3 Proposed Synthesis of Glucose 1C-Phosphonate Analogues

These analogues can be assembled by adding an anionic function, such as SO_3^- , CO_2^- , and Cl^- to the exocyclic methylene of **8**, in an analogous fashion to **50**. In addition to providing additional anionic charge, these analogues may enhance the acidity of the

phosphonic acid without compromising the enzymatic stability of the P-C bond. The key feature designed into these potential enzyme inhibitors is the additional charge associated with the methylene linker in the form of a sulfate and carboxylate group. The increase in electrostatic charge of the molecule will mimic the ternary transition state more closely, and it is anticipated that these molecules will bind more tightly. The same concept applies to **53**, in which its deprotection to the corresponding free acid may result in similar tight binding to the enzyme. As outlined in Chapter 1, one of the significant changes noted in the crystal structures of RmlA bound to its substrates, products and dTDP- β -L-rhamnose was the repositioning of residue R194 in the dTDP- β -L-rhamnose complex to interact with the β -phosphate.⁸ It is anticipated that these charged molecules will improve this interaction and provide additional binding energy.

The chloromethanephosphonate **54** will be prepared by treating **8** with NaOCl solution.⁸⁰ In order to afford **55**, **8** will be reacted with benzyl chloroformate in anhydrous THF⁸¹ while trimethylsilylation and the treatment of its anion with trimethylsilyl chlorosulfate in THF at room temperature will yield **56**.⁸¹ Compounds **54-56** can then be efficiently deprotected by reacting them with iodotrimethylsilane in anhydrous CH₂Cl₂ to afford the desired analogues of **1** (**57-59**).

Once prepared, these analogues will be evaluated as substrates for Cps2L as well as Cps2LQ24S. Standard HPLC methods, as outlined for the determination of progress curves for Cps2L, will be used to monitor the formation of the dTDP-sugar product. Relevant kinetic parameters will also be obtained for those analogues that are accepted as substrates by Cps2L.



Scheme 24: Proposed synthesis of ‘supercharged’ analogues of **1**

CHAPTER 6 EXPERIMENTAL

6.1 General Procedures and Instrumentation for Cps2L Studies

6.1.1 Purification of Cps2L

The overexpression and purification of Cps2L was performed as described in the literature.¹¹ Competent *E. coli* BL21 DE3 cells were transformed with the plasmid pSK001. The transformants that contain these plasmids were grown overnight in LB medium containing kanamycin (50 µg/mL) on a rotary shaker. The protein was diluted through the transfer of a 1% inoculum from the overnight culture into fresh LB-kanamycin medium. Once the optical density reached 0.6-0.8 (at 600 nm), isopropyl β-D-thiogalactopyranoside (IPTG) was added to induce protein expression (to a concentration of 1% v/v, 1 mM final concentration). The cells were then lysed by lysozyme with subsequent sonication, followed by purification of the His-tagged proteins by nickel affinity chromatography. The protein was eluted with increasing concentrations of imidazole (stepwise 25 mM to 250 mM) at 4 °C using fast protein liquid chromatography (FPLC). Residual imidazole salts were removed from the protein containing fractions using a PD-10 desalting column, in which the protein also undergoes buffer exchange. The purified Cps2L concentration was measured spectrophotometrically at 280 nm using a calculated extinction coefficient of 29,340 M⁻¹cm⁻¹. The purified enzyme had enzyme activities of 1 EU/µL, where 1 EU (enzyme unit) is the amount of enzyme required to catalyze the conversion of 1 µmol of dTTP and α-D-Glc 1-P per minute to product.

6.1.2 Determination of Progress Curves

Enzymatic reactions were analyzed using reversed-phase-HPLC performed on a Hewlett Packard Series 1050 instrument using an Agilent Zorbax 5 μm Rx-C18 column (150 cm x 4.6 mm). Compounds bearing a nucleotide base chromophore were monitored at an absorbance of 254 nm. Reactions were monitored by HPLC using a linear gradient from 90:10 A:B to 40:60 A:B over 8.0 min followed by a plateau at 40:60 A:B from 8.0 to 10.0 min at 1.0 mL/min where A is an aqueous buffer containing 12 mM *n*-Bu₄NBr, 10 mM KH₂PO₄, and 5% HPLC grade CH₃CN (pH 4.0) and B is 100% HPLC grade CH₃CN. Samples were analyzed by injecting 15 μL aliquots. Low resolution mass spectra were obtained using an Applied Biosystems hybrid triple quadrupole linear ion trap (*Qtrap 2000*) mass spectrometer equipped with an electrospray ionization (ESI) source, used in negative ion mode. The capillary voltage was set to -4500 kV with a declustering potential of -60 V and the curtain gas was set to 10 (arbitrary units). During sample analysis, the solvent (50:50 methanol:water) was constantly infused into the ion source at 10 $\mu\text{L}/\text{min}$ by the built-in syringe pump and the samples were directly injected into the mass spectrometer after dilution (to 1 μM) with the above solvent. An enhanced mass spectrum (EMS) was obtained by scanning from *m/z* 100 to 650. Product ions were then fragmented to confirm their identities with an enhanced product ion (EPI) scan using collision energy of -60 V.

Enzymatic reactions containing 1.0 mM NTP, 2.0 mM sugar-1- phosphate, 2.2 mM MgCl₂, and 0.5 EU inorganic pyrophosphatase were initiated by the addition of 2 EU nucleotidyltransferase in Tris-HCl buffer (20 mM final buffer concentration, 50 μL reaction volume). The reactions were incubated for 30 min or 24 h at 37 °C, quenched

with methanol (50 μ L), and centrifuged (5 min at 12,000 \times g) to precipitate the denatured enzymes prior to HPLC analysis. In the absence of nucleotidyltransferase, NTP, sugar 1-phosphate (or analogues thereof), or $MgCl_2$, no product formation was observed.

6.1.3 Determination of Apparent Kinetic Parameters

Enzymatic assays were performed using the same method as described above. Enzymatic reactions containing 1.0 mM dTTP, 2.2 mM $MgCl_2$, 2 EU inorganic pyrophosphatase, 100 μ M thymidine (internal standard) and 50 μ M, 75 μ M, 100 μ M, 200 μ M or 300 μ M sugar 1-phosphate were initiated by the addition of Cps2L (0.002 EU), Cps2L (32 EU), Cps2L(1.6 EU), and Cps2L (0.008 EU) for α -D-glucose 1-phosphonate, α -D-galactose 1-phosphonate, α -D-galactose 1-phosphate, and 2-deoxy-2-fluoro- α/β -D-glucose 1-phosphate respectively (200 μ L reaction volume). The enzymatic reactions were conducted at 37 $^{\circ}C$ and monitored at 1, 2, 4, 6, and 10 min (α -D-glc 1-phosphonate); 2, 4, 6, 10, and 15 min (α -D-gal 1-phosphonate); 10, 11, 13, 15, and 19 min (α -D-gal 1-phosphate); 1, 2, 4, 6, and 10 min (2F- α/β -D-glc 1-phosphate). Enzymatic reaction aliquots (40 μ L) were quenched with HPLC grade MeOH (40 μ L) and centrifuged (5 min at 12,000 \times g) to separate the precipitated denatured enzymes prior to HPLC analysis. The HPLC method used to determine conversions was as described above. Final concentrations of the sugar nucleotides were determined by comparing the peak area of the product to that of the thymidine internal standard. Initial rates were determined by plotting concentration of sugar nucleotide products versus time. Michaelis-Menten and Lineweaver-Burk plots were fitted to the Michaelis-Menten equation using GraFit 5.0 software.

6.1.4 Attempted Cps2L Inhibition Assays

Assays were prepared with either 0, 1, 5, 10, 20, or 40 mM of potential inhibitor (either **33** or **36**) in reaction tubes containing 0.1 mM uridine (internal standard), 0.6 mM Glc 1-P, 0.5 mM dTTP, 2.2 mM MgCl₂, and 0.2 EU of Cps2L added in Tris-HCl buffer (10 mM, pH 7.4) to a final volume of 40 μ L. Assays were incubated for 1 min at 37 $^{\circ}$ C and quenched with HPLC-grade methanol (40 μ L) before being centrifuged and analyzed by HPLC. Product conversions were calculated and compared to those of parallel assays without the presence of an inhibitor.

6.1.5 Characterization of Enzymatically Prepared Sugar Nucleotides

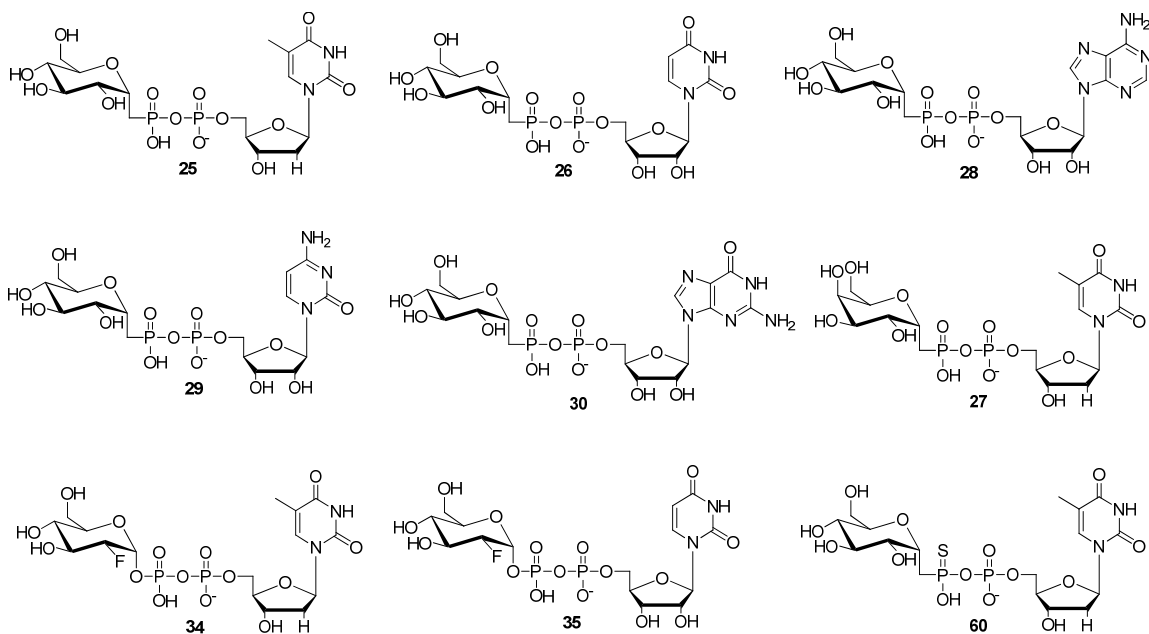


Figure 32: Structures of the sugar nucleotides characterized by ESI-MS/MS

dTDP-1CP-Glc (**25**) HRMS (ESI) Accurate Mass for C₁₇H₂₇N₂O₁₅P₂ [M-H]⁻ (*m/z* calcd 561.0892). Found: 561.0877; LRMS (ESI) = *m/z* 561.1 EPI fragments = *m/z* 321.1, 195.1, 176.9, 125.0 78.8.

UDP-1CP-Glc (**26**): HRMS (ESI) Accurate Mass for C₁₆H₂₅N₂O₁₆P₂ [M-H]⁻ (*m/z* calcd 563.0685). Found: 563.0682; LRMS (ESI) = *m/z* 563.0 EPI fragments = *m/z* 323.0, 280.0, 239.2, 211.0, 193.1

ADP-1CP-Glc (**28**): HRMS (ESI⁻) Accurate Mass for C₁₇H₂₆N₅O₁₄P₂[M-H]⁻ (*m/z* calcd 586.0957). Found: 586.0951; LRMS (ESI) = *m/z* 586.0. EPI fragments = *m/z* 550.1, 346.1, 239.1, 211.0

CDP-1CP-Glc (**29**): HRMS (ESI⁻) Accurate Mass for C₁₇H₂₆N₃O₁₅P₂[M-H]⁻ (*m/z* calcd 562.0845). Found: 562.0807; LRMS (ESI) = *m/z* 562.1, EPI fragments = *m/z* 525.8, 322.1, 255.4, 239.0, 211.02

GDP-1CP-Glc (**30**): HRMS (ESI⁻) Accurate Mass for C₁₇H₂₆N₅O₁₅P₂[M-H]⁻ (*m/z* calcd 602.0906). Found: 602.0878; LRMS (ESI) = *m/z* 602.0, EPI fragments = *m/z* 565.9, 547.6, 362.0, 300.9, 257.0, 211.1

dTDP-1CP-Gal (**27**): C₁₇H₂₇N₂O₁₅P₂[M-H]⁻ (*m/z* calcd 561.0892) LRMS (ESI) = *m/z* 561.1 EPI fragments = *m/z* 524.7, 321.0, 300.9, 257.0, 253.3, 234.9

dTDP-2F-Glc (**34**): HRMS (ESI⁻) Accurate Mass for C₁₇H₂₄FN₂O₁₅P₂[M-H]⁻ (*m/z* calcd 565.0641). Found: 565.1748; LRMS (ESI) = *m/z* 564.8 EPI fragments = *m/z* 564.8, 321.3, 300.1, 257.0, 253.3, 225.2

UDP-2F-Glc (**35**): HRMS (ESI⁻) Accurate Mass for C₁₇H₂₂FN₂O₁₆P₂[M-H]⁻ (*m/z* calcd 567.0434). Found: 567.1371; LRMS (ESI) = *m/z* 566.9 EPI fragments = *m/z* 566.9, 323.1, 280.1, 257.0, 253.3, 225.2

dTDP-1CPS-Glc (**60**): C₁₇H₂₇N₂O₁₄P₂S[M-H]⁻ (*m/z* calcd 577.0664) LRMS (ESI) = *m/z* 577.1 EPI fragments = *m/z* 577.1, 321.3, 311.2, 251.3, 227.1

6.2 Synthetic Procedures

NMR spectra were recorded on a Bruker AV 500 (¹H at 500, ¹³C at 125 MHz, ³¹P at 202.5 MHz) instrument at the Nuclear Magnetic Resonance Research Resource (NMR-3) or on the Bruker Avance/DRX-500 high-resolution spectrometer at the National Research Council Canada Institute for Marine Biosciences in Halifax. Except where specified, all reagents were purchased from commercial sources and were used without further purification, unless otherwise noted. Anhydrous THF was purified via filtration through alumina using an Innovative Technology solvent purification system and stored over 3Å molecular sieves. Solvents were reagent grade unless otherwise noted and were further dried when necessary. Chromatograms were initially examined under UV light and then

visualised with aqueous potassium permanganate (dip) followed by heating of the TLC plate with a heat gun. All anhydrous reactions were carried out in oven-dried glassware (>180 °C), which was cooled in a desiccator and was flushed with N₂ before use. Molecular sieves were activated before applications by storing in an oven (>180 °C) for 12 h. Evaporations were achieved using a Büchi rotary evaporator followed by drying using an Edward rotary vacuum pump. A Heto PowerDry LL1500 freeze dryer was used for lyophilization of samples.

6.2.1 3,4,5,7-Tetra-*O*-benzyl-1,2-dideoxy-D-glucoheptenitol (**6**)¹⁷

To a stirred suspension of methyltriphenylphosphonium bromide (23.0 g, 64.4 mmol) in anhydrous 1,2-dimethoxyethane (230 mL) at -78 °C under nitrogen atmosphere, *n*-BuLi (25.7 mL of 2.5 M in hexanes, 64.4 mmol) was added dropwise. The resulting orange reaction mixture was allowed to warm to room temperature over 30 min. In a separate flask under a nitrogen atmosphere and at -78 °C, *n*-BuLi (8.90 mL of 2.5 M in hexanes, 22.2 mmol) was added to a stirred solution of 2,3,4,6-tetra-*O*-benzyl-D-glucopyranose (**5**) (12.0 g, 22.2 mmol) in anhydrous 1,2-dimethoxyethane (300 mL). This mixture was allowed to warm to room temperature over 20 min and then added to the orange ylide solution prepared above. The resultant dark orange reaction mixture turned red after being stirred at 45 °C for 2 h. Acetone (132 mL) was added to the reaction mixture and immediately formed precipitate. The resulting solid gradually dissolved, yielding an orange solution that was stirred for an additional 2 h. After evaporation, the residue was suspended in brine (400 mL) and extracted with diethyl ether (400 mL x 2). The combined organic extracts were dried (MgSO₄), filtered and concentrated. Purification by flash chromatography (EtOAc/hexanes, 15/85) afforded compound **6** (9.47 g, 79%) as

a colorless liquid; R_f 0.41 (EtOAc/hexanes, 20/80); LRMS (ESI): found $(M+Na)^+$ 561.4. $C_{35}H_{38}O_5$ requires $(M+Na)^+$ 561.3.

6.2.2 C-(1-Deoxy-2,3,4,6-tetra-O-benzyl- α -D-glucopyranosyl) iodomethane (**7**)¹⁷

Under a nitrogen atmosphere, a solution of **6** (217 mg, 0.403 mmol) and mercuric trifluoroacetate (172 mg, 0.403 mmol) in anhydrous THF (4 mL) was stirred at rt for 18 h. The reaction mixture was then charged with KCl 0.8M (4 mL) and the solution was stirred for a further 5 h. THF was removed *in vacuo* and the remaining aqueous solution was extracted with DCM (15 mL x 2). The combined organic extracts were washed with brine (20 mL) and dried (Na_2SO_4), filtered and concentrated. This residue (a single spot, **6a**, R_f 0.27 (EtOAc/hexanes, 20/80) and iodine (161 mg, 0.634 mmol) were immediately dissolved in anhydrous DCM (6 mL) under a nitrogen atmosphere and stirred for 2 h. The reaction flask was then charged with 10% $Na_2S_2O_3$ (3 mL) and stirred for 10 min. The organic layer was removed and washed with 5% KI (5 mL), brine (5 mL), dried (Na_2SO_4) and concentrated. Silica column chromatography (EtOAc/hexanes, 10/90) gave a mixture of two compounds (R_f 0.60 and R_f 0.66, hexanes-EtOAc, 4:1) which were separated by a further column chromatography (EtOAc/hexanes, 8/92) to afford **7** (161 mg, 60%, 2 steps) as a colorless solid; R_f 0.66 (EtOAc/hexanes, 20/80).

6.2.3 Diethyl C-(1-deoxy-2,3,4,6-tetra-O-benzyl- α -D-glucopyranosyl) methanephosphonate (**8**)¹⁷

The iodo derivative **7** (198 mg, 0.298 mmol) was refluxed in triethyl phosphite (15 mL) for 16 h. The reaction mixture was concentrated under high vacuum and purified over silica column (EtOAc/hexanes, 40/60) to afford compound **8** (185 mg, 92%); R_f 0.24

(EtOAc/hexanes, 50:50); δ_{H} (500 MHz; CDCl_3) 1.27, 1.28 (6H, t, J 7.0 Hz, $2 \times \text{OCH}_2\text{CH}_3$), 2.20 (2H, m, 1'a-H and 1'b-H), 3.79-3.61 (6H, m, 2-H, 3-H, 4-H, 5-H, 6a-H and 6b-H), 4.09, 4.07 (each 2H, q, J 7.0 Hz, $2 \times \text{OCH}_2\text{CH}_3$), 4.54 (1H, m, $^1J_{\text{C,H}}$ 150 Hz, 1-H), 4.47, 4.50, 4.61, 4.64, 4.67, 4.77, 4.80, 4.88 (each 1H, d, $J \sim 12$ Hz, $4 \times \text{PhCH}_2$), 7.10-7.35 (20H, m, $4 \times \text{Ph}$); δ_{C} (125 MHz, CDCl_3) 16.6(x2) (CH_3 , d, $^3J_{\text{CH}_3,\text{P}}$ 6.1 Hz, OCH_2CH_3), 22.6 (CH_2 , d, $^1J_{\text{C}1',\text{P}}$ 145 Hz, C-1'), 61.6, 61.9 (each CH_2 , d, $^2J_{\text{CH}_2,\text{P}}$ 6.3 Hz, OCH_2CH_3), 68.8 (CH_2 , C-6), 69.9 (CH , d, $^2J_{\text{C}1,\text{P}}$ 5.3 Hz, C-1), 72.1 (CH , C-3 or C-4 or C-5), 73.3, 73.7, 75.1, 75.5 (all CH_2 , $4 \times \text{PhCH}_2$), 77.8 (CH , C-3 or C-4 or C-5), 79.3 (CH , d, $^3J_{\text{C}2,\text{P}}$ 13.0 Hz, C-2), 82.0 (CH , C-3 or C-4 or C-5), 127.8-138.7 (4C and 20CH, $4 \times \text{Ph}$); δ_{P} (202.5 MHz, CDCl_3) 29.18 (s); LRMS (ESI): found $(\text{M}+\text{Na})^+$ 697.3. $\text{C}_{39}\text{H}_{47}\text{O}_8\text{P}$ requires $(\text{M}+\text{Na})^+$, 697.3.

6.2.4 Ammonium C-(1-deoxy- α -D-glucopyranosyl)methane phosphonate (**1**)¹⁷

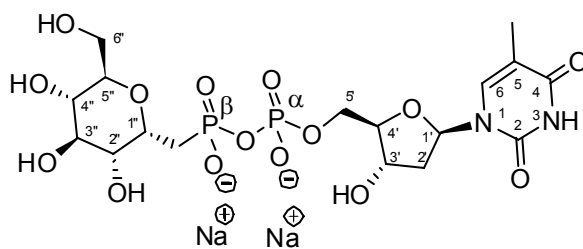
Under a nitrogen atmosphere and at 0 °C, a stirring solution of **8** (43 mg, 0.063 mmol) in anhydrous DCM (0.5 mL) was treated with iodotrimethylsilane (500 μL , 3.51 mmol) and allowed to warm to rt over 2 h. The reaction was quenched by methanol. The mixture was concentrated, dissolved in H_2O (10 mL) and washed with diethyl ether (10 mL x 8). The aqueous layer was passed through Amberlite IR-120 (H^+) ion exchange resin and the resulting acidic aqueous fraction was immediately adjusted to pH 8 with NH_4OH 0.2 M, concentrated to 5 mL, and lyophilized to afford the target phosphonate **5** as a colorless foam (18 mg, 100%); δ_{H} (500 MHz; D_2O) 1.78 (2H, m, 1'a-H and 1'b-H), 3.17 (1H, dd, $J_{3,4} \sim J_{4,5} \sim 9$ Hz, 4-H), 3.43-3.55 (4H, m, 2-H, 3-H, 5-H and 6a-H), 3.65 (1H, d, $^2J_{6b,6a}$ 11.8 Hz, 6b-H), 4.20 (1H, m, 1-H); δ_{C} (125 MHz; D_2O) 25.9 (CH_2 , d, $^1J_{\text{C}1',\text{P}}$ 129 Hz, C-

1'), 61.0 (CH₂, C-6), 70.4 (CH, C-4), 71.6 (CH, d, ³J_{C₂,P} 8.0 Hz, C-2), 72.5 (CH, d, ²J_{C₁,P} 2.1 Hz, C-1), 72.9 (CH, C-3 or C-5), 73.5 (CH, C-5 or C-3); δ_{C-H coupled} 72.5 (CH, d, ¹J_{C₁,H} 150 Hz, C-1); δ_P (202.5 MHz; D₂O) 19.90 (s); HRMS (ESI, negative mode): found (M-H)⁻, 257.0433. C₇H₁₄O₈P requires (M-H)⁻, 257.0432.

6.2.5 Phosphono analogue of dTDP-α-D-glucopyranose (dTDP-1CP-Glc) (**25**)

A modification of the assay conditions described above was used to scale up enzymatic coupling in order to purify and characterize the enzymatic coupling product of **1** and dTTP. A reaction was set up containing **1** (10.0 mg, 34.2 μmol), dTTP (27.0 mg, 47.8 μmol), MgCl₂ (4.9 mg, 51.3 μmol), and 5 EU inorganic pyrophosphatase, which was initiated by the addition of nucleotidyltransferase (336 EU, split into two equal portions) in Tris-HCl buffer (20 mM final buffer concentration pH 7.5, 2 mL reaction volume). The enzymatic reaction was monitored by HPLC and was stopped following 6 h (ca. 20 % conversion based on dTTP). This was done due to concern of possible product breakdown after prolonged incubation periods, in addition to a limited quantity of fresh enzyme. Following incubation for 6 h at 37 °C, alkaline phosphatase (80 EU) was added to the mixture, and allowed to incubate overnight at 25 °C. After the set time, the protein was precipitated with 2 mL methanol and the precipitate was washed with another 2 mL of methanol. The purification steps were performed as described in the literature with an extra desalting step.⁵² The sugar nucleotide product mixture was concentrated and re-dissolved in aqueous tributylammonium bicarbonate buffer (10 mM, ~2 mL) for purification via C18 ion-pair reversed-phase chromatography. The aqueous tributylammonium bicarbonate buffer was prepared by adding tributylamine (2.4 mL, 10 mmol/ L) to H₂O and bubbling CO₂ (obtained from the sublimation of dry ice) into the

solution (~2 h). Automated C18 reversed-phase ion-pair chromatography was performed using a 12 M (12 mm x 15 cm) Biotage C18 reversed-phase column. Compounds containing nucleotide base chromophores were monitored at 254 nm. A solvent system of 100/0 A/B (2 CV) followed by a linear gradient to 60/40 A/B over 15 CV and a plateau at 60/40 A/B (2 CV) was used where A represents 10 mM aqueous tributylammonium bicarbonate buffer and B represents HPLC MeOH at a flow rate of 10 mL/min. The C18 column was then washed with 0/100 A/B for 3 CV. All UV fractions containing sugar nucleotides, as judged by HPLC, were combined and concentrated to ~2 mL in volume and passed through a cation-exchange column (Dowex® 50W-X8 cation exchange resin (100-200 mesh, Na⁺ form, 18 mm x 14 cm)) in order to bind tributylammonium cations and generate the sodium salt of the desired sugar nucleotide. Further desalting of the product mixture was performed by using a Sephadex G10 column (1.5 cm x 100 cm) with water as eluant to afford compound dTDP-1CP-Glc (**25**), with an isolated yield of 6.8 mg (0.012 mmol, yield = 35% by mass, 34% by UV absorbance [$\epsilon = 9.7 \times 10^4 \text{ M}^{-1}\text{cm}^{-1}$ at a $\lambda_{\text{max}} = 267 \text{ nm}$]⁸⁹



δ_{H} (500 MHz; D₂O) 1.85 (3H, br s, 5CH₃-H), 2.06 (1H, ddd, $^2J_{1''\text{CH}2\text{a},\text{P}}$ 17 Hz, $^2J_{1''\text{CH}2\text{a},\text{b}}$ 16 Hz and $^3J_{1''\text{CH}2\text{a},1''}$ 4 Hz, 1''CH₂a-H), 2.15 (1H, ddd, $^2J_{1''\text{CH}2\text{b},\text{P}}$ 17 Hz, $^2J_{1''\text{CH}2\text{b},\text{a}}$ 16 Hz and $J_{1''\text{CH}2\text{b},1''}$ 11 Hz, 1''CH₂b-H), 2.25-2.34 (2H, m, 2'a-H and 2'b-H), 3.31 (1H, dd, $J_{4'',3''} \sim$

$J_{4'',5''} \sim 9.4$ Hz, 4''-H), 3.53 (1H, dd, $J_{3'',2''} \sim J_{3'',4''} \sim 9.4$ Hz, 3''-H), 3.58 (1H, ddd, $J_{5'',4''} 9.4$ Hz, $J_{5'',6''b} 5$ Hz and $J_{5'',6''a} 2.2$ Hz, 5''-H), 3.61-3.64 (1H, obscured m, 2''-H), 3.64 (1H, obscured dd, ${}^2J_{6''a,6''b} 12.2$ Hz and $J_{6''a,5''} 5$ Hz, 6''a-H), 3.76 (1H, dd, ${}^2J_{6''b,6''a} 12.2$ Hz and $J_{6''b,5''} 2.2$ Hz, 6''b-H), 4.08-4.11 (3H, m, 4'-H, 5'a-H and 5'b-H), 4.35 (1H, dddd, $J_{1'',P} \sim J_{1'',1''CH2b} \sim 10$ Hz and $J_{1'',2''} \sim J_{1'',1''CH2a} \sim 4$ Hz, 1''-H), 4.55 (1H, ddd, $J_{3',2'} \sim 6$ Hz, and $J_{3',2'a} \sim J_{3',4'} \sim 3$ Hz, 3'-H), 6.27 (1H, dd, $J_{1',2'a} \sim J_{1',2'b} \sim 7$ Hz, 1'-H), 7.67 (1H, s, 6-H); δ_C (125 MHz, D₂O) 11.7 (CH₃, 5-CH₃), 24.3 (CH₂, d, ${}^1J_{1''CH2,P} 139.7$ Hz, C-1''CH₂), 38.6 (CH₂, C-2'), 60.8 (CH₂, C-6''), 65.2 (CH₂, d, ${}^2J_{C5',P} 5.4$ Hz, C-5'), 70.1 (CH, C-4''), 70.9 (CH, C-3'), 71.1 (CH, d, ${}^3J_{C2'',P} 12.4$ Hz, C-2''), 72.0 (CH, d, ${}^2J_{C1'',P} 4.5$ Hz, C-1''), 72.6 (CH, C-5''), 73.2 (CH, C-3''), 85.0 (CH, C-1'), 85.4 (CH, d, ${}^3J_{C2'',P} 8.8$ Hz, C-4'), 111.8 (C, C-5), 137.4 (CH, C-6), 151.9 (C, C-2), 160.3 (C, C-4); δ_P (202.5 MHz, D₂O) -11.5 (1P, d, $J_{P\alpha,P\beta} 27$ Hz, P- α), 14.6 (1P, d, $J_{P\beta,P\alpha} 27$ Hz, P- β). HRMS (ESI): found [M-H]⁻ 561.0877. C₁₇H₂₇N₂O₁₅P₂ requires [M-H]⁻, 561.0892.

6.2.6 Tetraisopropyl mono- and difluoromethylenediphosphonate (**39,40**)

This reaction was performed under an inert atmosphere of nitrogen. Tetraisopropyl methylenediphosphonate (**38**) was distilled prior to conducting the experiment. **38** (0.198 g, 0.58 mmol) in DMF (2 mL) was cooled to 0 °C in an ice-bath. In a separate flask NaH (0.041 g, 1.74 mmol) was suspended in DMF (2 mL), cooled to 0 °C for 5 min, and added drop-wise via syringe to the flask containing the starting phosphonate. The mixture was stirred at 0 °C for a further 10 min, then at room temperature for 1 h, then cooled to 0 °C for 10 min. In a separate flask, Selectfluor® (1-chloromethyl-4-fluoro-1,4-diazabicyclo[2.2.2]octane bis(tetrafluoroborate) (5.14 g, 14.5 mmol) was dissolved in

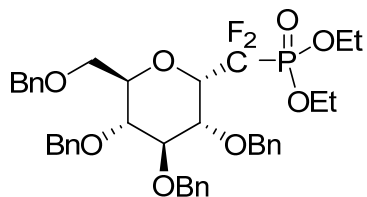
DMF (3 mL), cooled in an ice-bath for 15 min, and added all at once by syringe to the flask containing the anion of the **38**. The reaction mixture was stirred at 0 °C for 30 min, and then at room temperature for 1 h. The reaction progress was monitored by removing 0.6 mL aliquots for ^{31}P NMR spectroscopy [**38** 18.15 ppm(s); **39** 9.80 ppm, (d), $^2J_{\text{P,F}}$ 61.76 Hz; **40** 1.85 ppm, (t), $^2J_{\text{P,F}}$ 85.42 Hz], when a ratio of approximately 1:1:1 was observed, the reaction mixture was cooled in an ice-bath for 10 min, diluted with CH_2Cl_2 (15 mL) and quenched by the addition of saturated aqueous ammonium chloride (5-10 mL). The bottom layer was removed and the upper layer was extracted with CH_2Cl_2 (2 x 10 mL). The combined organic extracts were dried over anhydrous sodium sulfate, then concentrated to a syrup, which upon purification by silica gel column chromatography (EtOAc/hexane, 20/80) afforded 0.083 g of **39** (40 %) and 0.064 g of **40** (29 %). δP **39** 9.80 ppm (d, $^2J_{\text{P,F}}$ 61.31 Hz); **40** 1.85 ppm (t, $^2J_{\text{P,F}}$ 85.36 Hz].⁶³

6.2.7 Mono- and difluoromethylenediphosphonic acid (**39a**, **40a**)

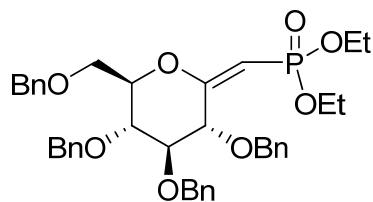
This reaction was not conducted under nitrogen. Compounds **39** and **40** in aqueous HCl (5 mL, 6 M) were refluxed for 24 h, after which time ^{31}P NMR spectroscopy indicated complete hydrolysis of the starting ester **39** (9.80 (d, $^2J_{\text{P,F}}$ 61.31 Hz)) into **39a** (11.12 (d $^2J_{\text{P,F}}$ 65.27 Hz)) and **40** (1.85 (d, $^2J_{\text{P,F}}$ 85.36 Hz)) into **40a** (3.58 (d, $^2J_{\text{P,F}}$ 87.79 Hz)) , the mixture was concentrated *in vacuo*. Methanol (5 x 5 mL) was added, and the volatiles were then removed *in vacuo*, to yield, after drying, 0.083 g of **39a** (100%) and 0.064 g of **40a** (100%)

6.2.8 Diethyl C-(1-deoxy-2,3,4,6-tetra-*O*-benzyl- α -D-glucopyranosyl) difluoromethanephosphonate (**41**)

Method C. This reaction was performed under an inert atmosphere of nitrogen.

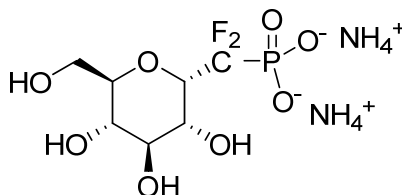


To a solution of **8** (0.068 g, 0.1 mmol) and *N*-fluorobenzenesulfonimide (0.078 g, 0.25 mmol) in dry THF (5 mL) at $-78\text{ }^{\circ}\text{C}$ was added NaHMDS (1.0 M in THF, 0.25 mL, 0.25 mmol) over 2 min. The reaction was stirred for 2 h at $-78\text{ }^{\circ}\text{C}$, and then allowed to warm to room temperature, and stirred for an additional 16 h. The reaction was quenched with a saturated solution of NH_4Cl solution, extracted with three portions of CH_2Cl_2 and washed with brine. The combined organic layers were dried over Na_2SO_4 , and then concentrated. The residue was subject to flash chromatography (EtOAc/hexanes, 30/70) which gave **41** as a colourless oil (0.0063 g, 9%) R_f 0.41 (EtOAc/hexanes, 50/50). δ_{H} (500 MHz; CDCl_3) 1.39 (6H, t, J 6.6, $2\times\text{OCH}_2\text{CH}_3$), 3.65 (2H, m, 6a-H and 6b-H), 4.30-4.11 (4H, m, 2-H, 3-H, 4-H), 4.12 (4H, q, $J \sim 6.0$ Hz, $2\times\text{OCH}_2\text{CH}_3$), 4.49, 4.51, 4.57, 4.64, 4.67, 4.71, 4.84, 4.94 (each 1H, d, $J \sim 12$ Hz, $4\times\text{PhCH}_2$), 4.60 (1H, app. ddd, $^3J_{\text{H,F}}$ 18 Hz, $^3J_{\text{H,P}}$ 12 Hz, $^3J_{\text{H}_1,\text{H}_2}$ 3 Hz, 1-H), 7.13-7.45 (20H, m, $4\times\text{Ph}$); δ_{C} (125 MHz, CDCl_3) 16.9 ($2\times\text{CH}_3$, d, $^3J_{\text{CH}_3,\text{P}}$ 5.4 Hz, OCH_2CH_3), 64.8 (CH, d, $^3J_{\text{C}_2,\text{P}}$ 13.0 Hz, C-2), 68.3 (CH_2 , C-6), 72.9, 73.8, 75.6, 81.3 (all CH_2 , $4\times\text{PhCH}_2$), 73.3 (CH, C-3 or C-4 or C-5), 77.8 (CH, C-3 or C-4 or C-5), 78.9 ($2\times\text{CH}_2$, d, $^2J_{\text{CH}_2,\text{P}}$ 7 Hz, OCH_2CH_3), 82.0 (CH, C-3 or C-4 or C-5), 90.2 (CF_2 , d, $^1J_{\text{C}_1',\text{P}}$ 145 Hz, C-1'), 102.9 (CH, m, C-1), 127.9-133.6 (4C and 20CH , $4\times\text{Ph}$); δ_{P} (202.5 MHz, CDCl_3) 6.95 (t, $^2J_{\text{P,F}}$ 115.46 Hz); HRMS (ESI): found $(\text{M}+\text{Na})^+$ 773.1076 $\text{C}_{39}\text{H}_{45}\text{O}_8\text{PF}_2$ requires $(\text{M}+\text{Na})^+$, 773.2712. LRMS (ESI): found $(\text{M}+\text{Na})^+$ 772.9



From the same column, the exo-glycal **41a** was isolated via flash chromatography (EtOAc/hexanes, 30/70) which resulted in a colourless oil (0.022 g, 33%): R_f 0.29 (EtOAc/hexanes, 50/50); δ_H (500 MHz; $CDCl_3$) 1.40 (6H, t, J 6.6, $2 \times OCH_2CH_3$), 3.68 (2H, m, 6a-H and 6b-H), 4.16-3.76 (3H, m, 3-H, 4-H, 5-H), 4.14 (4H, q, $J \sim 6.0$ Hz, $2 \times OCH_2CH_3$), 4.51 (1H, ddd, $^3J_{H_2-H_3}$ 10 Hz, $^4J_{H_{1'}-H_2}$ 1 Hz, $^4J_{H_2-P}$ 3 Hz, 2-H) 4.46, 4.48, 4.73, 4.76, 4.79, 4.84, 4.90, 4.94 (each 1H, d, J 11 Hz, $4 \times PhCH_2$), 5.51 (1H, dd, $^4J_{H_{1'}-H_2}$ 1.5 Hz, $^2J_{H_{1'}-P}$ 13 Hz, 1'-H), 7.16-7.43 (20H, m, $4 \times Ph$); δ_C (125 MHz, $CDCl_3$) 17.3 ($2 \times CH_3$, d, $^3J_{CH_3,P}$ 5.1 Hz, OCH_2CH_3), 68.2 (CH_2 , C-6), 72.6, 73.5, 75.2, 75.7 (all CH_2 , $4 \times PhCH_2$), 73.9 (CH, C-3 or C-4 or C-5), 74.4 (CH, d, $^3J_{C_2,P}$ 13.1 Hz, C-2), 78.0 (CH, C-3 or C-4 or C-5), 78.9 ($2 \times CH_2$, d, $^2J_{CH_2,P}$ 5.7 Hz, OCH_2CH_3), 81.8 (CH, C-3 or C-4 or C-5), 94.42 (CH, d, $^1J_{C_{1'}-P}$ 188.2 Hz, C-1'), 129.3-135.2 (4C and 20CH, $4 \times Ph$), 163.3 (CH, d, $^2J_{C_1-P}$ 1.2 Hz C-1); δ_P (202.5 MHz, $CDCl_3$) 17.11; HRMS (ESI): found $(M+Na)^+$ 695.2611 $C_{39}H_{45}O_8P$ requires $(M+Na)^+$, 695.2750. LRMS (ESI): found $(M+Na)^+$ 695.3

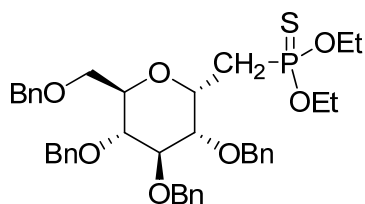
6.2.9 Ammonium C-(1-deoxy- α -D-glucopyranosyl)methane difluorophosphonate (**36**)



Under a nitrogen atmosphere and at 0 °C, a stirring solution of **41** (6.3 mg, 0.008 mmol)

in anhydrous DCM (0.5 mL) was treated with iodotrimethylsilane (60 μ L, 0.4 mmol) and allowed to warm to rt over 2 h. Monitored by TLC using 6/3/1 n-propanol-NH₃-H₂O (R_f : 0.34). After quenching with methanol, the mixture was concentrated and dissolved in H₂O (10 mL) and washed with diethyl ether (10 mL x 8). The resulting acidic aqueous layer was immediately adjusted to pH 8 with NH₄OH 0.2 M, concentrated to 5 mL, purified by cellulose column (1.5 x 10 cm, 2.5 g) (n-propanol-NH₃-H₂O, 8/1/1). The resulting fraction was lyophilized to afford the target phosphonate **36** as a white film (2.4 mg, 88%); δ_H (500 MHz; D₂O) 3.22 (1H, dd, 4-H), 3.41-3.63 (4H, m, 2-H, 3-H, 5-H, 6a-H and 6b-H), 4.52 (1H, m, 1-H); δ_C (125 MHz; D₂O) 63.4 (CH₂, C-6), 71.4 (CH, C-4), 72.9 (CH, app. d, C-2), 73.7 (CH, C-3), 74.4 (CH, C-5); 72.5 (CH, d, $^2J_{C1,P}$ 2.1 Hz, C-1), 92.2 (CF₂, br. m, C-1') δ_P (202.5 MHz; D₂O) -9.8 (t, $^2J_{P,F}$ 108.31 Hz). HRMS (ESI): found (M-H)⁻, 292.9842. C₇H₁₂F₂O₈P requires (M-H)⁻, 293.0243. LRMS (ESI): found (M-H)⁻ 292.8

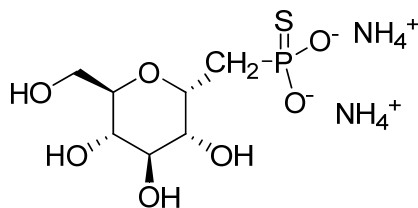
6.2.10 Diethyl C-(1-deoxy-2,3,4,6-tetra-O-benzyl- α -D-glucopyranosyl) methane thiophosphonate (**49**)



To a suspension of **8** (98.9 mg, 0.146 mmol) in toluene (8 mL) was added Lawesson's reagent (58.6 mg, 0.146 mmol) in one portion. The reaction was warmed to 55 °C for 12 h and then cooled to room temperature. The yellow reaction mixture was filtered, and then the filtrate was concentrated and chromatographed (EtOAc/hexanes, 15/85) to afford **49** (72.4 mg, 0.105 mmol, 71%) as a white solid: R_f 0.61 (EtOAc/hexanes, 80/20); δ_H

(500 MHz; CDCl₃) 1.28, 1.33 (6H, t, *J* 7.0 Hz, 2xOCH₂CH₃), 2.47 (2H, m, 1'a-H and 1'b-H), 3.82-3.66 (6H, m, 2-H, 3-H, 4-H, 5-H, 6a-H and 6b-H), 4.16, 4.12 (each 2H, q, *J* 7.0 Hz, 2xOCH₂CH₃), 4.59 (1H, m, ¹J_{C,H} 142 Hz, 1-H), 4.45, 4.49, 4.64, 4.66, 4.71, 4.76, 4.82, 4.87 (each 1H, d, *J* ~11 Hz, 4xPhCH₂), 7.17- 7.39 (20H, m, 4xPh); δC (125 MHz, CDCl₃) 16.4(x2) (CH₃, d, ³J_{CH₃,P} 7.3 Hz, OCH₂CH₃), 30.5 (CH₂, d, ¹J_{C1',P} 116 Hz, C-1'), 62.6, 62.7 (each CH₂, d, ²J_{CH₂,P} 6.9 Hz, OCH₂CH₃), 68.7 (CH₂, C-6), 70.2 (CH, d, ²J_{C1,P} 3.2 Hz, C-1), 72.1 (CH, C-3 or C-4 or C-5), 73.3, 73.7, 75.2, 75.6 (all CH₂, 4xPhCH₂), 77.8 (CH, C-3 or C-4 or C-5), 79.3 (CH, d, ³J_{C₂,P} 14.1 Hz, C-2), 82.2 (CH, C-3 or C-4 or C-5), 127.7-138.8 (4C and 20CH, 4xPh); δP (202.5 MHz, CDCl₃) 96.81(s); HRMS (ESI): found (M+Na)⁺ 713.2494 C₃₉H₄₇O₇PS requires (M+Na)⁺, 713.2672. LRMS (ESI): found (M+Na)⁺ 713.1 requires (M+Na)⁺, 713.3

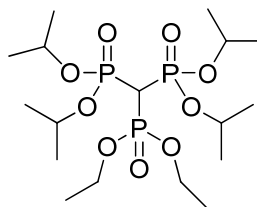
6.2.11 Ammonium C-(1-deoxy-α-D-glucopyranosyl)methane thiophosphonate (**37**)



Under a nitrogen atmosphere and at 0 °C, a stirring solution of **49** (72.4 mg, 0.105 mmol) in anhydrous DCM (0.5 mL) was treated with iodotrimethylsilane (740 μL, 5.25 mmol) and allowed to warm to rt over 2 h. Monitored by TLC using 6:3:1 n-propanol-NH₃-H₂O (R_f: 0.70). The reaction was quenched by methanol. The mixture was concentrated, dissolved in H₂O (10 mL) and washed with diethyl ether (10 mL x 8). The resulting acidic aqueous layer was immediately adjusted to pH 8 with NH₄OH 0.2 M, concentrated to 5 mL, purified by cellulose column (1.5 x 10 cm, 2.5 g) (n-propanol-NH₃-H₂O, 8/1/1).

The resulting fraction was lyophilized to afford the target phosphonate **37** as a white film (13 mg, 42%); δ_{H} (500 MHz; D₂O) 2.41 (2H, m, 1'a-H and 1'b-H), 3.37 (1H, m, 4-H), 3.44-3.56 (4H, m, 2-H, 3-H, 5-H and 6a-H), 3.68 (1H, d, $^2J_{6b,6a}$ 11.2 Hz, 6b-H), 4.43 (1H, m, 1-H); δ_{C} (125 MHz; D₂O) 28.7 (CH₂, d, $^1J_{\text{C}1',\text{P}}$ 112 Hz, C-1'), 60.4 (CH₂, C-6), 69.5 (CH, C-4), 70.3 (CH, d, $^3J_{\text{C}2,\text{P}}$ 13.7 Hz, C-2), 71.4 (CH, C-3 or C-5), 72.1 (CH, d, $^2J_{\text{C}1,\text{P}}$ 4.1 Hz, C-1), 73.5 (CH, C-5 or C-3); δ_{P} (202.5 MHz; D₂O) 87.9 (s); HRMS (ESI⁻): found (M-H)⁻, 257.0463. C₇H₁₄O₇PS requires (M-H)⁻, 257.0245. LRMS (ESI⁻): found (M-H)⁻, 257.1

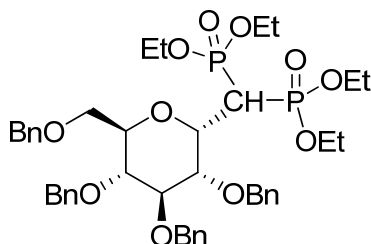
6.2.12 Diethyl tetraisopropyl methylenetrphosphonate (**52**)



Under an inert atmosphere of nitrogen, tetraisopropyl methylenebisphosphonate **38** (89.3 μL , 0.28 mmol) was dissolved in THF (8 mL) and was stirred at -78 °C. To this solution, four equivalents of NaHMDS (1.12 mL, 1.12 mmol) were added dropwise via syringe. The resulting mixture was allowed to stir for 30 min at which time four equivalents of diethyl chlorophosphite (159.6 μL , 1.12 mmol) slowly added to the reaction. The reaction was stirred at this temperature for 2 h, and then was allowed to warm to 0 °C over 30 min. The P(III) intermediate (**51**) was then oxidized *in situ* by quenching the reaction by slow addition of hydrogen peroxide (30%, 0.62 mL, 5 eq), and the resulting mixture was stirred vigorously at 0 °C for 10 min. THF was removed *in vacuo* and the remaining aqueous solution was extracted with DCM (15 mL x 3). The combined organic extracts

were washed with brine (25 mL), dried (Na₂SO₄), filtered, and concentrated. The extracts were then chromatographed (EtOAc/hexanes, 80/20), and aliquots were monitored by ESI-MS/MS until **52** was eluted and collected (96.1 mg, 0.20 mmol, 72%) as a clear oil; δ_{H} (500 MHz, CDCl₃) 1.28-1.44 (30H, m), 3.09 (1H, q, *J* 25.1 Hz), 4.10-4.33 (4H, m), 4.74-5.01 (4H, m) δ_{C} (125 MHz, CDCl₃) 17.1 (CH₃, OCH₂CH₃), 25.2 (CH₃, OCH(CH₃)₂), 51.1 (CH, br. m, CH(P(O)OR₂)), 59.8 (CH₂, OCH₂CH₃), 69.9 (CH₃, OCH(CH₃)₂); δ_{P} (202.5 MHz, CDCl₃) 12.78 (d, *J* 34.97 Hz), 15.21 (t, *J* 34.97 Hz); HRMS (ESI): found (M+Na)⁺ 503.1605 C₁₇H₄₀O₉P₃ requires (M+Na)⁺, 503.1699 LRMS (ESI⁺): found (M+Na)⁺, 503.1

6.2.13 Diethyl C-(1-deoxy-2,3,4,6-tetra-O-benzyl- α -D-glucopyranosyl) methane bisphosphonate (**53**)



Under an inert atmosphere of nitrogen, **8** (39.1 mg, 0.058 mmol) was dissolved in THF (6 mL) and was stirred at -78 °C. To this solution, four equivalents of NaHMDS (0.23 mL, 0.23 mmol) were added dropwise via syringe. The resulting mixture was allowed to stir for 30 min at which time four equivalents of diethyl chlorophosphite (33 μ L, 0.23 mmol) slowly added to the reaction. The reaction was stirred at this temperature for 2 h, and then was allowed to warm to 0 °C over 30 min. The P(III) intermediate was then oxidized *in situ* by quenching the reaction by slow addition of hydrogen peroxide (30%, 0.62 mL, 5 eq), and the resulting mixture was stirred vigorously at 0 °C for 10 min. THF was

removed *in vacuo* and the remaining aqueous solution was extracted with DCM (15 mL x 3). The combined organic extracts were washed with brine (25 mL), dried (Na₂SO₄), filtered, and concentrated. The extracts were then chromatographed twice (EtOAc/hexanes, 75/25 to 90/10), and aliquots were monitored by ESI-MS/MS until **53** was eluted and collected (6.6 mg, 0.008 mmol, 14%) as a pale yellow oil: R_f 0.12 (EtOAc/hexanes, 80/20) δ_H (500 MHz; CDCl₃) 1.27, 1.29 (12H, t, *J* 6.8, 2xOCH₂CH₃), 2.23 (m, 1H, ³*J*_{CH,H} 7.2 Hz, ²*J*_{CH,P1} and ²*J*_{CH,P2} 12.4 Hz, H-1'), 3.89-3.58 (m, 6H, H-2, H-3, H-4, H-5, H-6a, H-6b), 4.11 (8H, q, *J* 6.8 Hz, 2xOCH₂CH₃), 4.42, 4.56, 4.58, 4.65, 4.67, 4.76, 4.80, 4.89 (each 1H, d, *J* ~12.1 Hz, 4xPhCH₂), 4.60 (1H, m, 1-H), 7.13-7.45 (20H, m, 4xPh); δ_C (125 MHz, CDCl₃) 16.4 (x2) (CH₃, t, ³*J*_{CH3,P} 5.9 Hz, OCH₂CH₃), 43.6 (CH, t, ¹*J*_{C1',P1} and ¹*J*_{C1',P2} 141 Hz, C-1'), 62.3 (CH₂, t, ²*J*_{CH2,P} 6.4 Hz, OCH₂CH₃), 68.7 (CH₂, C-6), 69.2 (CH, t, ²*J*_{C1,P} 5.4 Hz, C-1), 72.0 (CH, C-3 or C-4 or C-5), 73.3, 73.5, 75.3, 75.5 (all CH₂, 4xPhCH₂), 77.9 (CH, C-3 or C-4 or C-5), 79.1 (CH, t, ³*J*_{C2,P} 12.8 Hz, C-2), 82.3 (CH, C-3 or C-4 or C-5), 125.6-139.4 (4C and 20CH, 4xPh); δ_P (202.5 MHz, CDCl₃) 18.63 (s); HRMS (ESI⁺): found (M+Na)⁺ 833.2736. C₄₃H₅₆O₁₁P₂ requires (M+Na)⁺, 833.3190. LRMS (ESI⁺): found (M+Na)⁺, 833.1

REFERENCES

- (1) Moretti, R.; Thorson, J. S. *J. Biol. Chem.* **2007**, *282*, 16942-16947.
- (2) Zuccotti, S.; Zanardi, D.; Rosano, C.; Sturla, L.; Tonetti, M.; Bolognesi, M. *J. Mol. Biol.* **2001**, *313*, 831-843.
- (3) Melo, A.; Glaser, L. *J. Biol. Chem.* **1965**, *240*, 398-405.
- (4) Ko, K. S.; Zea, C. J.; Pohl, N. L. *J. Org. Chem.* **2005**, *70*, 1919-1921.
- (5) Jin, X.; Ballicora, M. A.; Preiss, J.; Geiger, J. H. *EMBO J.* **2005**, *24*, 694-704.
- (6) Steiner, T.; Lamerz, A. C.; Hess, P.; Breithaupt, C.; Krapp, S.; Bourenkov, G.; Huber, R.; Gerardy-Schahn, R.; Jacob, U. *J. Biol. Chem.* **2007**, *282*, 13003-13010.
- (7) Sivaraman, J.; Sauve, V.; Matte, A.; Cygler, M. *J. Biol. Chem.* **2002**, *277*, 44214-44219.
- (8) Blankenfeldt, W.; Asuncion, M.; Lam, J. S.; Naismith, J. H. *EMBO J.* **2000**, *19*, 6652-6663.
- (9) Sheu, K. R.; Richard, J. P.; Frey, P. A. *Biochemistry* **1979**, *18*, 5548-5556.
- (10) Barton, W. A.; Lesniak, J.; Biggins, J. B.; Jeffrey, P. D.; Jiang, J. Q.; Rajashankar, K. R.; Thorson, J. S.; Nikolov, D. B. *Nat. Struct. Biol.* **2001**, *8*, 545-551.
- (11) Timmons, S. C.; Mosher, R. H.; Knowles, S. A.; Jakeman, D. L. *Org. Lett.* **2007**, *9*, 857-860.
- (12) Huestis, M. P.; Aish, G. A.; Hui, J. P.; Soo, E. C.; Jakeman, D. L. *Org. Biomol. Chem.* **2008**, *6*, 477-484.
- (13) Timmons, S. C.; Hui, J. P.; Pearson, J. L.; Peltier, P.; Daniellou, R.; Nugier-Chauvin, C.; Soo, E. C.; Syvitski, R. T.; Ferrieres, V.; Jakeman, D. L. *Org. Lett.* **2008**, *10*, 161-163.
- (14) Jiang, J. Q.; Biggins, J. B.; Thorson, J. S. *J. Am. Chem. Soc.* **2000**, *122*, 6803-6804.
- (15) Barton, W. A.; Biggins, J. B.; Jiang, J.; Thorson, J. S.; Nikolov, D. B. *Proc. Natl. Acad. Sci.* **2002**, *99*, 13397-13402.
- (16) Kornfeld, S.; Glaser, L. *J. Biol. Chem.* **1961**, *236*, 1791-1794.
- (17) Beaton, S. A.; Huestis, M. P.; Sadeghi-Khomami, A.; Thomas, N. R.; Jakeman, D. L. *Chem. Commun.* **2009**, 238-240.

- (18) Jakeman, D. L.; Young, J. L.; Huestis, M. P.; Peltier, P.; Daniellou, R.; Nugier-Chauvin, C.; Ferrieres, V. *Biochemistry* **2008**, *47*, 8719-8725.
- (19) Mizanur, R. M.; Zea, C. J.; Pohl, N. L. *J. Am. Chem. Soc.* **2004**, *126*, 15993-15998.
- (20) Jiang, J.; Biggins, J. B.; Thorson, J. S. *Angew. Chem. Int. Edit.* **2001**, *40*, 1502-1505.
- (21) Levy, D. E.; Fügedi, P.; Eds.; In *The Organic Chemistry of Sugars*; CRC/Taylor & Francis: Boca Raton, FL, **2006**, 286-363.
- (22) Nicotra, F. Synthesis of C-glycosides of biological interest. *Glycoscience Synthesis of Substrate Analogs and Mimetics* **1997**, 55-83.
- (23) De Clercq, E. *Biochem. Pharmacol.* **2007**, *73*, 911-922.
- (24) Russell, R. G. G.; Rogers, M. J. *Bone* **1999**, *25*, 97-106.
- (25) Chapleur, Y.; *Carbohydrate Mimics: Concepts and Methods*; John Wiley & Sons Canada, Ltd., **1998**; 67-85
- (26) Zhang, C.; Griffith, B. R.; Fu, Q.; Albermann, C.; Fu, X.; Lee, I.; Li, L.; Thorson, J. S. *Science* **2006**, *313*, 1291-1294.
- (27) Minami, A.; Uchida, R.; Eguchi, T.; Kakinuma, K. *J. Am. Chem. Soc.* **2005**, *127*, 6148-6149.
- (28) Breton, C.; Snajdrova, L.; Jeanneau, C.; Koca, J.; Imberty, A. *Glycobiology* **2006**, *16*, 29R-37R.
- (29) Lovering, A. L.; de Castro, L. H.; Lim, D.; Strynadka, N. C. *Science* **2007**, *315*, 1402-1405.
- (30) Gordon, R. D.; Sivarajah, P.; Satkunarajah, M.; Ma, D.; Tarling, C. A.; Vizitiu, D.; Withers, S. G.; Rini, J. M. *J. Mol. Biol.* **2006**, *360*, 67-79.
- (31) Postema, M. H. D. *C-Glycoside Synthesis*; CRC Press: London, 1995.
- (32) Bertozzi, C.; Bednarski, M. *Synthesis of C-Glycosides: Stable Mimics of O-Glycosidic Linkages*, Khan, S. H.; O'Neill, R. A., Eds. In *Modern Methods in Carbohydrate Synthesis*; Harwood Academic; United Kingdom, **1996**; 316-351
- (33) Engel, R. *Chem. Rev.* **1977**, *77*, 349-367.
- (34) Cipolla, L.; La Ferla, B.; Nicotra, F. *Carbohydr. Polym.* **1998**, *37*, 291-298.
- (35) Vasella, A.; Baudin, G.; Panza, L. *Heteroat. Chem.* **1991**, *2*, 151-161.
- (36) Ray, W. J.; Post, C. B.; Puvathingal, J. M. *Biochemistry* **1993**, *32*, 38-47.

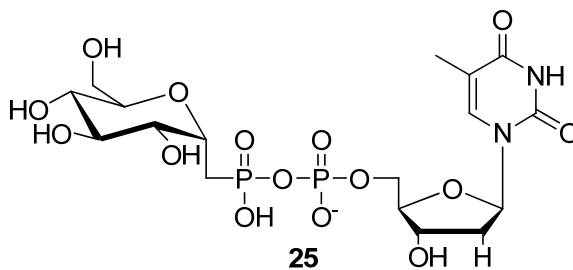
- (37) Becker, S.; Schnackerz, K. D.; Schinzel, R. *Biochim. Biophys. Acta, Gen. Subj.* **1995**, *1243*, 381-385.
- (38) Chmielewski, M.; BeMiller, J. N.; Cerretti, D. P. *Carbohydr. Res.* **1981**, *97*, C1-C4.
- (39) Nicotra, F.; Ronchetti, F.; Russo, G. *J. Org. Chem.* **1982**, *47*, 4459-4462.
- (40) Sadeghi-Khomami, A. Design, synthesis and evaluation of UDP-galactopyranose mutaseinhibitors as new anti-tuberculosis agents, Nottingham University, United Kingdom, 2004. PhD thesis.
- (41) Nicotra, F.; Perego, R.; Ronchetti, F.; Russo, G.; Toma, L. *Carb. Res.* **1984**, *131*, 180-184.
- (42) Cipolla, L.; Ferla, B. L.; Nicotra, F.; Panza, L. *Tetrahedron Lett.* **1997**, *38*, 5567-5568.
- (43) Cipolla, L.; La Ferla, B.; Panza, L.; Nicotra, F. *J. Carbohydr. Chem.* **1998**, *17*, 1003-1013.
- (44) Street, I. P.; Withers, S. G. *Biochem. J.* **1995**, *308*, 1017-1023.
- (45) Pougny, J.; Nassr, M. A. M.; Sinaÿ, P. *Chem. Commun.* **1981**, 375-376.
- (46) Nicotra, F.; Panza, L.; Ronchetti, F.; Russo, G.; Toma, L. *Carbohydr. Res.* **1987**, *171*, 49-57.
- (47) Nicotra, F.; Perego, R.; Ronchetti, F.; Russo, G.; Toma, L. *Gazz. Chim. Ital* **1984**, *114*, 193-195.
- (48) Freeman, F.; Robarge, K. D. *Carbohydr. Res.* **1986**, *154*, 270-274.
- (49) Boschetti, A.; Nicotra, F.; Panza, L.; Russo, G. *J. Org. Chem.* **1988**, *53*, 4181-4185.
- (50) Casero, F.; Cipolla, L.; Lay, L.; Nicotra, F.; Panza, L.; Russo, G. *J. Org. Chem.* **1996**, *61*, 3428-3432.
- (51) Lichtenthaler, F. W.; Kaji, E. *Liebigs Ann. Chem.* **1985**, *1985*, 1659-1668.
- (52) Timmons, S. C.; Jakeman, D. L. *Org. Lett.* **2007**, *9*, 1227-1230.
- (53) Rose, N. L.; Zheng, R. B.; Pearcey, J.; Zhou, R.; Completo, G. C.; Lowary, T. L. *Carbohydr. Res.* **2008**, *343*, 2130-2139.
- (54) Matsumura, F.; Oka, N.; Wada, T. *Org. Lett.* **2008**, *10*, 1557-1560.
- (55) Li, P.; Sergueeva, Z. A.; Dobrikov, M.; Shaw, B. R. *Chem. Rev.* **2007**, *107*, 4746-4796.

- (56) Wolucka, B. A.; Rush, J. S.; Waechter, C. J.; Shibaev, V. N.; de Hoffmann, E. *Anal. Biochem.* **1998**, *255*, 244-251.
- (57) Berkowitz, D. B.; Bose, M. *J. Fluorine Chem.* **2001**, *112*, 13-33.
- (58) Romanenko, V. D.; Kukhar, V. P. *Chem. Rev.* **2006**, *106*, 3868-3935.
- (59) Berkowitz, D. B.; Bose, M.; Pfannenstiel, T. J.; Doukov, T. *J. Org. Chem.* **2000**, *65*, 4498-4508.
- (60) O'Hagan, D.; Rzepa, H. S. *Chem. Commun.* **1997**, 645-652.
- (61) Swierczek, K.; Pandey, A. S.; Peters, J. W.; Hengge, A. C. *J. Med. Chem.* **2003**, *46*, 3703-3708.
- (62) Ko, K. S.; Zea, C. J.; Pohl, N. L. *J. Am. Chem. Soc.* **2004**, *126*, 13188-13189.
- (63) Mohamady, S.; Jakeman, D. L. *J. Org. Chem.* **2005**, *70*, 10588-10591.
- (64) Xu, Y.; Qian, L.; Prestwich, G. D. *Org. Lett.* **2003**, *5*, 2267-2270.
- (65) Banks, E. R.; Murtagh, V.; An, I.; Maleczka Jr., R. E. In *1-(Chloromethyl)-4-fluoro-1,4-diazoniabicyclo[2.2.2]octane Bis(tetrafluoroborate)*; e-EROS Encyclopedia of Reagents for Organic Synthesis; John Wiley & Sons, Ltd: 2007.
- (66) Poss, A. J. In *N-Fluorobenzenesulfonimide*; e-EROS Encyclopedia of Reagents for Organic Synthesis; John Wiley & Sons, Ltd: 2003; .
- (67) O'Donnell, K.; Bacon, R.; Chellappa, K. L.; Schowen, R. L.; Lee, J. K. *J. Am. Chem. Soc.* **1972**, *94*, 2500-2505.
- (68) Gawley, R. E.; Hennings, D. D. In *Sodium Hydride*; e-EROS Encyclopedia of Reagents for Organic Synthesis; John Wiley & Sons, Ltd. 2006.
- (69) Fraser, R. R.; Mansour, T. S.; Savard, S. *J. Org. Chem.* **1985**, *50*, 3232-3234.
- (70) Smith, M. B.; March, J. In *Acids and Bases*; March's Advanced Organic Chemistry (Sixth Edition); John Wiley & Sons, Ltd. 2007; pp 356-394.
- (71) Taylor, S. D.; Kotoris, C. C.; Hum, G. *Tetrahedron* **1999**, *55*, 12431-12477.
- (72) Hussain, M.; Ahmed, V.; Hill, B.; Ahmed, Z.; Taylor, S. D. *Bioorg. Med. Chem.* **2008**, *16*, 6764-6777.
- (73) Differding, E.; Duthaler, R. O.; Kreiger, A.; Ruegg, G. G.; Schmit, C. *Synlett* **1991**, 395-396.
- (74) Burton, D. J.; Kesling, H. S.; Naae, D. G. *J. Fluorine Chem.* **1981**, *18*, 293-298.
- (75) Burton, D. J.; Yang, Z.; Qiu, W. *Chem. Rev.* **1996**, *96*, 1641-1716.

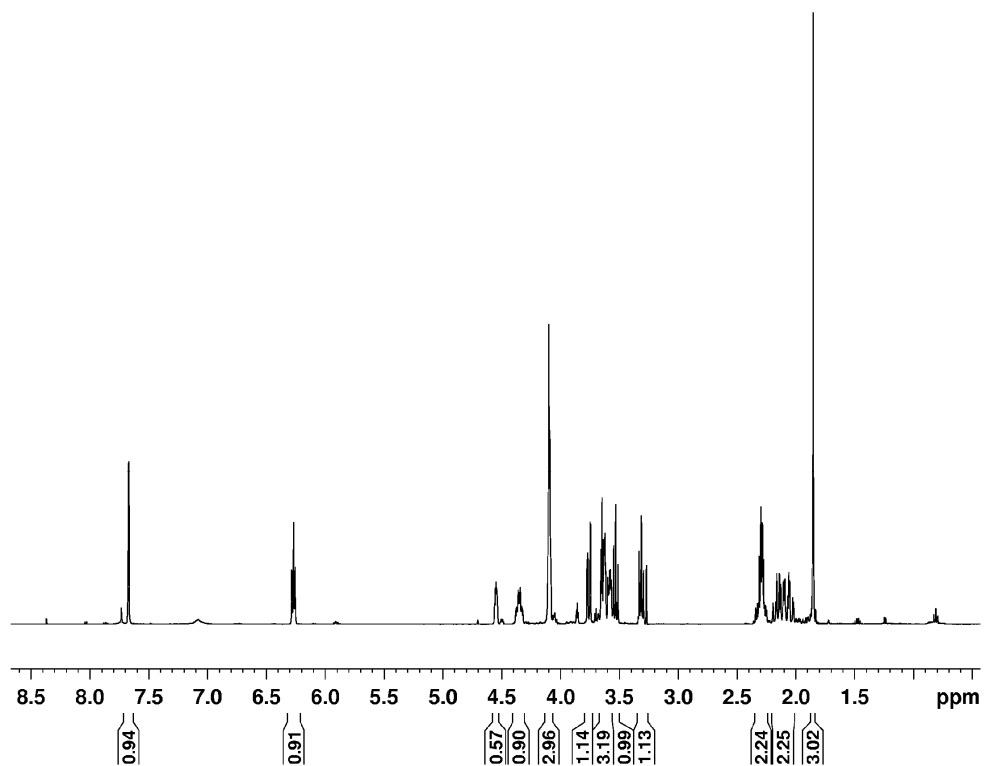
- (76) Bhadury, P. S.; Palit, M.; Sharma, M.; Raza, S. K.; Jaiswal, D. K. *J. Fluorine Chem.* **2002**, *116*, 75-80.
- (77) Ozturk, T.; Ertas, E.; Mert, O. *Chem. Rev.* **2007**, *107*, 5210-5278.
- (78) Karp, G. M. *J. Org. Chem.* **1999**, *64*, 8156-8160.
- (79) Vassiliou, S.; Grabowiecka, A.; Kosikowska, P.; Yiotakis, A.; Kafarski, P.; Berlicki, A. *J. Med. Chem.* **2008**, *51*, 5736-5744.
- (80) Liu, X.; Adams, H.; Blackburn, G. M. *Chem. Commun.* **1998**, 2619-2620.
- (81) Liu, X. H.; Zhang, X. R.; Blackburn, G. M. *Chem. Commun.* **1997**, 87-88.
- (82) Cvetovich, R. J. *Organic Process Research & Development* **2010**, *14*, 295-297.
- (83) Du, Y.; Jung, K.; Wiemer, D. F. *Tetrahedron Lett.* **2002**, *43*, 8665-8668.
- (84) Beaucage, S. L. In *Synthetic Strategies and Parameters Involved in the Synthesis of Oligodeoxyribonucleotides According to the Phosphoramidite Method*; Beaucage, S. L., Bergstrom, D. E., Glick, G. D. and Jones, R. A., Eds.; *Current Protocols in Nucleic Acid Chemistry*; John Wiley & Sons: New York, NY, 2001.
- (85) Ogilvie, K. K.; Nemer, M. J. *Tetrahedron Lett.* **1981**, *22*, 2531-2532.
- (86) Chellmani, A.; Suresh, R. *React. Kinet. Catal. Lett.* **1988**, *37*, 501-505.
- (87) Denney, D. B.; Goodyear, W. F.; Goldstein, B. *J. Am. Chem. Soc.* **1960**, *82*, 1393-1395.
- (88) Wen, X.; Hultin, P. G. *Tetrahedron Lett.* **2004**, *45*, 1773-1775.
- (89) *The Merck Index*; Windholz, M., Ed.; Merck & Co, Inc.: Rathway, N.J., 1983; p. 1347, #9245.

APPENDIX 1. Selected NMR Spectra of Representative Compounds

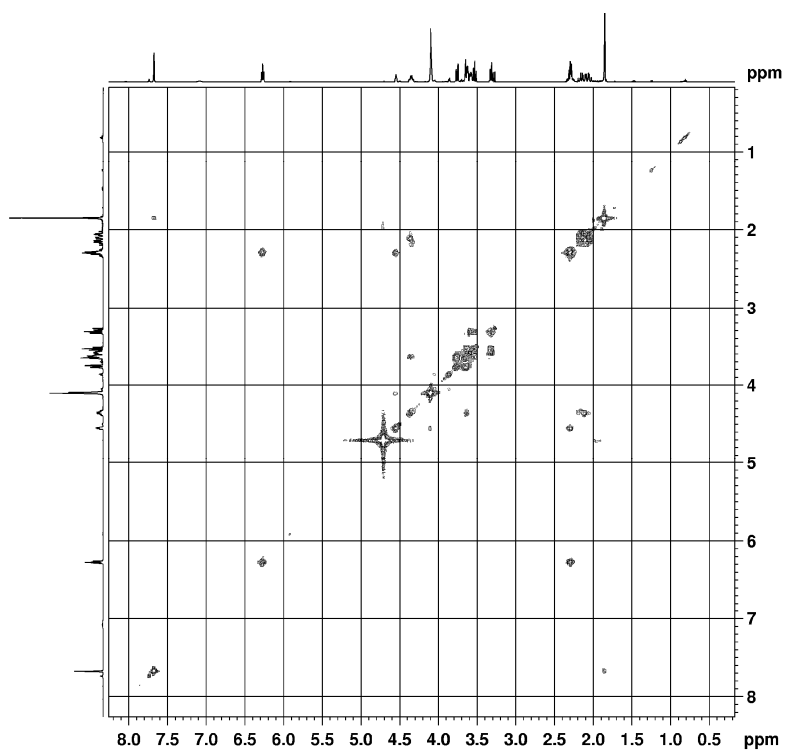
Figure 33: NMR spectra of purified phosphono analogue of dTDP- α -D-glucopyranose (**25**)



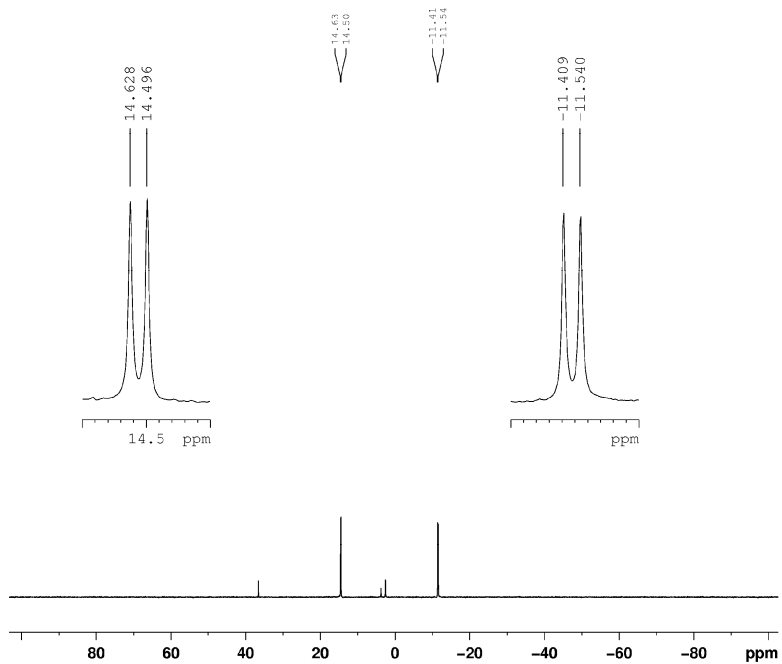
(a) ^1H NMR spectrum of **25**



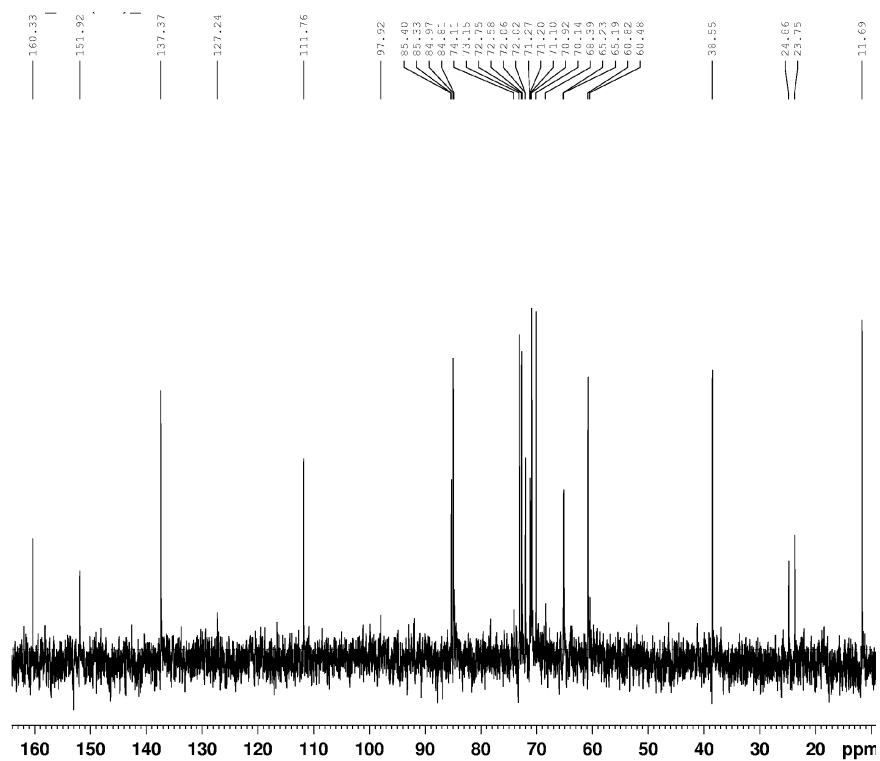
(b) COSY NMR spectrum of **25**



(c) ^{31}P NMR spectrum of **25**



(d) $^{13}\text{C}\{^1\text{H}\}$ NMR spectrum of **25**



(a) $^{13}\text{C}\text{-}^1\text{H}$ HSQC spectrum of **25**

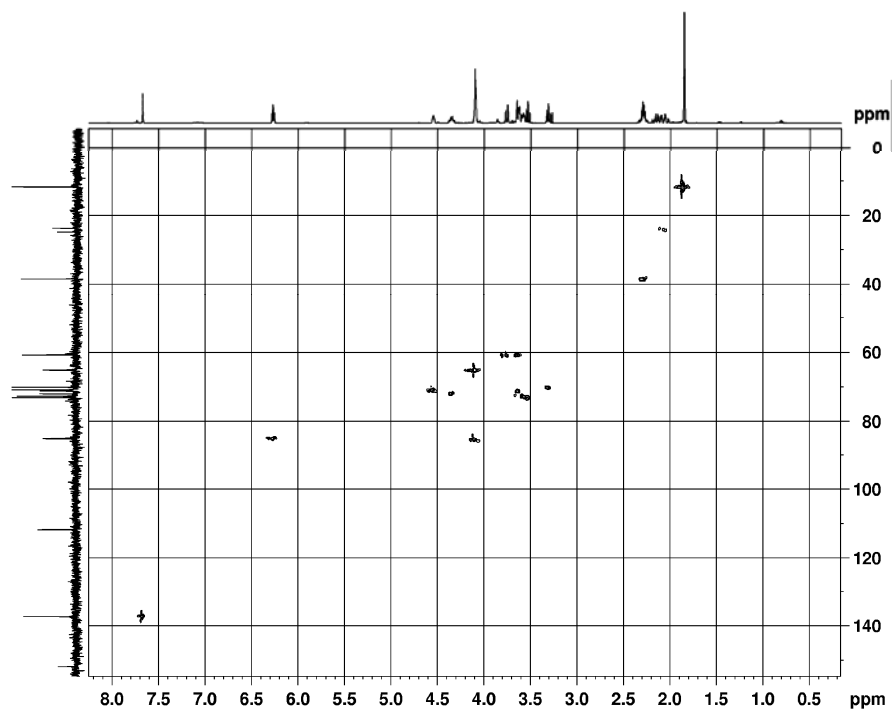
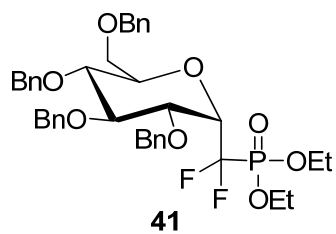
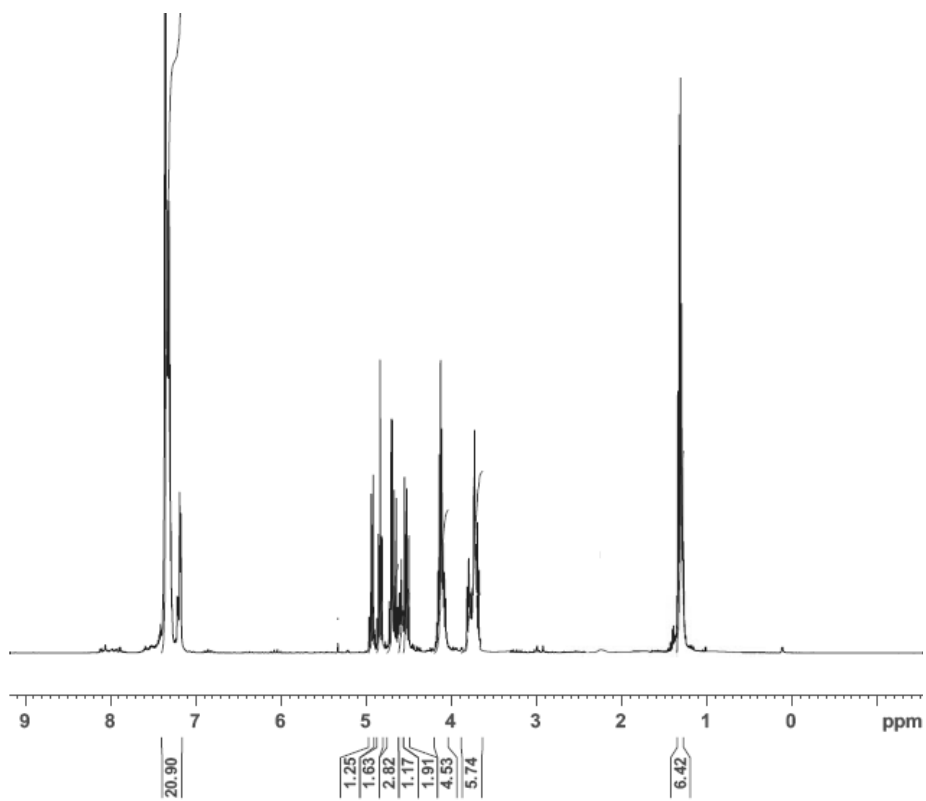


Figure 34: NMR spectra of diethyl *C*-(1-deoxy-2,3,4,6-tetra-*O*-benzyl- α -D-glucopyranosyl) difluoromethanephosphonate (**41**)



(a) ^1H NMR spectrum of **41**



(b) ^{31}P NMR spectrum of **41**

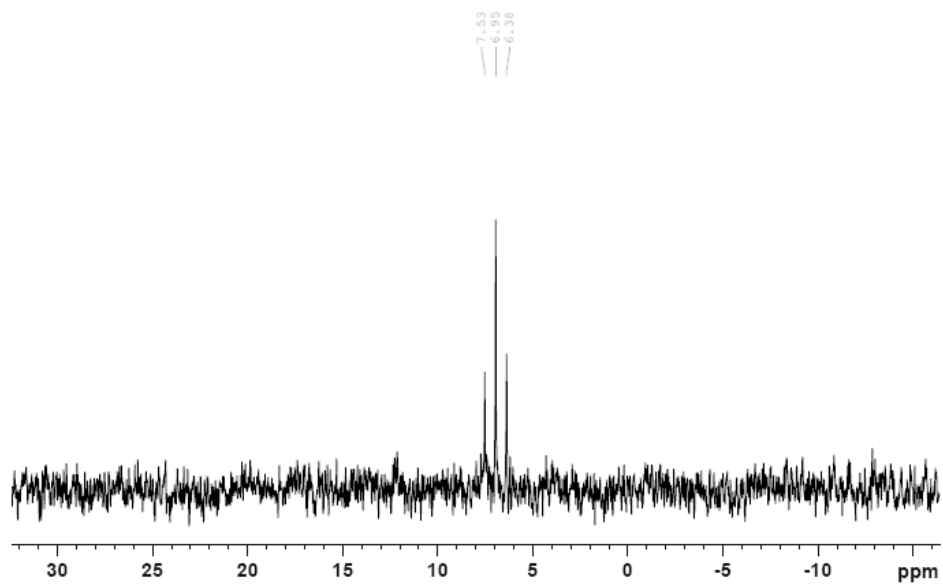
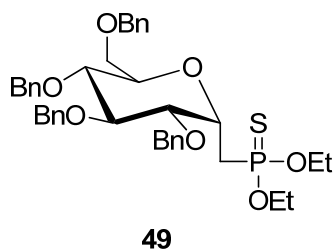
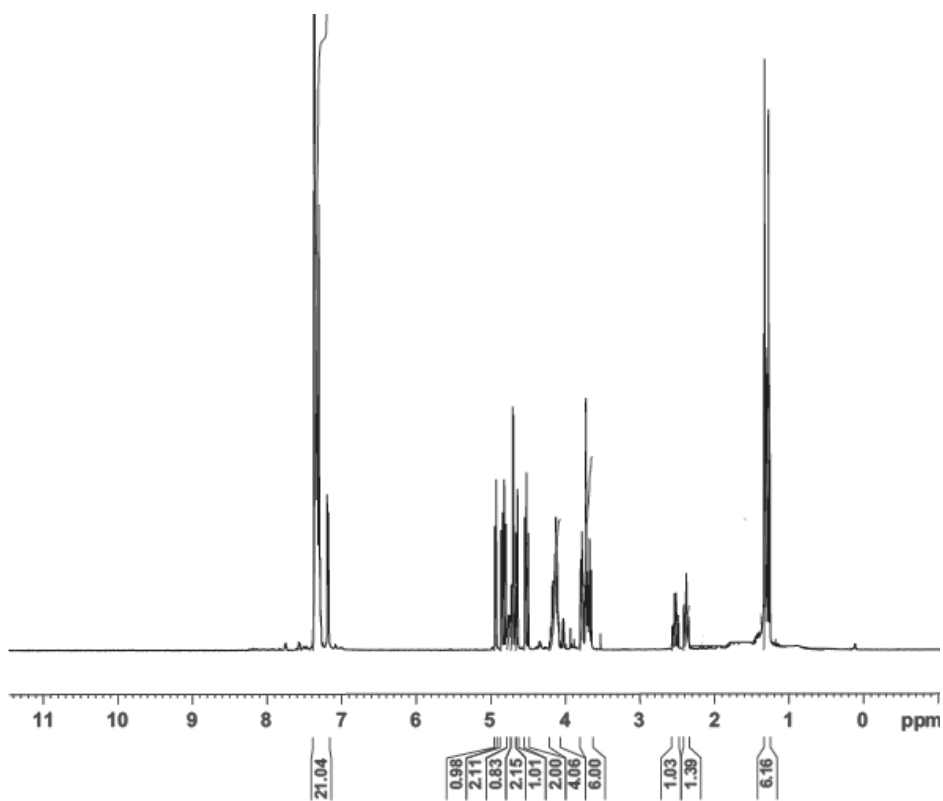


Figure 35: NMR spectra of diethyl C-(1-deoxy-2,3,4,6-tetra-O-benzyl- α -D-glucopyranosyl) methane thiophosphonate (**49**)



(a) ^1H NMR spectrum of **49**



(b) ^{31}P NMR spectrum of **49**

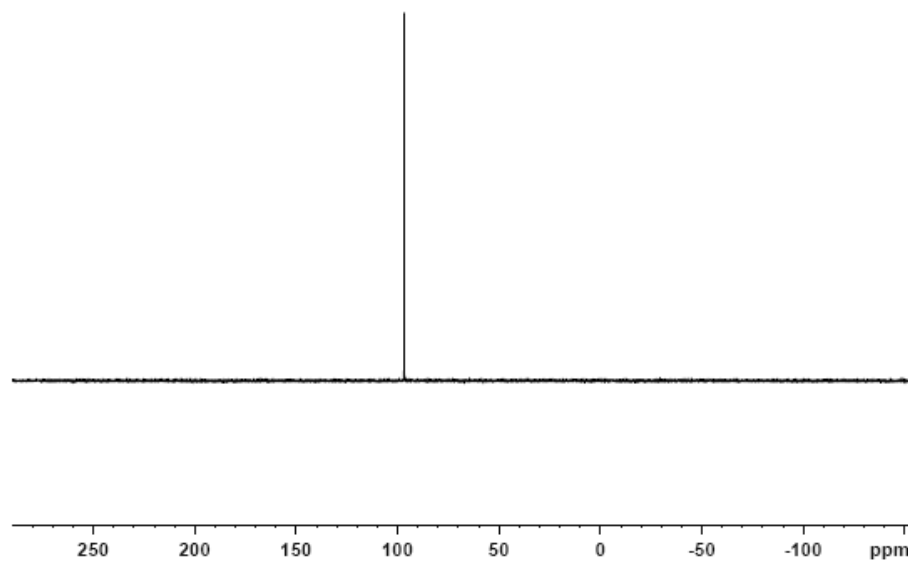
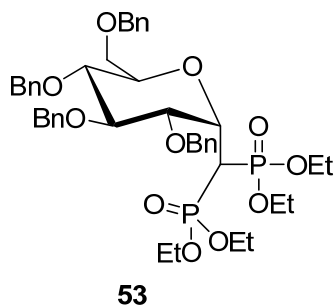
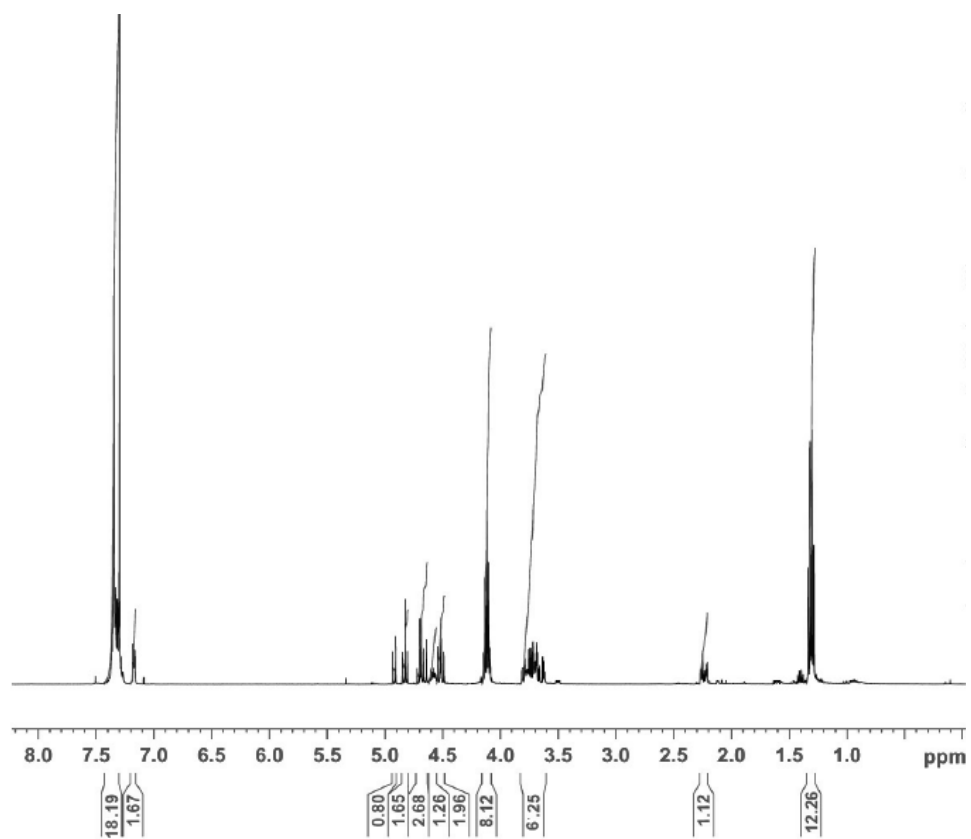


Figure 36: NMR spectra of diethyl C-(1-deoxy-2,3,4,6-tetra-O-benzyl- α -D-glucopyranosyl) methane bisphosphonate (**50**)



(a) ^1H NMR spectrum of **53**



(b) ^{31}P NMR spectrum of **53**

